

An efficient and exact noncommutative quantum Gibbs sampler

Chi-Fang Chen,^{1,2,*} Michael J. Kastoryano,^{2,3} and András Gilyén⁴

¹*Institute for Quantum Information and Matter,*

California Institute of Technology, Pasadena, CA, USA

²*AWS Center for Quantum Computing, Pasadena, CA*

³*IT University of Copenhagen, Denmark*

⁴*Alfréd Rényi Institute of Mathematics, HUN-REN, Budapest, Hungary*

Preparing thermal and ground states is an essential quantum algorithmic task for quantum simulation. In this work, we construct the first efficiently implementable and exactly detailed-balanced Lindbladian for Gibbs states of arbitrary noncommutative Hamiltonians. Our construction can also be regarded as a continuous-time quantum analog of the Metropolis-Hastings algorithm. To prepare the quantum Gibbs state, our algorithm invokes Hamiltonian simulation for a time proportional to the mixing time and the inverse temperature β , up to polylogarithmic factors. Moreover, the gate complexity reduces significantly for lattice Hamiltonians as the corresponding Lindblad operators are (quasi-) local (with radius $\sim \beta$) and only depend on local Hamiltonian patches. Meanwhile, purifying our Lindbladians yields a temperature-dependent family of frustration-free “parent Hamiltonians”, prescribing an adiabatic path for the canonical purified Gibbs state (i.e., the Thermal Field Double state). These favorable features suggest that our construction is the ideal quantum algorithmic counterpart of classical Markov chain Monte Carlo sampling.

I. INTRODUCTION

One of the leading candidate applications of quantum computers [DMB⁺23] is to simulate quantum systems [Fey82]. In particular, the preparation of thermal states or ground states for materials and molecules has received significant attention [BWM⁺18, CNA⁺20, LBG⁺21, vBLH⁺21]. Surprisingly, there has not been a consensus on the “go-to” quantum algorithm for this task due to a lack of provable guarantees or empirical evidence [LLZ⁺22]. Recently, several Monte Carlo-style, nonunitary quantum algorithms have been proposed [TOV⁺11, YAG12, WT21, RWW22, CKBG23, DCL23]. While their efficacy has only been validated using small-scale numerics and under strong theoretical assumptions [CB21, SM21, DCL23], there are reasons for optimism. On physical grounds, these algorithms resemble naturally occurring system-bath dynamics [ML20]; if a system rapidly cools in a refrigerator, the same plausibly applies to a “cooling algorithm” that emulates this process. Alternatively, from a computer science perspective, these algorithms are cousins of classical Markov chain Monte Carlo (MCMC) methods but with quantum mechanical effects and complications. This work sets out to complete this line of thought and construct an ideal quantum MCMC algorithm where the robustness, simplicity, and empirical success of the classical case may be transferrable.

The cornerstone of classical Markov chain Monte Carlo methods is *detailed balance* (see, e.g., [LPW⁺17]): given a target state π , we impose a certain symmetry of the Markov chain \mathbf{M}

$$\mathbf{M}_{s's} \pi_s = \pi_{s'} \mathbf{M}_{s's'} \quad \text{for each configuration } s, s', \quad \text{ensuring stationarity } \mathbf{M}[\pi] = \pi.$$

This simple recipe for the stationary state has been crucial in constructing and analyzing the Metropolis-Hastings algorithm and related Markov chains. Notably, detailed balance gives a conceptually simple picture of convergence via the spectral gap \mathbf{M} , a quantity amenable to numerical and analytic bounds. If the problem at hand has a local structure, detailed balance can often be imposed locally and efficiently, relegating the algorithm’s complexity to the *mixing time*, the time scale of convergence towards stationarity. While the mixing time may be challenging to analyze, MCMC methods can often be employed heuristically. In particular, we are often interested in sampling the *Gibbs distribution* $\pi_\beta \propto e^{-\beta H}$ of a certain energy functional H at temperature $1/\beta$. Analogously, the central idea of *quantum Gibbs sampling* is to construct a detailed-balanced quantum process where the quantum Gibbs state is stationary. In this work, we focus on designing a Lindbladian \mathcal{L}_β (the quantum analog of a continuous-time Markov chain generator) such that

$$e^{\mathcal{L}_\beta t}[\rho_\beta] = \rho_\beta \quad \text{where } \rho_\beta := e^{-\beta H} / \text{Tr}(e^{-\beta H}),$$

for *any* target quantum Hamiltonian \mathbf{H} . As in the classical case, we can prepare samples of quantum Gibbs states if the Lindbladian evolution can be *efficiently* implemented and the state converges *rapidly* to the Gibbs state.

The main issue with existing quantum Gibbs sampling algorithms is that *quantum detailed balance* (Figure 1) only holds *approximately* unless we can distinguish individual energy eigenstates exactly, which is generally

* chifang@caltech.edu

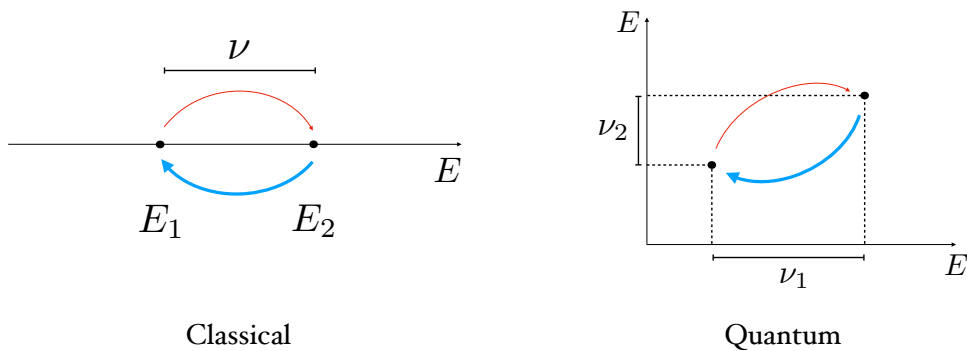


Figure 1. (Left) For the classical Gibbs distribution, the detailed balance condition is a pairwise relation between heating (red) and cooling (blue) transition rates, depending on the energy difference ν of states. (Right) For the quantum Gibbs state, the detailed balance condition refers to pairs of matrix elements of the density operator (expanded in the energy basis), where each matrix element is described by a pair of energies (of the basis elements in the ket and bra respectively) therefore the relation depends on both of the respective energy differences ν_1 and ν_2 .

intractable except for fast-forwardable Hamiltonians (e.g., Hamiltonians with commuting terms). Consequently, we either lose accuracy guarantees for the stationary state or the efficiency for the individual steps of the Gibbs sampling algorithm, leading to significant aggregated complexity plaguing various constructions; see Ref. [CKBG23] for a comprehensive catalog. The algorithmic challenge in enforcing quantum detailed balance is the energy-time uncertainty principle rooted in *metrology*: for each energy estimate, the uncertainty scales inversely proportional to the Hamiltonian simulation time. Indeed, all existing quantum MCMC algorithms attempt to attain detailed balance via an “energy estimation” subroutine (quantum phase estimation [TOV+11, WT21, RWW22] or operator Fourier Transform [CKBG23, Appendix A]). Consequently, this error propagates to the desired Gibbs state and impacts the implementation cost.

To our knowledge, the best general lower-bound on the Hamiltonian simulation time is $\Omega(\beta)$ per Gibbs sample [CKBG23, Proposition G.5]. This comes from a sensitivity argument that the Gibbs state is a smooth matrix function of \mathbf{H} with derivatives bounded by $\mathcal{O}(\beta)$. This conceptual gap motivates our guiding question:

Can we design an efficiently implementable yet exactly detailed-balanced quantum Gibbs sampler?

If so, we may recover both the simplicity and versatility of classical MCMC algorithms. In this work, we answer this question in the affirmative by explicitly constructing an exactly detailed-balanced Lindbladian at a moderate cost: $\tilde{\mathcal{O}}(\beta)$ -Hamiltonian simulation cost per *unit time* of Lindbladian evolution $e^{\mathcal{L}}$. (The unit-time evolution for a continuous-time generator should be regarded as “one step,” corresponding to one discrete Markov chain update.) Furthermore, for lattice Hamiltonians (with local jumps), our Lindbladian is (quasi-)local with locality scaling as $\tilde{\mathcal{O}}(\beta)$. Thus, one step of the algorithm only needs to simulate localized Hamiltonian patches; this starkly contrasts with previous works, whose cost per unit time step generally scales with the system size due to simulating the *global* Hamiltonian. The mathematical and conceptual simplicity of our result immediately initiates a list of new directions, which we discuss in detail in Section IV.

The key revelation behind our construction is that that quantum detailed balance can be enforced *smoothly* without ever knowing the energy. Indeed, the standard *metrology* lower bound $\sim \Omega(\frac{1}{\epsilon})$ is not an obstruction because having access to a detailed-balanced Lindbladian (or the Gibbs state) does not give energy estimates. We have seen that Quantum Signal Processing [LC17] or Quantum Singular Value Transform (QSVT) [GSLW19] allows one to directly access smooth (polynomial) functions of Hamiltonians without a phase-estimation subroutine; the costs often scale linearly with the largest derivatives and only *logarithmically* with the precision. However, Lindbladians, as superoperators, are more restrictive to manipulate than Hermitian matrices. A key design ingredient is a carefully chosen *coherent* term in our Lindbladian

$$\mathcal{L}_\beta[\rho] = -i \underbrace{[\mathbf{B}, \rho]}_{\text{“coherent”}} + (\text{“dissipative”}),$$

which appears necessary to *coherently* and *exactly* cancel out certain unwanted errors from the dissipative part.

As a by-product, purifying our Lindbladian yields a temperature-dependent family of “parent Hamiltonians” whose zero-eigenstate is a canonical purification of the Gibbs state.¹ Similarly to how classical Markov chains can be “quantized” to prepare the purified stationary state, here we prepare the purified Gibbs state by following a prescribed adiabatic path (called *quantum simulated annealing* [Szeg04, YAG12]), drawing a surprisingly simple

¹ This purification coincides with the *Thermal Field Double* state featured in recent quantum gravity discussions. See, e.g., [MS13].

connection between thermal dissipation and adiabatic evolution. In particular, for lattice Hamiltonians, the parent Hamiltonian inherits the (quasi-)locality, which curiously connects the purified Gibbs state to the ground state of (quasi-)local Hamiltonians.

A. Main results

Our main results, based on the algorithmic framework of [CKBG23, Section III], consider the following Lindbladian in the Schrodinger picture

$$\mathcal{L}_\beta[\cdot] := \underbrace{-i[\mathbf{B}, \cdot]}_{\text{“coherent”}} + \sum_{a \in A} \int_{-\infty}^{\infty} \gamma(\omega) \left(\underbrace{\hat{\mathbf{A}}^a(\omega)(\cdot)\hat{\mathbf{A}}^a(\omega)^\dagger}_{\text{“transition”}} - \underbrace{\frac{1}{2}\{\hat{\mathbf{A}}^a(\omega)^\dagger\hat{\mathbf{A}}^a(\omega), \cdot\}}_{\text{“decay”}} \right) d\omega \quad (1.1)$$

which is parameterized by the following terms (with convenient normalization conditions [CKBG23, Section I.B]):

- The distinct *jump operators* \mathbf{A}^a “drive” the transitions, and can be chosen arbitrarily as long as their adjoints are included

$$\{\mathbf{A}^a : a \in A\} = \{\mathbf{A}^{a^\dagger} : a \in A\} \quad \text{and} \quad \left\| \sum_{a \in A} \mathbf{A}^{a^\dagger} \mathbf{A}^a \right\| \leq 1. \quad (1.2)$$

For better mixing and ergodicity, the jumps should be “scrambling” and not commute with the Hamiltonian (e.g., breaking the symmetries of the Hamiltonian). For lattice Hamiltonians, the jump operators may be chosen simply to be the single-site Pauli operators, but global jumps could also be helpful in some cases as in the classical case (e.g., cluster updates).

- The *Operator Fourier Transform* (OFT)² (Section II A) weighted by a Gaussian *filter* with a tunable width $\sim \sigma_E^{-1}$

$$\begin{aligned} \hat{\mathbf{A}}^a(\omega) &:= \frac{1}{\sqrt{2\pi}} \int_{-\infty}^{\infty} e^{i\mathbf{H}t} \mathbf{A}^a e^{-i\mathbf{H}t} e^{-i\omega t} f(t) dt \quad \text{where} \quad f(t) := e^{-\sigma_E^2 t^2} \sqrt{\sigma_E \sqrt{2/\pi}} \\ &= \frac{e^{-t^2/\beta^2}}{\sqrt{\beta \sqrt{\pi/2}}} \quad \text{if} \quad \sigma_E = \frac{1}{\beta}. \end{aligned} \quad (1.3)$$

In particular, the Gaussian is normalized $\int_{-\infty}^{\infty} |f(t)|^2 dt = 1$. Naturally, the Heisenberg evolution $e^{i\mathbf{H}t} \mathbf{A}^a e^{-i\mathbf{H}t}$ diagnoses the energy difference ω before and after the jump. Integrating over time $\frac{1}{\sqrt{2\pi}} \int_{-\infty}^{\infty} (\cdot) e^{-i\omega t} f(t) dt$ yields the operator Fourier Transform $\hat{\mathbf{A}}^a(\omega)$, which selects the transitions of \mathbf{A}^a that *increase* the energy by roughly $\sim \omega \pm \mathcal{O}(\sigma_E)$. At first glance, the Gaussian filter seems to merely ensure good concentration for both the frequency and time domain, but it turns out to have a more intimate connection [Mou19] to quantum detailed balance (see also Section D for an alternative justification).

- The *transition weight* $\gamma(\omega)$ follows (yet another) Gaussian with a tunable variance $\sigma_\gamma > 0$:

$$\gamma(\omega) = \exp\left(-\frac{(\omega + \omega_\gamma)^2}{2\sigma_\gamma^2}\right) \quad \text{with shift} \quad \sigma_\gamma^2 := \frac{2\omega_\gamma}{\beta} - \sigma_E^2 \quad (1.4)$$

$$= \exp\left(-\frac{(\beta\omega + 1)^2}{2}\right) \quad \text{if} \quad \sigma_E = \sigma_\gamma = \omega_\gamma = \frac{1}{\beta}. \quad (1.5)$$

The normalization is such that $\|\gamma(\omega)\|_\infty \leq 1$, and the maximum is attained at $\omega = -\omega_\gamma$.

- A coherent (i.e., nondissipative) term generated by a fine-tuned Hermitian matrix \mathbf{B} . The expression depends on $\omega_\gamma, \sigma_E, \beta$ in the general case (see Corollary III.1), but it simplifies to

$$\mathbf{B} := \sum_{a \in A} \int_{-\infty}^{\infty} b_1(t) e^{-i\beta \mathbf{H}t} \left(\int_{-\infty}^{\infty} b_2(t') e^{i\beta \mathbf{H}t'} \mathbf{A}^{a^\dagger} e^{-2i\beta \mathbf{H}t'} \mathbf{A}^a e^{i\beta \mathbf{H}t'} dt' \right) e^{i\beta \mathbf{H}t} dt \quad \text{if} \quad \omega_\gamma = \sigma_E = \sigma_\gamma = \frac{1}{\beta} \quad (1.6)$$

² Note the sign convention, which might differ from that of other works in the literature.

for some carefully chosen smooth and rapidly decaying functions b_1, b_2 normalized by $\|b_1\|_1, \|b_2\|_1 \leq 1$. The coherent term \mathbf{B} may appear intimidating but plays a crucial role in ensuring *quantum detailed balance* for the Gibbs state ρ_β , defined as:

$$\mathcal{L}_\beta^\dagger[\cdot] = \sqrt{\rho_\beta}^{-1} \mathcal{L}_\beta[\sqrt{\rho_\beta} \cdot \sqrt{\rho_\beta}] \sqrt{\rho_\beta}^{-1} \quad \text{for fixed } \beta, \mathbf{H}. \quad (1.7)$$

It implies the stationarity of Gibbs state exactly (see [Definition II.1](#)).

The Gaussian transition weight (1.4) is inspired by an observation of [\[Mou19\]](#):³ the functional form of Gaussians is naturally compatible with exact detailed balance⁴ if we make conscious choices of ω_γ, σ_E

$$\exp\left(-\frac{(\omega + \omega_\gamma)^2}{2\sigma^2}\right) = \exp\left(-\frac{2\omega_\gamma}{\sigma^2} \cdot \omega\right) \exp\left(-\frac{(-\omega + \omega_\gamma)^2}{2\sigma^2}\right).$$

Compared with the usual step-function-like Metropolis weight $\min(1, e^{-\beta\omega})$, the Gaussian weight is more selective, only allowing energy transitions $-\omega_\gamma \pm \mathcal{O}(\sigma_\gamma)$; this narrower window could potentially freeze the dynamics, leading to long mixing time.

Fortunately, quantum detailed balance 1.7 is preserved under *linear combination* of Lindbladians; hence, choosing a linear combination of γ covering a range of different width σ_γ can remove the heavy restriction on energy transitions. Surprisingly, a suitable linear combination recovers Metropolis-like transition weights, which we focus on as the representative. To obtain the corresponding exactly detailed-balanced Lindbladian, the only change compared to (1.4)-(1.6) is the choice of transition weight

$$\text{(Metropolis-Style)} \quad \gamma^M(\omega) := \exp\left(-\beta \max\left(\omega + \frac{1}{2\beta}, 0\right)\right) \quad \text{if } \sigma_E = \frac{1}{\beta} \quad (1.8)$$

with the corresponding coherent term \mathbf{B}^M parameterized by another function $b_2^M(t)$ (the function $b_1^M(t) = b_1(t)$ remains the same as in (1.6)).⁵

Now, we present the first main result: the Gibbs state is an *exact* stationary state of the advertised Lindbladian (see [Section II C 2](#) for the proof). Although we have mainly focused on the Gibbs state, we can formally invoke Gibbs sampling for $\beta\mathbf{H} = \log(\rho_{fix})$ for arbitrary target stationary state ρ_{fix} , albeit with potential overhead from implementing the matrix logarithm.

Theorem I.1 (Gibbs state is stationary). *For any $\beta \geq 0$, the Lindbladian (1.1)-(1.3) with $\sigma_E = \frac{1}{\beta}$, Gaussian transition weight (1.5), and the coherent term \mathbf{B} (1.6) satisfies detailed balance (1.7) exactly. Therefore, the Gibbs state is stationary*

$$\mathcal{L}_\beta[\rho_\beta] = 0.$$

The same applies for the Metropolis transition weight $\gamma^M(\omega)$ (1.8) with the corresponding coherent term \mathbf{B}^M .

Furthermore, building on the algorithmic machinery developed in Ref. [\[CKBG23, Section III\]](#), the Lindbladian can be efficiently simulated at a moderate cost (see [Section III D](#) for the proof).

Theorem I.2 (Efficient implementation). *Instantiate the Lindbladian parameters of [Theorem I.1](#) for either the Gaussian $\gamma(\omega)$ or Metropolis $\gamma^M(\omega)$ transition weight. Then, the Lindbladian evolution*

$$e^{\mathcal{L}_\beta t} \quad \text{for each } t \geq 1$$

can be implemented efficiently in ϵ -diamond distance with cost:

$$\begin{aligned} \tilde{\mathcal{O}}(t \cdot \beta) & \quad \text{(total Hamiltonian simulation time)} \\ \tilde{\mathcal{O}}(1) & \quad \text{(resettable ancilla)} \\ \tilde{\mathcal{O}}(t) & \quad \text{(block-encodings for the jumps } \sum_{a \in A} |a\rangle \otimes \mathbf{A}^a) \\ \tilde{\mathcal{O}}(t) & \quad \text{(other two-qubit gates).} \end{aligned}$$

The $\tilde{\mathcal{O}}(\cdot)$ notation absorbs logarithmic dependencies on $t, \beta, \|\mathbf{H}\|, n, 1/\epsilon, |A|$.

³ Their algorithm [\[Mou19\]](#) seems qualitatively different from Monte Carlo style quantum algorithms [\[TOV+11, YAG12, WT21, RWW22, CKBG23\]](#) and closer to performing phase estimation on trial states; see the discussion in [\[Mou19, Page 5\]](#).

⁴ We thank Jonathan Moussa for pointing us to his paper and raising the question of whether detailed balance can hold exactly in the precursor of this work [\[CKBG23\]](#).

⁵ The generalized function (distribution) $b_2^M(t)$ should be interpreted as the Cauchy principal value $\lim_{\eta \rightarrow 0^+} \mathbb{1}(|t| > \eta) b_2^M(t)$. In case $[\mathbf{H}, \sum_{a \in A} \mathbf{A}^{a\dagger} \mathbf{A}^a] \neq 0$ an additional correction term $\frac{1}{16\sqrt{2}\pi} \delta(t)$ should be added.

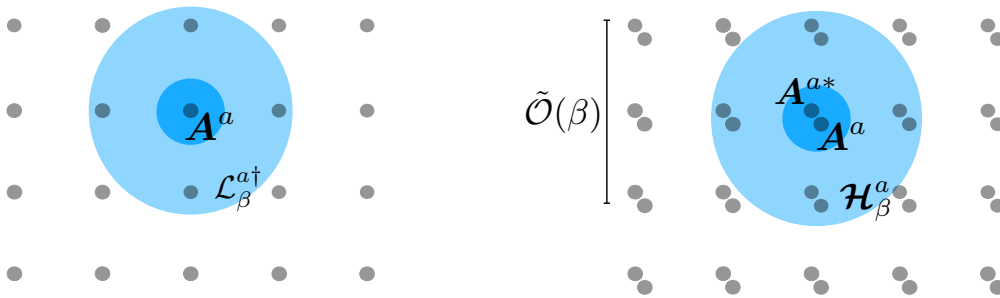


Figure 2. (Left) For lattice Hamiltonians, our Lindbladian is a sum of quasi-local terms \mathcal{L}_β^a localized around each jump \mathbf{A}^a with radius $\tilde{\mathcal{O}}(\beta)$. Indeed, detailed balance is really about the *energy difference*, which can be diagnosed by Fourier Transforming the Heisenberg evolution $\mathbf{A}^a(t) = e^{i\mathbf{H}t}\mathbf{A}^ae^{-i\mathbf{H}t}$. Due to the Lieb-Robinson bounds, the localized Lindbladian terms effectively only depend on the local Hamiltonian patch nearby (up to exponentially decaying tail). (Right) This locality persists after purification, where two copies of the system are glued together.

Here, our Lindbladian is normalized (1.2), (1.3), (1.4), (1.6) (or the Metropolis-like weight (1.8) with its coherent term \mathbf{B}^M) such that

$$\|\mathcal{L}_\beta\|_{1-1} = \tilde{\mathcal{O}}(1).$$

Therefore, evolving for unit time $t = 1$ corresponds to a $\tilde{\mathcal{O}}(1)$ -strength update $e^{\mathcal{L}_\beta}$ and only requires a characteristic Hamiltonian simulation time $\sim \beta$. This is precisely the cost for implementing both the operator Fourier Transform (1.3) and the coherent term (1.6) via Linear Combination of Unitaries. To be more careful, the $\tilde{\mathcal{O}}(\cdot)$ notation also includes polylogarithmic factors due to discretization, truncation, and Hamiltonian simulation error, which is typical in quantum algorithms. To clarify, the idealized map \mathcal{L}_β remains exactly detailed-balanced (the nice object to analyze), and the algorithmic implementation error can be made arbitrarily small given the desired runtime.

We expect the *total Hamiltonian simulation time* to be the figure of merit for the algorithmic cost, among others. The jump operators \mathbf{A}^a can be as simple as Pauli operators, but we consider a black-box query model in case more complex jumps are needed for faster mixing. In the last line, the use of other two-qubit gates comes from easier-to-implement unitaries, including the Quantum Fourier Transform, state preparation unitary for the Gaussian filter $|f\rangle$, controlled transition weight; see Section III C and [CKBG23, Section III.B].

Combining Theorem I.1 and Theorem I.2, we can prepare the Gibbs state by simulating the Lindbladian until convergence, resulting in the cost

$$(\text{total Hamiltonian simulation time per Gibbs sample}) = \tilde{\mathcal{O}}(t_{\text{mix}}(\mathcal{L}_\beta) \cdot \beta).$$

Formally, the *mixing time* $t_{\text{mix}}(\mathcal{L}_\beta)$ quantifies the shortest time scale that any two input states become indistinguishable (see Proposition E.4). To obtain end-to-end gate complexities, we should also instantiate the Hamiltonian simulation cost, a subroutine whose complexity for various systems has been thoroughly studied. For example, on D -dimensional lattices with local jumps \mathbf{A}^a , we expect the actual cost to be (up to logarithmic error dependence)

$$(\text{gate complexity per unit evolution time}) \sim \underbrace{\beta}_{\text{Ham. sim. time}} \times \underbrace{(v_{LR}\beta)^D}_{\text{volume}}, \quad (\text{spatially local Hamiltonians})$$

where v_{LR} is the Lieb-Robinson velocity and $v_{LR}\beta$ is roughly the radius of the Heisenberg evolution $\mathbf{A}^a(\cdot)$ at time $\sim \beta$. Indeed, the Lindbladian is a sum over quasi-local Lindbladian operators (Figure 2)

$$\mathcal{L}_\beta = \sum_{a \in A} \mathcal{L}_\beta^a \quad \text{each centered at } \mathbf{A}^a \quad \text{with radius } \tilde{\mathcal{O}}(v_{LR}\beta).$$

In particular, the cost per unit Lindbladian evolution time is essentially *independent* of the system size (up to logarithmic dependencies), as we only need to simulate the Hamiltonian patch surrounding each jump \mathbf{A}^a .⁶

1. Purifying the Lindbladians

We may purify the Lindbladian to prepare the *purified Gibbs state* [WT21]

$$|\sqrt{\rho_\beta}\rangle := \frac{1}{\sqrt{\text{Tr}[e^{-\beta\mathbf{H}}]}} \sum_i e^{-\beta E_i/2} |\psi_i\rangle \otimes |\psi_i^*\rangle; \quad (1.9)$$

⁶ In fact, we can further parallelize the Lindbladian evolution to improve the circuit depth; see Section C.

this particular purification is reminiscent of the quantum walk formalism for detailed-balanced classical Markov chains. The relevant “parent Hamiltonian” (playing the role of a “quantum walk” operator) is the *discriminant* associated with the Lindbladian; the expression may appear intimidating but resembles how classical detailed-balanced Markov chains are quantized

$$\mathcal{H}_\beta := \rho^{-1/4} \mathcal{L}[\rho^{1/4} \cdot \rho^{1/4}] \rho^{-1/4}.$$

The above should be regarded as the Lindbladian under similarity transformation. Further, to implement the quantum walk, the superoperator needs to be *vectorized* into an operator on duplicated Hilbert spaces

$$\text{(vectorization)} \quad \mathcal{H}_\beta : \mathcal{B}(\mathbb{C}^{2^n}) \rightarrow \mathcal{B}(\mathbb{C}^{2^n}) \simeq \mathcal{H}_\beta \in \mathcal{B}(\mathbb{C}^{2^n} \otimes \mathbb{C}^{2^n}).$$

Indeed, the Gibbs state ρ_β , as the Lindbladian stationary state, corresponds to the purified Gibbs state $|\sqrt{\rho_\beta}\rangle$ (1.9), as a zero-eigenvector of the discriminant. As a sanity check, the quantum detailed balance condition 1.7 naturally ensures that the operator is Hermitian $\mathcal{H}_\beta = \mathcal{H}_\beta^\dagger$.

Proposition I.1 (Purifying Lindbladians). *Instantiate the Lindbladian parameters of Theorem I.1 for the Gaussian or Metropolis transition weight. Then, the corresponding discriminant \mathcal{H}_β is Hermitian, frustration-free, and annihilates the purified Gibbs state.*

$$\mathcal{H}_\beta = \sum_{a \in A} \mathcal{H}_\beta^a \quad \text{such that} \quad \mathcal{H}_\beta^a |\sqrt{\rho_\beta}\rangle = 0 \quad \text{for each } a \in A.$$

In other words, preparing the purified Gibbs state boils down to the *ground state* problem (up to a negative sign) for a *frustration-free* parent Hamiltonian parameterized by β^7 ; for lattice Hamiltonian with local jumps \mathbf{A}^a , the parent Hamiltonian inherits the *quasi-locality* of our Lindbladian, with individual terms of radius $\sim v_{LR}\beta$. The algorithmic cost to implement the parent Hamiltonian is analogous to the Lindbladian case, where \mathbf{H}_β roughly corresponds to a constant-time Lindbladian evolution.

Theorem I.3 (Block encodings for the discriminants). *Instantiate the Lindbladian parameters of Theorem I.1 for either the Gaussian or Metropolis transition weight. Then, the corresponding discriminant $\frac{1}{\mathcal{O}(1)} \mathcal{H}_\beta$ can be block-encoded approximately in ϵ -spectral norm using*

$$\begin{aligned} \tilde{\mathcal{O}}(\beta) & \quad (\text{Hamiltonian simulation time}) \\ \tilde{\mathcal{O}}(1) & \quad (\text{resettable ancilla}) \\ \tilde{\mathcal{O}}(1) & \quad (\text{block-encodings for the jumps } \sum_{a \in A} |a\rangle \otimes \mathbf{A}^a \text{ and its transposes } \sum_{a \in A} |a\rangle \otimes (\mathbf{A}^a)^T) \\ \tilde{\mathcal{O}}(1) & \quad (\text{other two-qubit gates}). \end{aligned}$$

The $\tilde{\mathcal{O}}(\cdot)$ notation absorbs logarithmic dependencies on $t, \beta, \|\mathbf{H}\|, n, 1/\epsilon, |A|$.

Like in Theorem I.2, we have expanded many other unitaries in the last line; see Section III C. Note that we had to downscale the discriminant to implement the block encodings; see Section III E for the proof. For readers familiar with quantum walks, obtaining a block-encoding for $\mathbf{I} + \mathcal{H}_\beta$ (instead of \mathcal{H}_β) would be nicer as it leads to a quadratic speedup in terms of the spectral gap of \mathcal{H}_β . However, we have not found such a direct block-encoding for our particular construction, leaving this an open problem. This is in contrast with our earlier approximate construction [WT21, CKBG23], where such a direct block-encoding was possible, which might be advantageous in some cases.

B. Roadmap

The remaining body of text is organized thematically by the analysis and the algorithm. We begin with the analysis (Section II) regarding how we design our Lindbladian to satisfy quantum detailed balance exactly. Next, we give efficient algorithms (Section III) in terms of modularized block encodings to implement the advertised Lindbladian and its purification.

In the appendix, we include a dictionary of notations (Section IV) and independent expositions: A connection between the discriminant gap, mixing time, and the area law of entanglement (Section C) and an alternative heuristic derivation of our detailed balance Lindbladian in the time domain (Section D).

⁷ Strictly speaking, originating from a Lindbladian, here the parent Hamiltonian is negative semi-definite, and the purified Gibbs state is the top-eigenstate. Introducing a global negative sign will make it the ground state.

II. ANALYSIS

In this section, we execute the calculations circling the exact detailed balance condition. First, we review the operator Fourier Transform in the frequency domain. Second, we review the notion of detailed balance, including the stationary state and spectral theory of convergence. Third, we plug in the advertised functional forms and derive the required coherent term \mathbf{B} for achieving detailed balance.

A. Operator Fourier Transform

Our Lindbladian features the operator Fourier Transform $\hat{\mathbf{A}}(\omega)$ of a jump operator \mathbf{A} according to the Hamiltonian \mathbf{H} (dropping the jump label for this section). To analyze it, we need to consider the frequency domain representation instead of the time domain. Decompose the operator in the energy basis, and regroup in terms of the energy change (called the *Bohr frequencies* $\nu \in B(\mathbf{H}) := \{E_i - E_j \mid E_i, E_j \in \text{Spec}(\mathbf{H})\}$)

$$\mathbf{A} := \sum_{E_1, E_2 \in \text{Spec}(\mathbf{H})} \mathbf{P}_{E_2} \mathbf{A} \mathbf{P}_{E_1} = \sum_{\nu \in B(\mathbf{H})} \sum_{E_2 - E_1 = \nu} \mathbf{P}_{E_2} \mathbf{A} \mathbf{P}_{E_1} =: \sum_{\nu \in B(\mathbf{H})} \mathbf{A}_\nu \quad \text{such that} \quad (\mathbf{A}_\nu)^\dagger = (\mathbf{A}^\dagger)_{-\nu}$$

where \mathbf{P}_E denotes the orthogonal projector onto the eigensubspace of \mathbf{H} with *exact* energy E . This decomposition naturally solves the Heisenberg evolution

$$e^{i\mathbf{H}t} \mathbf{A} e^{-i\mathbf{H}t} = \sum_{\nu \in B} \mathbf{A}_\nu e^{i\nu t} \quad \text{since} \quad [\mathbf{H}, \mathbf{A}_\nu] = \nu \mathbf{A}_\nu.$$

Indeed, the energy differences $\nu \in B$ (shorthand of $B(\mathbf{H})$) naturally arise from the commutator (as opposed to the absolute energies $E \in \text{spec}(\mathbf{H})$).

At first glance, the reference to the exact energies seems unphysical as each of them individually requires a long (likely exponential) Hamiltonian simulation time to access algorithmically. Fortunately, all that we are manipulating are the *smooth* weights on these Bohr frequencies; indeed, the operator Fourier Transform can be conveniently expressed by

$$\hat{\mathbf{A}}_f(\omega) = \frac{1}{\sqrt{2\pi}} \int_{-\infty}^{\infty} e^{i\mathbf{H}t} \mathbf{A} e^{-i\mathbf{H}t} e^{-i\omega t} f(t) dt = \sum_{\nu \in B} \mathbf{A}_\nu \hat{f}(\omega - \nu),$$

where $\hat{f}(\omega) = \frac{1}{\sqrt{2\pi}} \int_{-\infty}^{\infty} f(t) e^{-i\omega t} dt$ is the Fourier Transform of the filter function $f(t)$. Our choice of $f(t)$ is

$$f(t) := e^{-\sigma_E^2 t^2} \sqrt{\sigma_E \sqrt{2/\pi}} \quad \text{such that} \quad \hat{f}(\omega) = \frac{1}{\sqrt{2\sigma_E \sqrt{2\pi}}} \exp\left(-\frac{\omega^2}{4\sigma_E^2}\right) \quad \text{and} \quad \int_{-\infty}^{\infty} |f(t)|^2 dt = 1,$$

therefore $\hat{\mathbf{A}}(\omega)$ becomes simply

$$\hat{\mathbf{A}}(\omega) = \frac{1}{\sqrt{2\sigma_E \sqrt{2\pi}}} \sum_{\nu \in B} \exp\left(-\frac{(\omega - \nu)^2}{4\sigma_E^2}\right) \mathbf{A}_\nu.$$

The above uses the Gaussian integrals, which will also be constantly recalled.

Fact II.1 (Gaussian integrals). *For any $b \in \mathbb{C}$ and $\sigma > 0$, we have that $\int_{-\infty}^{\infty} e^{-\frac{(\omega-b)^2}{2\sigma^2}} d\omega = \sqrt{2\pi}\sigma$.*

We can think of the width σ_E as the uncertainty in energy, which scales inversely proportionally to the time width $\sim \sigma_E^{-1}$.

B. Exact detailed balance from that of the transition part

Our notion of detailed balance for Lindbladians is analogous to its classical cousin, ensuring a stationary state ρ . For the mathematical audience, we should mention that other forms of quantum detailed balance have also been studied (see [Section E](#)), but we will dominantly focus on the following as it appears to be especially nice.

Definition II.1 (Kubo–Martin–Schwinger detailed balance condition). *For a normalized, full-rank state $\rho \succ 0$, we say that an super-operator \mathcal{L} satisfies ρ -detailed balance (or ρ -DB in short) if*

$$\mathcal{L}^\dagger[\cdot] = \rho^{-1/2} \mathcal{L}[\rho^{1/2} \cdot \rho^{1/2}] \rho^{-1/2},$$

or equivalently, whenever the associated discriminant is self-adjoint with respect to ρ , i.e.,

$$\begin{aligned}\mathcal{D}(\rho, \mathcal{L}) &:= \rho^{-1/4} \mathcal{L}[\rho^{1/4} \cdot \rho^{1/4}] \rho^{-1/4} \\ &= \rho^{1/4} \mathcal{L}^\dagger[\rho^{-1/4} \cdot \rho^{-1/4}] \rho^{1/4} = \mathcal{D}(\rho, \mathcal{L})^\dagger.\end{aligned}$$

In the above, $(\mathcal{L})^\dagger$ denotes the adjoint for superoperators with respect to trace (i.e., the Hilbert Schmidt inner product).

One may interpret the conjugation with the state as a similarity transformation under which the Lindbladian becomes Hermitian (w.r.t. to the KMS inner product). The above generalizes classical detailed balance by considering super-operators and permitting the stationary distribution to be an operator.

Proposition II.1 (Fixed point). *If a Lindbladian \mathcal{L} is ρ -detailed-balanced, then*

$$\mathcal{L}[\rho] = 0.$$

Recently, *quantum approximate detailed balance* has also been studied in the precursor of this work [CKBG23, Section II.A], discussing nonasymptotic error bounds relating mixing times to fixed point error. Exact detailed balance gives a much simpler conceptual picture. Still, we may again need to recall approximate detailed balance for non-fine-tuned Lindbladians (such as those from Nature) or amid intermediate steps of analysis (such as when truncating the radius of the quasi-local jumps).

At first glance, the detailed balance condition is merely a linear equation that can be solved abstractly. However, the difficulty arises due to two additional constraints.

- (**Complete Positivity**.) Lindbladians have a particular *quadratic* dependence on the Lindblad operators to ensure complete positivity and trace preservation of $e^{t\mathcal{L}}$ for any t .
- (**Efficiency**.) The Lindbladian (i.e., the block-encoding for the jumps and the Hamiltonian) must be efficiently implemented using a limited Hamiltonian simulation time.

The main challenge is to satisfy both constraints simultaneously. Indeed, Davies' generator [Dav74, Dav76] satisfies the first but not the second because it uses an infinite-time operator Fourier Transform; using QSVT, one might be able directly to implement the Boltzmann weight smoothly at moderate costs, but it may break the Lindbladian structure. Our approach begins by isolating the “transition” part of the Lindbladian (1.1) with abstract Lindblad operators L_j

$$\mathcal{L}[\cdot] := -i[B, \cdot] + \underbrace{\sum_j L_j \cdot L_j^\dagger}_{\mathcal{T}:=} - \frac{1}{2} \left\{ \underbrace{\sum_j L_j^\dagger L_j}_{\mathcal{R}:=}, \cdot \right\}$$

where B and R are both Hermitian. This decomposition is helpful because conjugating with the stationary state preserves the form of the transition part

$$\sqrt{\rho}^{-1} \left(\sum_j L_j (\sqrt{\rho} \cdot \sqrt{\rho}) L_j^\dagger \right) \sqrt{\rho}^{-1} = \sum_j L'_j(\cdot) L'_j{}^\dagger.$$

However, the commutator B and anti-commutator terms R mix with each other under conjugation with Gibbs state. Based on the above observation, our recipe for constructing a detailed-balanced Lindbladian consists of three steps:

1. *Guess* a set of Lindblad operators L_j such that the transition part (which is $\mathcal{T} = \sum_a \int_{-\infty}^{\infty} \gamma(\omega) \hat{A}^a(\omega) \cdot \hat{A}^a(\omega)^\dagger d\omega$ in our case) obeys detailed balance.
2. According to the transition part \mathcal{T} , determine the decay part parameterized by R . This gives a purely dissipative Lindbladian.
3. According to the decay part R , tailor the commutator term B to ensure detailed balance. Remarkably, such a B always exists, can be found explicitly, and is essentially *unique*. Of course, whether the map is efficiently implementable is a separate question.⁸

⁸ This is inspired by a related ongoing work [GHC⁺on] at an early stage.

To simplify the presentation, we introduce the following notation for conjugating any full-rank state ρ :

$$\Gamma_\rho[\cdot] := \rho^{1/2}(\cdot)\rho^{1/2} \quad \text{and} \quad \Lambda_\rho[\cdot] := \rho^{-1/2}(\cdot)\rho^{1/2}.$$

Observe that for Hermitian operator \mathbf{X} , we have the identities $\Gamma_\rho[\mathbf{X}]^\dagger = \Gamma_\rho[\mathbf{X}]$ and $\Lambda_\rho[\mathbf{X}]^\dagger = \Lambda_\rho^{-1}[\mathbf{X}]$. When the context is clear, we will omit subscript ρ .

The main calculation of this section is summarized as follows. For any \mathbf{R} , we can give a general solution for the coherent term \mathbf{B} ; this calculation is possible because the coherent term is not constrained by the complete-positivity structure of Lindbladians and only needs to be Hermitian.

Lemma II.1 (Prescribing the coherent term). *For any full-rank state ρ and Hermitian operator \mathbf{R} , there exists a unique Hermitian operator \mathbf{B} (up to adding any scalar multiples of the identity \mathbf{I}) such that the super-operator*

$$\mathcal{S}[\cdot] := -i[\mathbf{B}, \cdot] - \frac{1}{2}\{\mathbf{R}, \cdot\}$$

satisfies ρ -DB.⁹ For a Gibbs state $\rho \propto \exp(-\beta\mathbf{H})$, we can express the solution decomposed according to the Bohr frequencies $\nu \in B$ as

$$\mathbf{B} = \frac{i}{2} \sum_{\nu \in B} \tanh\left(\frac{\beta\nu}{4}\right) \mathbf{R}_\nu.$$

The above can be applied to a purely dissipative Lindbladian, where the transition part already satisfies ρ -DB.

Corollary II.1 (ρ -DB Lindbladians). *Suppose we have a purely-dissipative \mathcal{L}_{diss} Lindbladian such that the transition part satisfies ρ -DB for a full-rank state ρ*

$$\Gamma_\rho^{-1} \circ \mathcal{T} \circ \Gamma_\rho = \mathcal{T}^\dagger,$$

then we can accordingly prescribe \mathbf{B} such that $-i[\mathbf{B}, \cdot] + \mathcal{L}_{diss}$ satisfies ρ -DB.

Proof of Lemma II.1. Let $\mathbf{K} := \mathbf{B} - \frac{i}{2}\mathbf{R}$ and observe that

$$\begin{aligned} \mathcal{S}[\cdot] &:= -i[\mathbf{B}, \cdot] - \frac{1}{2}\{\mathbf{R}, \cdot\} = -i\mathbf{K}(\cdot) + i(\cdot)\mathbf{K}^\dagger \\ \mathcal{S}^\dagger[\cdot] &:= i[\mathbf{B}, \cdot] - \frac{1}{2}\{\mathbf{R}, \cdot\} = i\mathbf{K}^\dagger(\cdot) - i(\cdot)\mathbf{K} \end{aligned}$$

using that \mathbf{B} and \mathbf{R} are Hermitian. Then,

$$\begin{aligned} \mathcal{S}^\dagger[\cdot] - \Gamma^{-1} \circ \mathcal{S} \circ \Gamma[\cdot] &= i\mathbf{K}^\dagger(\cdot) - i(\cdot)\mathbf{K} + i\Gamma^{-1}(\mathbf{K}\Gamma[\cdot] - \Gamma[\cdot]\mathbf{K}^\dagger) \\ &= i(\mathbf{K}^\dagger + \Lambda[\mathbf{K}])(\cdot) - i(\cdot)(\mathbf{K} + (\Lambda[\mathbf{K}])^\dagger) \quad (\text{using that } \Gamma^{-1}\mathbf{K}\Gamma[\cdot] = \Lambda[\mathbf{K}](\cdot)) \\ &=: i(\mathbf{Q}(\cdot) - (\cdot)\mathbf{Q}^\dagger), \end{aligned}$$

where we define $\mathbf{Q} := \mathbf{K}^\dagger + \Lambda[\mathbf{K}]$. To ensure quantum detailed balance, we need the RHS to vanish

$$\mathbf{Q}(\cdot) - (\cdot)\mathbf{Q}^\dagger = 0 \quad \iff \quad \mathbf{Q} = 0 + \lambda\mathbf{I} \quad \text{for } \lambda \in \mathbb{R},$$

that is, \mathbf{Q} vanishes up to a real multiple of the identity $\lambda\mathbf{I}$; for simplicity, the identity part can be dropped for now and added back. Since ρ has full rank, we can assume without loss of generality that $\rho \propto \exp(-\beta\mathbf{H})$ for some \mathbf{H} . Now we compute

$$\begin{aligned} \mathbf{Q} &= \mathbf{K}^\dagger + \Lambda[\mathbf{K}] \\ &= (1 + \Lambda)\mathbf{B} + \frac{i}{2}(1 - \Lambda)\mathbf{R} \\ &= \sum_{\nu \in B} (1 + e^{\beta\nu/2})\mathbf{B}_\nu + \frac{i}{2}(1 - e^{\beta\nu/2})\mathbf{R}_\nu. \quad (\text{using that } \Lambda(\mathbf{B}_\nu) = e^{\beta\nu/2}\mathbf{B}_\nu) \end{aligned}$$

⁹ Actually, our proof shows an even stronger statement: for any Hermitian \mathbf{F} commuting with ρ there is a unique \mathbf{B} (up to an additive term proportional to \mathbf{I}) such that $\mathcal{S}^\dagger[\cdot] - \Gamma^{-1} \circ \mathcal{S} \circ \Gamma[\cdot] = -i[\mathbf{F}, \cdot]$. The only change is that one should set $\mathbf{B}_0 := -\frac{1}{2}\mathbf{F}$. This relates to a more general notion of detailed balance that allows for a unitary drift [Definition E.1](#), see also [\[FF07, Section 5\]](#). This might be useful for breaking degeneracies of the state ρ (or the Hamiltonian \mathbf{H}).

where we denote $B := B(\mathbf{H})$ the set of Bohr frequencies of \mathbf{H} . Since the operators \mathbf{B}_ν (and \mathbf{R}_ν) are linearly independent for different Bohr frequencies,

$$\mathbf{Q} = 0 \iff \mathbf{B}_\nu = \frac{i}{2} \tanh\left(\frac{\beta\nu}{4}\right) \mathbf{R}_\nu \quad \text{for each } \nu \in B. \quad (\text{using that } \tanh(x) = \frac{e^{2x}-1}{e^{2x}+1})$$

In particular, $\mathbf{B}_0 = 0$ since $\tanh(0) = 0$.

Finally, since \mathbf{R} is Hermitian and $\tanh(\omega)$ is an odd function, we have that \mathbf{B} is Hermitian as well by

$$\begin{aligned} \sum_{\nu \in B} (\mathbf{B}_\nu)^\dagger &= \frac{i}{2} \sum_{\nu \in B} \tanh\left(-\frac{\beta\nu}{4}\right) (\mathbf{R}_\nu)^\dagger. && (\text{Using } -\tanh(x) = \tanh(-x)) \\ &= \frac{i}{2} \sum_{\nu \in B} \tanh\left(-\frac{\beta\nu}{4}\right) \mathbf{R}_{-\nu} && (\text{Using that } \mathbf{R} = \mathbf{R}^\dagger \text{ implies } (\mathbf{R}_\nu)^\dagger = \mathbf{R}_{-\nu}) \\ &= \frac{i}{2} \sum_{\nu \in B} \tanh\left(\frac{\beta\nu}{4}\right) \mathbf{R}_\nu = \sum_{\nu \in B} \mathbf{B}_\nu. && (\text{Change of variables } \nu \rightarrow -\nu) \quad \blacksquare \end{aligned}$$

Adding the identity part $\lambda \mathbf{I}$ to conclude the proof.

C. Exact detailed balance for Gaussian weights and their linear combinations

In this section, we carry out the abstract recipe for our advertised Lindbladian to prove the exact detailed balance condition (Definition II.1). We begin with the transition part and then solve for the coherent term.

1. Exact detailed balance of the transition part

First, we show that the Gaussian ansatz indeed leads to detailed balance for the “transition” part

$$\Gamma_\rho^{-1} \circ \mathcal{T} \circ \Gamma_\rho = \mathcal{T}^\dagger.$$

It is instructive to rewrite the abstract equation above in terms of Bohr-frequencies. Let (\cdot) be any input matrix, then the transition part of our Lindbladian reads

$$\begin{aligned} \mathcal{T} &= \sum_{a \in A} \int_{-\infty}^{\infty} \gamma(\omega) \hat{\mathbf{A}}^a(\omega)(\cdot) \hat{\mathbf{A}}^a(\omega)^\dagger d\omega = \frac{1}{2\sigma_E \sqrt{2\pi}} \sum_{a \in A} \sum_{\nu_1, \nu_2 \in B} \int_{-\infty}^{\infty} e^{-\frac{(\omega+\omega_\gamma)^2}{2\sigma_\gamma^2}} e^{-\frac{(\omega-\nu_1)^2}{4\sigma_E^2}} e^{-\frac{(\omega-\nu_2)^2}{4\sigma_E^2}} \mathbf{A}_{\nu_1}^a(\cdot) (\mathbf{A}_{\nu_2}^a)^\dagger d\omega \\ &=: \sum_{a \in A} \sum_{\nu_1, \nu_2 \in B} \alpha_{\nu_1, \nu_2}^{(\omega_\gamma, \sigma_\gamma)} \mathbf{A}_{\nu_1}^a(\cdot) (\mathbf{A}_{\nu_2}^a)^\dagger. \end{aligned} \quad (2.2)$$

Since the bilinear expression holds for any input (\cdot) , taking traces on both sides yields that

$$\sum_{a \in A} \int_{-\infty}^{\infty} \gamma(\omega) \hat{\mathbf{A}}^a(\omega)^\dagger \hat{\mathbf{A}}^a(\omega) d\omega = \sum_{a \in A} \sum_{\nu_1, \nu_2 \in B} \alpha_{\nu_1, \nu_2}^{(\omega_\gamma, \sigma_\gamma)} (\mathbf{A}_{\nu_2}^a)^\dagger \mathbf{A}_{\nu_1}^a.$$

In terms of Bohr frequencies, the exact detailed balance condition is a certain symmetry of the coefficient matrix $\alpha^{(\omega_\gamma, \sigma_\gamma)}$.

Proposition II.2 (Detailed balance in the Energy domain). *Consider a super-operator parameterized by a Hamiltonian \mathbf{H} , β , and a set of operators including its adjoints $\{\mathbf{A}^a : a \in A\} = \{\mathbf{A}^{a^\dagger} : a \in A\}$:*

$$\mathcal{T} = \sum_{a \in A} \sum_{\nu_1, \nu_2 \in B} \alpha_{\nu_1, \nu_2} \mathbf{A}_{\nu_1}^a(\cdot) (\mathbf{A}_{\nu_2}^a)^\dagger \quad \text{such that} \quad \alpha_{\nu_1, \nu_2} = \alpha_{-\nu_2, -\nu_1} e^{-\beta(\nu_1 + \nu_2)/2} \quad \text{for each } \nu_1, \nu_2 \in B$$

Then,

$$\Gamma_\rho^{-1} \circ \mathcal{T} \circ \Gamma_\rho = \mathcal{T}^\dagger.$$

Indeed, one recovers the classical detailed balance condition for inputs diagonal in the energy basis. However, the quantum detailed balance condition also constrains the amplitudes between off-diagonal matrix elements (Figure 1).

Proof. We can directly calculate

$$\begin{aligned}
\Gamma_{\rho}^{-1} \circ \mathcal{T} \circ \Gamma_{\rho}^1 &= \sum_{a \in A} \sum_{\nu_1, \nu_2 \in B} \alpha_{\nu_1, \nu_2} \sqrt{\rho_{\beta}^{-1}} \mathbf{A}_{\nu_1}^a \sqrt{\rho_{\beta}}(\cdot) \sqrt{\rho_{\beta}}(\mathbf{A}_{\nu_2}^a)^{\dagger} \sqrt{\rho_{\beta}^{-1}} \\
&= \sum_{a \in A} \sum_{\nu_1, \nu_2 \in B} \alpha_{\nu_1, \nu_2} e^{\frac{\beta}{2} \nu_1} \mathbf{A}_{\nu_1}^a(\cdot) (\mathbf{A}_{\nu_2}^a)^{\dagger} e^{\frac{\beta}{2} \nu_2} && \text{(since } \rho_{\beta} \propto e^{-\beta \mathbf{H}} \text{)} \\
&= \sum_{a \in A} \sum_{\nu_1, \nu_2 \in B} \alpha_{-\nu_2, -\nu_1} \mathbf{A}_{\nu_1}^a(\cdot) (\mathbf{A}_{\nu_2}^a)^{\dagger} && \text{(since } \alpha_{\nu_1, \nu_2} e^{\frac{\beta(\nu_1 + \nu_2)}{2}} = \alpha_{-\nu_2, -\nu_1} \text{)} \\
&= \sum_{a \in A} \sum_{\nu_1, \nu_2 \in B} \alpha_{-\nu_2, -\nu_1} ((\mathbf{A}^{a\dagger})_{-\nu_1})^{\dagger}(\cdot) (\mathbf{A}^{a\dagger})_{-\nu_2} && \text{(since } (\mathbf{A}_{\nu})^{\dagger} = (\mathbf{A}^{\dagger})_{-\nu} \text{)} \\
&= \sum_{a \in A} \sum_{\nu_1, \nu_2 \in B} \alpha_{-\nu_2, -\nu_1} (\mathbf{A}_{-\nu_1}^a)^{\dagger}(\cdot) \mathbf{A}_{-\nu_2}^a && \text{(since } \{\mathbf{A}^a : a \in A\} = \{\mathbf{A}^{a\dagger} : a \in A\} \text{)} \\
&= \sum_{a \in A} \sum_{\nu_1, \nu_2 \in B} \alpha_{\nu_2, \nu_1} (\mathbf{A}_{\nu_1}^a)^{\dagger}(\cdot) \mathbf{A}_{\nu_2}^a && \text{(since } B = \text{spec}(\mathbf{H}) - \text{spec}(\mathbf{H}) = -B \text{)} \\
&= \sum_{a \in A} \sum_{\nu_1, \nu_2 \in B} \alpha_{\nu_1, \nu_2} (\mathbf{A}_{\nu_2}^a)^{\dagger}(\cdot) \mathbf{A}_{\nu_1}^a = \mathcal{T}^{\dagger}. && \text{(relabelling } \nu_1 \leftrightarrow \nu_2 \text{)} \quad \blacksquare
\end{aligned}$$

While the above representation explicitly addresses the energy basis, we note that positivity becomes obscured as the left and right energy labels ν_1, ν_2 can differ. The positivity now becomes implicit in the coefficient matrix.

Proposition II.3 (Positive semi-definite). *If the coefficients α_{ν_1, ν_2} as a matrix α is positive-semi-definite*

$$\alpha \geq 0,$$

(and thus Hermitian $\alpha_{\nu_1, \nu_2} = (\alpha_{\nu_2, \nu_1})^*$), then

$$\sum_{a \in A} \sum_{\nu_1, \nu_2 \in B} \alpha_{\nu_1, \nu_2} \left(\mathbf{A}_{\nu_1}^a(\cdot) (\mathbf{A}_{\nu_2}^a)^{\dagger} - \frac{1}{2} \{ (\mathbf{A}_{\nu_2}^a)^{\dagger} \mathbf{A}_{\nu_1}^a, \cdot \} \right) \text{ gives a Lindbladian.}$$

Positivity indeed holds for (2.2) and can be seen by the integral form of the coefficients. To conclude this section, it remains to verify that the coefficients arising from Gaussian indeed satisfy the symmetry.

Lemma II.2 (Exact “skew-symmetry” of coefficients). *For each $\omega_{\gamma}, \sigma_{\gamma}$, the coefficients $\alpha_{\nu_1, \nu_2}^{(\omega_{\gamma}, \sigma_{\gamma})}$ defined by (2.2) factorize*

$$\alpha_{\nu_1, \nu_2}^{(\omega_{\gamma}, \sigma_{\gamma})} = \frac{\sigma_{\gamma}}{2\sqrt{\sigma_E^2 + \sigma_{\gamma}^2}} \cdot \exp\left(-\frac{(\nu_1 + \nu_2 + 2\omega_{\gamma})^2}{8(\sigma_E^2 + \sigma_{\gamma}^2)}\right) \cdot \exp\left(-\frac{(\nu_1 - \nu_2)^2}{8\sigma_E^2}\right), \quad (2.3)$$

and have a certain “skew-symmetry” under negation and transpose

$$\alpha_{\nu_1, \nu_2}^{(\omega_{\gamma}, \sigma_{\gamma})} = \alpha_{-\nu_2, -\nu_1}^{(\omega_{\gamma}, \sigma_{\gamma})} e^{-\beta(\nu_1 + \nu_2)/2} \quad \text{for } \beta := \frac{2\omega_{\gamma}}{\sigma_E^2 + \sigma_{\gamma}^2}. \quad (2.4)$$

Proof. We directly calculate the Gaussian integrals in (2.2), preserving the quadratic nature of the exponents.

$$\begin{aligned}
\alpha_{\nu_1, \nu_2}^{(\omega_{\gamma}, \sigma_{\gamma})} &= \frac{1}{\sigma_E \sqrt{8\pi}} \int_{-\infty}^{\infty} \exp\left(-\frac{\omega^2}{2} \cdot \left(\frac{1}{\sigma_{\gamma}^2} + \frac{1}{\sigma_E^2}\right) - \omega \cdot \left(\frac{\omega_{\gamma}}{\sigma_{\gamma}^2} - \frac{\nu_1 + \nu_2}{2\sigma_E^2}\right) - \frac{\nu_1^2 + \nu_2^2}{4\sigma_E^2} - \frac{\omega_{\gamma}^2}{2\sigma_{\gamma}^2}\right) d\omega = \\
&= \frac{1}{\sigma_E \sqrt{8\pi}} \int_{-\infty}^{\infty} \exp\left(-\frac{\left(\omega + \left(\frac{1}{\sigma_{\gamma}^2} + \frac{1}{\sigma_E^2}\right)^{-1} \left(\frac{\omega_{\gamma}}{\sigma_{\gamma}^2} - \frac{\nu_1 + \nu_2}{2\sigma_E^2}\right)\right)^2}{2\left(\frac{1}{\sigma_{\gamma}^2} + \frac{1}{\sigma_E^2}\right)^{-1}} + \frac{\left(\frac{1}{\sigma_{\gamma}^2} + \frac{1}{\sigma_E^2}\right)^{-1} \left(\frac{\omega_{\gamma}}{\sigma_{\gamma}^2} - \frac{\nu_1 + \nu_2}{2\sigma_E^2}\right)^2}{2} - \frac{\nu_1^2 + \nu_2^2}{4\sigma_E^2} - \frac{\omega_{\gamma}^2}{2\sigma_{\gamma}^2}\right) d\omega \\
&= \frac{1}{2\sigma_E} \cdot \frac{1}{\sqrt{\frac{1}{\sigma_{\gamma}^2} + \frac{1}{\sigma_E^2}}} \exp\left(\frac{1}{2\left(\frac{1}{\sigma_{\gamma}^2} + \frac{1}{\sigma_E^2}\right)} \left(\frac{\omega_{\gamma}}{\sigma_{\gamma}^2} - \frac{\nu_1 + \nu_2}{2\sigma_E^2}\right)^2 - \frac{\nu_1^2 + \nu_2^2}{4\sigma_E^2} - \frac{\omega_{\gamma}^2}{2\sigma_{\gamma}^2}\right) && \text{(by Fact II.1)} \\
&= \frac{1}{2\sqrt{\frac{\sigma_E^2}{\sigma_{\gamma}^2} + 1}} \cdot \exp\left(-\frac{(\nu_1 + \nu_2 + 2\omega_{\gamma})^2}{8(\sigma_E^2 + \sigma_{\gamma}^2)}\right) \cdot \exp\left(-\frac{(\nu_1 - \nu_2)^2}{8\sigma_E^2}\right) && \text{(since } 2(\nu_1^2 + \nu_2^2) = (\nu_1 + \nu_2)^2 + (\nu_1 - \nu_2)^2 \text{)} \\
&= \alpha_{-\nu_2, -\nu_1}^{(\omega_{\gamma}, \sigma_{\gamma})} e^{-\beta(\nu_1 + \nu_2)/2}. && \text{(due to our choice of } \beta \text{)} \quad \blacksquare
\end{aligned}$$

We see that we may tune the parameters to match a desirable exponent β . Remarkably, the width σ_E can be finite (i.e., do not scale linearly the precision $\frac{1}{\epsilon}$ like in metrology) while retaining exact detailed balance; a reasonable choice is, e.g.,

$$\omega_\gamma = \sigma_E = \sigma_\gamma = \frac{1}{\beta}.$$

This will imply that the algorithmic cost for implementing the Gaussian weighted operator Fourier Transform will only need to scale with β (and polylogarithmically with the precision due to discretization and truncation error)! However, the Gaussian transition weight comes with the price of a narrower band of transitions peaked at $\omega_\gamma \pm \mathcal{O}(\sigma_\gamma)$, which might result in a substantially increased mixing time compared to, e.g., Metropolis weight $\gamma(\omega) = \min(1, e^{-\beta\omega})$; we will revisit this issue by taking *linear combinations* of Gaussians at [Section II C 3](#) since all our calculation are linear. For clarity, we first focus on the Gaussian weights.

Why does Gaussian interplay so perfectly with quantum detailed balance? In [Section D](#), we attempted to derive Gaussian from the first principle. Indeed, Gaussians are very natural if we impose several conditions on the function.

2. Adding the unitary term

Now that the “transition” part satisfies the detailed balance condition exactly, we proceed to complete the Lindbladian by adding the “decay” part and the “coherent” part. The decay part is fixed by trace-preserving; [Lemma II.1](#) then uniquely prescribes the required coherent term, which we display as follows in the frequency domain. The explicit form will be useful for implementation.

Corollary II.2 (An exactly detailed-balanced Lindbladian with Gaussian filtering). *The Lindbladian*

$$\mathcal{L}[\cdot] := -i \sum_{\nu \in B} [B_\nu, \cdot] + \sum_{a \in A} \sum_{\nu_1, \nu_2 \in B} \alpha_{\nu_1, \nu_2} \left(\mathbf{A}_{\nu_1}^a (\cdot) (\mathbf{A}_{\nu_2}^a)^\dagger - \frac{1}{2} \{ (\mathbf{A}_{\nu_2}^a)^\dagger \mathbf{A}_{\nu_1}^a, \cdot \} \right)$$

corresponding to a self-adjoint set of jump operators $\{\mathbf{A}^a : a \in A\} = \{\mathbf{A}^{a\dagger} : a \in A\}$, parametrized by coefficients $\alpha_{\nu_1, \nu_2} \in \mathbb{C}$ satisfying $\alpha_{\nu_1, \nu_2}^* = \alpha_{\nu_2, \nu_1}$ and

$$\alpha_{\nu_1, \nu_2} e^{\frac{\beta(\nu_1 + \nu_2)}{2}} = \alpha_{-\nu_2, -\nu_1},$$

and amended by the coherent terms

$$B_\nu := \sum_{a \in A} \sum_{\substack{\nu_1 - \nu_2 = \nu \\ \nu_1, \nu_2 \in B}} \underbrace{\frac{\tanh(-\beta(\nu_1 - \nu_2)/4)}{2i}}_{\hat{f}(\nu_1, \nu_2) :=} \alpha_{\nu_1, \nu_2} (\mathbf{A}_{\nu_2}^a)^\dagger \mathbf{A}_{\nu_1}^a \quad (2.5)$$

satisfies ρ_β -detailed balance.

Proof. Apply [Lemma II.1](#). Note that the operator

$$(\mathbf{A}_{\nu_2}^a)^\dagger \mathbf{A}_{\nu_1}^a = \sum_{E_i - E_j = \nu_1, E_i - E_k = \nu_2} P_{E_k} \mathbf{A}^{a\dagger} P_{E_i} \mathbf{A}^a P_{E_j}$$

must have the energy difference contained in the set of Bohr frequencies B

$$\begin{aligned} \nu_1 - \nu_2 &= E_i - E_j - (E_i - E_k) \quad \text{for some } E_i, E_j, E_k \in \text{Spec}(\mathbf{H}) \\ &= E_k - E_j \in B. \end{aligned}$$

■

The above corollary essentially leads to [Theorem I.1](#) but is written in the Bohr-frequency decomposition.

Proof of Theorem I.1. Combine [Proposition II.3](#), [Lemma II.2](#), [Proposition II.1](#), and [Corollary II.2](#) to conclude the proof. ■

3. Linear combination of Gaussians

Can we go beyond Gaussians? As we discussed, the Gaussians have a narrower band of transitions; it would be desirable to lift this restriction to accelerate the mixing time. In this section, we give a family of filters by exploiting the freedom to tune the Gaussian parameters $(\omega_\gamma, \sigma_E, \sigma_\gamma)$ and taking a linear combination of Gaussians.

Corollary II.3 (Linear combination of Gaussians). *Fix σ_E and $g \in \ell_1(\mathbb{R})$ and set $\gamma^{(g)}(\omega) := \int_{\frac{\beta\sigma_E^2}{2}}^{\infty} g(x) e^{-\frac{(\omega+x)^2}{4x/\beta - 2\sigma_E^2}} dx$.*¹⁰ Then, analogous to (2.2), the coefficients as a linear combination over integration variable x

$$\alpha_{\nu_1, \nu_2}^{(g)} := \int_{\frac{\beta\sigma_E^2}{2}}^{\infty} g(x) \alpha_{\nu_1, \nu_2}^{(\omega_\gamma, \sigma_\gamma)} dx \quad \text{for } (\omega_\gamma(x), \sigma_\gamma(x)) = (x, \sqrt{2x/\beta - \sigma_E^2}), \quad (2.6)$$

satisfy the symmetries $\alpha_{\nu_1, \nu_2}^{(g)*} = \alpha_{\nu_2, \nu_1}^{(g)}$ and $\alpha_{\nu_1, \nu_2}^{(g)} = \alpha_{-\nu_1, -\nu_2}^{(g)} e^{-\beta(\nu_1 + \nu_2)/2}$ for each $\nu_1, \nu_2 \in \mathbb{R}$. If $g(x) \geq 0$ for each x , then we also have that $\alpha^{(g)} \geq 0$, however, this is not a necessary condition.

Proof. Recall the meaning of the superscripts $\alpha_{\nu_1, \nu_2}^{(\omega_\gamma, \sigma_\gamma)}$. The proof is merely the linearity of symmetries and that convex combination preserves the cone of positive semidefinite matrices. \blacksquare

To widen the band of transitions, a natural choice is to weigh each Gaussian $e^{-\frac{(\omega+\omega_\gamma)^2}{2\sigma_\gamma^2}}$ with its inverse ℓ_1 -weight. Surprisingly, this leads to filters that resemble the Metropolis and Glauber weights; while other choices are plausible, we spell out the calculation for this as a natural representative.

Proposition II.4 (Metropolis and Glauber-like filters). *Setting $g(\omega_\gamma) = \frac{1}{\sqrt{2\pi}\sigma_\gamma} = \frac{1}{\sqrt{2\pi(\frac{2\omega_\gamma}{\beta} - \sigma_E^2)}}$ yields*

$$\begin{aligned} \gamma_{\sigma_E}^{(s)}(\omega) &:= \int_{\frac{\beta\sigma_E^2}{2}}^{\frac{\beta\sigma_E^2}{2} + \frac{s^2}{\beta}} \frac{e^{-\frac{(\omega+x)^2}{4x/\beta - 2\sigma_E^2}}}{\sqrt{2\pi(2x/\beta - \sigma_E^2)}} dx \\ &= e^{-\beta \max\left(\omega + \frac{\beta\sigma_E^2}{2}, 0\right)} \cdot \underbrace{\frac{1}{2} \left[\left(\operatorname{erf}\left(\frac{s}{2} - \frac{\beta}{s} \left| \omega + \frac{\beta\sigma_E^2}{2} \right| \right) + 1 \right) + e^{\beta \left| \omega + \frac{\beta\sigma_E^2}{2} \right|} \left(\operatorname{erf}\left(\frac{s}{2} + \frac{\beta}{s} \left| \omega + \frac{\beta\sigma_E^2}{2} \right| \right) - 1 \right) \right]}_{\leq 1}, \end{aligned} \quad (2.7)$$

which, in the $s \rightarrow \infty$ limit, coincides with the Metropolis weight shifted by $\frac{\beta\sigma_E^2}{2}$:

$$\gamma_{\sigma_E}^{(\infty)}(\omega) = e^{-\beta \max\left(\omega + \frac{\beta\sigma_E^2}{2}, 0\right)}. \quad (2.8)$$

Restricting the above $g(\omega_\gamma)$ to the interval $\omega_\gamma \in \left(\frac{3\beta\sigma_E^2}{2}, \infty\right)$ results in the following smooth variant of (2.8)

$$\tilde{\gamma}_{\sigma_E}^{(\infty)}(\omega) = e^{-\beta \max\left(\omega + \frac{\beta\sigma_E^2}{2}, 0\right)} \cdot \underbrace{\frac{1}{2} \left[\operatorname{erfc}\left(\frac{1}{\sigma_E} \left(\frac{\beta\sigma_E^2}{2} - \left| \omega + \frac{\beta\sigma_E^2}{2} \right| \right)\right) + e^{\beta \left| \omega + \frac{\beta\sigma_E^2}{2} \right|} \operatorname{erfc}\left(\frac{1}{\sigma_E} \left(\frac{\beta\sigma_E^2}{2} + \left| \omega + \frac{\beta\sigma_E^2}{2} \right| \right)\right) \right]}_{\leq 1}, \quad (2.9)$$

which resembles the Glauber filter also shifted by $\frac{\beta\sigma_E^2}{2}$ (Figure 3).

Proof. We directly found the above by Mathematica; see Section F for the code. \blacksquare

III. ALGORITHMS

This section presents efficient quantum algorithms for simulating the advertised Lindbladian and the associated parent Hamiltonian. The former mainly builds on black-box Lindbladian simulation algorithms [CW17, CL17, LW22], more precisely their improved variant described in [CKBG23, Theorem III.2] whose complexity boils

¹⁰ Note that in principle we could also vary σ_E , but that would complicate both the analysis and the implementation due to the required adjustments to the parameters of the performed operator Fourier Transform.

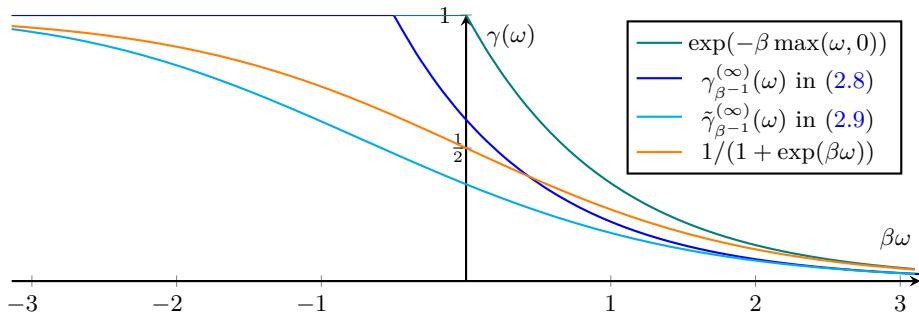


Figure 3. A plot of the filter functions $\gamma(\omega)$ for Metropolis, Glauber and our filters arising from Gaussian linear combination (2.8)-(2.9) (with $\sigma_E = \frac{1}{\beta}$).

down to constructing block encoding for the Lindblad operators (Definition III.1); the latter merely requires block-encoding the parent Hamiltonian, which feeds into quantum simulated annealing (see [CKBG23, Appendix G] for a modern discussion) to prepare the purified Gibbs state.

Thus, the main algorithmic contribution is to assemble the block encodings associated with our synthetic Lindbladian (1.1) and our parent Hamiltonians (Theorem I.3). The frequency domain representation (Section II), which is natural in the context of analyzing quantum detailed balance, is less instructive for algorithmic implementation. Indeed, addressing the exact energy eigenstates (or the exact Bohr frequencies) is generally inefficient. Nevertheless, the algorithmic task becomes straightforward in the time domain representation. Indeed, our Lindbladian can be expressed in terms of weighted time integrals $\int(\cdot)dt$ of some rapidly decaying functions; a standard Linear-Combination-of-Unitary argument (under suitable discretization) leads to the algorithmic complexity in terms of controlled Hamiltonian simulation time.

For the Lindbladian (1.1), block-encodings for the dissipative part are already constructed in [CKBG23, Section III.B]. Thus, it remains to construct the coherent term; for the parent Hamiltonian, we will need to construct block encodings from scratch, but the manipulations are analogous. In the following sections, we first present the time-domain expressions (Section III A-III B), which immediately yield the corresponding block encodings (Section III C) and the overall complexities (Section III D-III E).

A. Time-domain representation of our Lindbladians

Applying a two-dimensional Fourier Transform for the coherent term (2.5) leads to the following time-domain representation where LCU techniques are naturally applicable. See Section A 1 for the calculations.

Corollary III.1 (Coherent term for the Gaussian case). *For each $\beta > 0$ and parameters $\sigma_E = \sigma_\gamma = \omega_\gamma = \frac{1}{\beta}$, the coherent term \mathbf{B} (2.5) corresponding to the Gaussian weight $\gamma(\omega) = \exp\left(-\frac{(\beta\omega+1)^2}{2}\right)$ can be written as*

$$\mathbf{B} := \sum_{a \in A} \int_{-\infty}^{\infty} b_1(t) e^{-i\beta \mathbf{H}t} \left(\int_{-\infty}^{\infty} b_2(t') \mathbf{A}^{a\dagger}(\beta t') \mathbf{A}^a(-\beta t') dt' \right) e^{i\beta \mathbf{H}t} dt, \quad (3.1)$$

where

$$b_1(t) := 2\sqrt{\pi} e^{\frac{1}{8}} \left(\frac{1}{\cosh(2\pi t)} *_t \sin(-t) \exp(-2t^2) \right) \quad \text{such that } \|b_1\|_1 < 1 \quad (3.2)$$

$$b_2(t) := \frac{1}{2\pi} \sqrt{\frac{1}{\pi}} \exp(-4t^2 - 2it) \quad \text{such that } \|b_2\|_1 < \frac{1}{16}. \quad (3.3)$$

Indeed, we can verify that \mathbf{B} is Hermitian by

$$\begin{aligned} \mathbf{B}^\dagger &= \sum_{a \in A} \int_{-\infty}^{\infty} b_1^*(t) e^{-i\beta \mathbf{H}t} \left(\int_{-\infty}^{\infty} b_2^*(t') \mathbf{A}^{a\dagger}(-\beta t') \mathbf{A}^a(\beta t') dt' \right) e^{i\beta \mathbf{H}t} dt \\ &= \sum_{a \in A} \int_{-\infty}^{\infty} b_1(t) e^{-i\beta \mathbf{H}t} \left(\int_{-\infty}^{\infty} b_2(-t') \mathbf{A}^{a\dagger}(-\beta t') \mathbf{A}^a(\beta t') dt' \right) e^{i\beta \mathbf{H}t} dt \quad (\text{By } b_1^*(t) = b_1(t) \text{ and } b_2^*(t) = b_2(-t)) \\ &= \sum_{a \in A} \int_{-\infty}^{\infty} b_1(t) e^{-i\beta \mathbf{H}t} \left(\int_{-\infty}^{\infty} b_2(t') \mathbf{A}^{a\dagger}(\beta t') \mathbf{A}^a(-\beta t') dt' \right) e^{i\beta \mathbf{H}t} dt = \mathbf{B}. \quad (\text{Change of variable } t' \rightarrow -t') \end{aligned}$$

The explicit weights corresponding to Metropolis weights are slightly more cumbersome due to taming a mild (logarithmic) singularity. We can also verify that $\mathbf{B}^{M,\eta}$ is Hermitian by $b_2^{M,\eta*}(t) = b_2^{M,\eta}(-t)$.

Corollary III.2 (Approximate coherent term for the Metropolis-like weight). *If $\sigma_E = \frac{1}{\beta}$, then the coherent term \mathbf{B}^M corresponding to the Metropolis-like weight $\gamma^M(\omega) = \exp\left(-\beta \max\left(\omega + \frac{1}{2\beta}, 0\right)\right)$ satisfies*

$$\|\mathbf{B}^M - \mathbf{B}^{M,\eta}\| \leq \left\| \sum_{a \in A} \mathbf{A}^{a\dagger} \mathbf{A}^a \right\| \min\left(\frac{\eta\beta\|\mathbf{H}\|}{\sqrt{2\pi}}, \mathcal{O}((\eta\beta\|\mathbf{H}\|)^3)\right), \quad (3.4)$$

where

$$\mathbf{B}^{M,\eta} := \sum_{a \in A} \int_{-\infty}^{\infty} b_1(t) e^{-i\beta \mathbf{H}t} \left(\int_{-\infty}^{\infty} b_2^{M,\eta}(t') \mathbf{A}^{a\dagger}(\beta t') \mathbf{A}^a(-\beta t') dt' + \frac{1}{16\sqrt{2\pi}} \mathbf{A}^{a\dagger} \mathbf{A}^a \right) e^{i\beta \mathbf{H}t} dt, \quad (3.5)$$

with $b_1(t)$ as in (3.2), and

$$b_2^{M,\eta}(t) := \frac{1}{4\sqrt{2\pi}} \frac{\exp(-2t^2 - it) + \mathbb{1}(|t| \leq \eta) i(2t + i)}{t(2t + i)} \quad \text{such that} \quad \|b_2^{M,\eta}\|_1 < \frac{1}{5} + \frac{1}{2\sqrt{2\pi}} \ln(1/\eta). \quad (3.6)$$

Further, if $[\sum_{a \in A} \mathbf{A}^{a\dagger} \mathbf{A}^a, \mathbf{H}] = 0$, we can drop the second term in (3.5) after the integral in t' since $\int_{-\infty}^{\infty} b_1(t) = 0$.

See Section B for the proof. After suitable truncation, this merely incurs a *logarithmic* overhead ($\sim \log(\beta\|\mathbf{H}\|/\epsilon)$) to the algorithmic cost for an ϵ -approximation due to subnormalization $\frac{1}{\|b_2^{M,\eta}\|_1}$.

B. Time-domain representation of our parent Hamiltonians

Recall that the central mathematical object for coherent Gibbs sampling is the *discriminant* (i.e., the Lindbladian under a similarity transformation)

$$\mathcal{H}(\rho, \mathcal{L}) := \rho^{-1/4} \mathcal{L}[\rho^{1/4} \cdot \rho^{1/4}] \rho^{-1/4}$$

This amounts to a mild calculation that transfers the heavy lifting done already in the Lindbladian context. One adaption for the coherent algorithm is that the fundamental object is not a superoperator but an operator on a doubled Hilbert space. Formally, we define the *vectorization* of a super-operator by

$$\mathcal{C}[\cdot] = \sum_j \alpha_j \mathbf{A}_j[\cdot] \mathbf{B}_j \rightarrow \mathbf{C} = \sum_j \alpha_j \mathbf{A}_j \otimes \mathbf{B}_j^T \quad (\text{vectorization})$$

where \mathbf{B}_j^T denotes the transpose of the matrix \mathbf{B}_j in the computational basis $|i\rangle$. We use curly fonts \mathcal{C} for super-operators and bold fonts \mathbf{C} for the vectorized super-operators (which is, a matrix). For a matrix ρ , let us denote its vectorized version by

$$|\rho\rangle := (I \otimes T^{-1})\rho \quad \text{where} \quad T|i\rangle = \langle i| \quad \text{for each} \quad |i\rangle.$$

In the time domain, our parent Hamiltonian takes the following form (see Section A 2 for the calculations)

$$\mathcal{H}_\beta = \underbrace{\sum_{a \in A} \int_{-\infty}^{\infty} \int_{-\infty}^{\infty} h_-(t_-) h_+(t_+) \cdot \mathbf{A}^a(t_+ - t_-) \otimes \mathbf{A}^a(-t_- - t_+)^T dt_+ dt_-}_{\text{transition part}} + \underbrace{\frac{1}{2}(\mathbf{N} \otimes \mathbf{I} + \mathbf{I} \otimes \mathbf{N}^*)}_{\text{decay and coherent part}}.$$

Compared with the Lindbladian case, the first term is essentially the transition part under a similarity transformation, and the second term combines the decay and coherent part. Here, we do not care about complete positivity or trace-preserving but merely Hermiticity.

1. The transition part

The transition parts for both Gaussian and Metropolis weights are as follows.

Corollary III.3 (The transition part for Gaussian weights). *For the Gaussian weight $\gamma(\omega) = \exp\left(-\frac{(\beta\omega+1)^2}{2}\right)$ with $\omega_\gamma = \sigma_E = \sigma_\gamma = 1/\beta$, the discriminant \mathcal{H}_β is described in the time domain by*

$$h_+(t) = \frac{1}{\beta} e^{-1/4} \exp\left(-\frac{4t^2}{\beta^2}\right) \quad \text{and} \quad h_-(t) = \frac{1}{\pi\beta} \exp\left(-\frac{2t^2}{\beta^2}\right) \quad \text{such that} \quad \|h_-\|_1, \|h_+\|_1 \leq 1. \quad (3.7)$$

Corollary III.4 (The transition part for Metropolis weights). For $\sigma_E = \frac{1}{\beta}$, the Metropolis-like weight $\gamma^M(\omega) = \exp\left(-\beta \max\left(\omega + \frac{1}{2\beta}, 0\right)\right)$ yields \mathcal{H}_β described in the time domain by the same $h_-(t)$ as in Eq. (3.7) and by

$$h_+(t) = \frac{e^{-1/8}}{\beta} \frac{e^{-2t^2/\beta^2}}{4\sqrt{2\pi}\left(\frac{t^2}{\beta^2} + \frac{1}{16}\right)} \quad \text{such that} \quad \|h_+(t)\|_1 \leq 1.$$

2. The \mathbf{N} -term

The time-domain presentation of the \mathbf{N} term is as follows.

Corollary III.5 (\mathbf{N} term for Gaussian weights). For each β , the Gaussian weight $\gamma(\omega) = \exp\left(-\frac{(\beta\omega+1)^2}{2}\right)$ with $\sigma_E = \sigma_\gamma = \omega_\gamma = \frac{1}{\beta}$ corresponds to the discriminant where

$$\mathbf{N} = \sum_{a \in A} \int_{-\infty}^{\infty} n_1(t) e^{-i\beta \mathbf{H}t} \left(\int_{-\infty}^{\infty} n_2(t') \mathbf{A}^{a\dagger}(\beta t') \mathbf{A}^a(-\beta t') dt' \right) e^{i\beta \mathbf{H}t} dt,$$

where

$$\begin{aligned} n_1(t) &:= \frac{1}{4} \cdot 2\sqrt{\pi} \left(\frac{1}{\cosh(2\pi t)} *_t \exp(-2t^2) \right) & \text{such that} \quad \|n_1\|_1 = \frac{\pi}{4\sqrt{2}} < 1 \\ n_2(t) &:= 4 \cdot 2 \cdot \frac{1}{2\pi} \sqrt{\frac{1}{\pi}} \exp(-4t^2 - 2it) = 8 \cdot b_2(t) & \text{such that} \quad \|n_2\|_1 < \frac{1}{2} \end{aligned} \quad (3.8)$$

with b_2 as in (3.3).

Corollary III.6 (\mathbf{N} term for Metropolis weights). If $\sigma_E = \frac{1}{\beta}$, then the Metropolis-like weight $\gamma^M(\omega) = \exp\left(-\beta \max\left(\omega + \frac{1}{2\beta}, 0\right)\right)$ corresponds to the discriminant where \mathbf{N}^M satisfies

$$\|\mathbf{N}^M - \mathbf{N}^{M,\eta}\| \leq \sum_{a \in A} \|\mathbf{A}^{a\dagger} \mathbf{A}^a\| \min\left(\frac{\eta\beta\|\mathbf{H}\|}{\sqrt{2\pi}}, \mathcal{O}((\eta\beta\|\mathbf{H}\|)^3)\right),$$

where

$$\mathbf{N}^{M,\eta} := \sum_{a \in A} \int_{-\infty}^{\infty} n_1(t) e^{-i\beta \mathbf{H}t} \left(\int_{-\infty}^{\infty} n_2^{M,\eta}(t') \mathbf{A}^{a\dagger}(\beta t') \mathbf{A}^a(-\beta t') dt' + \frac{1}{16\sqrt{2\pi}} \mathbf{A}^{a\dagger} \mathbf{A}^a \right) e^{i\beta \mathbf{H}t} dt,$$

with $n_1(t)$ as in (3.8), and $n_2^{M,\eta} = b_2^{M,\eta}$ as in (3.6).

In the above cases, we can verify that \mathbf{N} is Hermitian by $n_1^*(t) = n_1(t)$ and $n_2^*(t) = n_2(-t)$. For \mathbf{N}^M , we also use that $(\mathbf{A}^{a\dagger} \mathbf{A}^a)^\dagger = \mathbf{A}^{a\dagger} \mathbf{A}^a$.

C. Block-encodings

Our simulation algorithm extensively uses block encodings that are largely borrowed from [CKBG23]. This section aims to instantiate them to state the theorems appropriately, and the curious reader may refer to [CKBG23, Section III.B].

Definition III.1 (Block-encoding for Lindbladian). Given a purely irreversible Lindbladian

$$\mathcal{L}[\rho] := \sum_{j \in J} \left(\mathbf{L}_j \rho \mathbf{L}_j^\dagger - \frac{1}{2} \mathbf{L}_j^\dagger \mathbf{L}_j \rho - \frac{1}{2} \rho \mathbf{L}_j^\dagger \mathbf{L}_j \right),$$

we say that a unitary \mathbf{U} is a block-encoding for Lindblad operators $\{\mathbf{L}_j\}_{j \in J}$ if¹¹

$$\langle\langle 0^b | \otimes \mathbf{I} \rangle\rangle \cdot \mathbf{U} \cdot (|0^c\rangle \otimes \mathbf{I}) = \sum_{j \in J} |j\rangle \otimes \mathbf{L}_j \quad \text{for} \quad b \leq c \in \mathbb{Z}^+.$$

¹¹ In the first register, we could use any orthonormal basis. Sticking to computational basis elements $|j\rangle$ is just for ease of presentation. Intuitively, one can think about b as the number of ancilla qubits used for implementing the Lindblad operators \mathbf{L}_j , while typically $a - b \approx \log |J|$.

- Block-encoding V_{jump} of the jump operators A^a in the form of [Definition III.1](#):

$$(\langle 0^b | \otimes I_a \otimes I_{sys}) \cdot V_{jump} \cdot (|0^c\rangle \otimes I_{sys}) = \sum_{a \in A} |a\rangle \otimes A^a.$$

To implement the discriminant, we also assume access to a block-encoding V_{jumpT} for the partial transpose $\sum_{a \in A} |a\rangle \otimes (A^a)^T$.

- Quantum Fourier Transform

$$QFT_N : |\bar{t}\rangle \rightarrow \frac{1}{\sqrt{N}} \sum_{\bar{\omega} \in S_{\omega_0}} e^{-i\bar{\omega}\bar{t}} |\bar{\omega}\rangle.$$

We use “bar” to denote variables taking discrete values. In particular, the Fourier frequencies $\bar{\omega}$ and times \bar{t} are integer multiples of ω_0 and t_0 respectively such that

$$\begin{aligned} \omega_0 t_0 &= \frac{2\pi}{N}, \quad \text{and} \quad S^{[N]} := \left\{ -\lfloor (N-1)/2 \rfloor, \dots, -1, 0, 1, \dots, \lfloor (N-1)/2 \rfloor \right\}, \\ \text{and} \quad S_{\omega_0}^{[N]} &:= \omega_0 \cdot S^{[N]}, \quad S_{t_0}^{[N]} := t_0 \cdot S^{[N]}. \end{aligned}$$

- Controlled Hamiltonian simulation

$$\sum_{\bar{t} \in S_{t_0}} |\bar{t}\rangle \langle \bar{t}| \otimes e^{\pm i\bar{t}\mathbf{H}}.$$

- State preparation oracles for the Fourier Transform weights, acting on the frequency register

$$Prep_f : |\bar{0}\rangle \rightarrow |f\rangle.$$

- Controlled filter for the Boltzmann factors acting on the frequency register and the Boltzmann weight register

$$\mathbf{W} := \sum_{\bar{\omega} \in S_{\omega_0}} \mathbf{Y}_{1-\gamma(\bar{\omega})} \otimes |\bar{\omega}\rangle \langle \bar{\omega}| \quad \text{where} \quad 0 \leq \gamma(\bar{\omega}) \leq 1 \quad \text{and} \quad \gamma(\bar{\omega}) = \gamma(-\bar{\omega}) e^{-\beta \bar{\omega}}.$$

- Single qubit Pauli-Y rotations

$$\mathbf{Y}_\theta := \begin{pmatrix} \sqrt{1-\theta} & -\sqrt{\theta} \\ \sqrt{\theta} & \sqrt{1-\theta} \end{pmatrix}.$$

- Reflection on b -qubits

$$\mathbf{R}_b := 2|0^b\rangle \langle 0^b| - I_b$$

To feed into the black-box Lindbladian simulation algorithm [[CKBG23](#), Theorem III.2], we need block-encodings for the dissipative part and the coherent term; for the coherent Gibbs sampler, we need block-encoding for the discriminant \mathcal{H}_β , which we obtain by adding the transition part and the \mathbf{N} part.

Proposition III.1 (Block-encoding for the coherent term). *Suppose $\|f_-\|_1, \|f_+\|_1 \leq 1$. Then, there is a block-encoding for*

$$\sum_{\bar{t}_- \in S_{t_0}} f_-(\bar{t}_-) e^{-i\mathbf{H}\bar{t}_-} \left(\sum_{\bar{t}_+ \in S_{t_0}} f_+(\bar{t}_+) \sum_{a \in A} A^{a\dagger}(\bar{t}_+) A^a(-\bar{t}_+) \right) e^{i\mathbf{H}\bar{t}_-}$$

using constant calls to controlled Hamiltonian simulation, V_{jump} , $prep_{\sqrt{|f_+|}}$, $prep_{f_+/\sqrt{|f_+|}}$, $prep_{\sqrt{|f_+|}}$, $prep_{f_+/\sqrt{|f_+|}}$ and their adjoints.

The identical statement applies to the \mathbf{N} term by replacing $f_\pm \rightarrow n_\pm$.

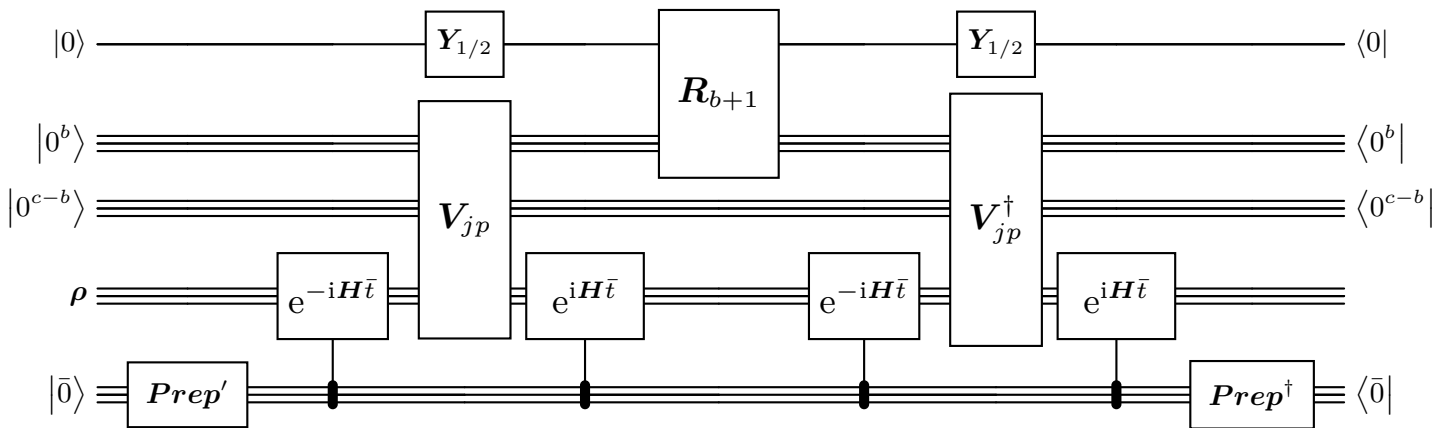


Figure 4. Circuit for block-encoding (3.9). The gate prep is a shorthand for $\mathit{Prep}_{\sqrt{|f_+|}}$ and prep' for $\mathit{Prep}_{f_+/\sqrt{|f_+|}}$.

Proof. It suffices to construct

$$\sum_{\bar{t}_+ \in S_{t_0}} f_+(\bar{t}_+) \sum_{a \in A} A^{a\dagger}(\bar{t}_+) A^a(-\bar{t}_+) \quad (3.9)$$

and then apply the operator Fourier Transform. When there is only one jump ($|A| = 1$), this merely uses iterations of LCU and controlled Hamiltonian simulation. When a block-encoding gives the set of jumps, see Figure 4. To see that this yields the desired expression, observe that

$$Y_{1/2}|0\rangle = |+\rangle \quad \text{and} \quad Y_{1/2}^\dagger|0\rangle = |-\rangle.$$

Thus, the expression remains the same if we drop the $-I_{b+1}$ term in R_{b+1} . \blacksquare

Proposition III.2 (Bilinear). *Suppose $\|h_-\|_1 = \|h_+\|_1 = 1$. Then, there is a block-encoding for*

$$\sum_{\bar{t}_- \in S_{t_0}} \sum_{\bar{t}_+ \in S_{t_0}} \sum_{a \in A} h_-(\bar{t}_-) h_+(\bar{t}_+) \cdot A^a(\bar{t}_+ - \bar{t}_-) \otimes A^a(-\bar{t}_- - \bar{t}_+)^T$$

using constant calls to controlled Hamiltonian simulation, $V_{j\text{ump}}$, $V_{j\text{ump}}^T$, $\mathit{prep}_{\sqrt{|h_+|}}$, $\mathit{prep}_{h_+/\sqrt{|h_+|}}$, $\mathit{prep}_{\sqrt{|h_+|}}$, $\mathit{prep}_{h_+/\sqrt{|h_+|}}$ and their adjoints.

Proof. The proof is a modification of Proposition III.1 by replacing $V_{j\text{ump}}^\dagger$ with $V_{j\text{ump}}^T$ and duplicating the system register. \blacksquare

D. Proving Theorem I.2: complexity for Lindbladian simulation

We now combine the block-encoding to give the overall cost of Gibbs sampling. We can implement the controlled time-evolution up to a truncation time as long as the profiles f_+ , f_- are well-concentrated and smooth in the time domain (and that the Fourier Transforms are well-defined), which is the case since the frequency profiles \hat{f}_+ , \hat{f}_- are smooth and concentrated Corollary III.1-Proposition B.1. Also, the following results all require discretization of the time integrals, which is fortunately handled by [CKBG23, Appendix C]; this sets the required size of the Fourier Transform register, which uses polylogarithmically many qubits.

Proof of Theorem I.2. Use the black-box Lindbladian simulation algorithm [CKBG23, Theorem III.2] for block-encoding for the coherent term (Proposition III.1) and the dissipative part [CKBG23, Section III.B.1]. For the Metropolis weight, a logarithmic overhead is incurred for taming the mild singularity in the b_2^M ; especially, \mathbf{B} is subnormalized by $\|b_2^M\|_1^{-1} = 1/\mathcal{O}(\log(\beta\|H\|/\epsilon))$ to fit an approximation of \mathbf{B} into a unitary block encoding. \blacksquare

E. Proving Theorem I.3: complexity for the discriminant

We may now construct the advertised block encoding for the discriminant. The N term is analogous to the coherent term (Proposition III.1).

Proof of Theorem I.3. Add the block encodings for the transition part (from Proposition III.2), $\mathbf{N} \otimes \mathbf{I}$, and $\mathbf{I} \otimes \mathbf{N}$ (from Proposition III.1), up to mild subnormalization. Again, the Metropolis case incurs an additional logarithmic factor. ■

Note that we do not implement $\mathbf{I} + \mathcal{H}_\beta$ (as in [CKBG23, Proposition III.5]) but rather \mathcal{H}_β itself; implementing the former would allow us to obtain a quadratic speedup on the discriminant gap, which we current do not have.

IV. DISCUSSION

We have constructed the quantum analog of the classical Monte Carlo algorithms with desirable features. We highlight potential future directions as listed.

- **Quantum simulation applications.** A key factor in industrial quantum simulation applications [CNAA+20, vBLH+21, LBG+21] is effective quantum algorithms for low-energy states. Our algorithm can be employed for any Hamiltonian *without* substantial variational parameters or a case-by-case trial state or adiabatic path. While the mixing time can vary widely, the fact that physically relevant states (molecules or materials) *exist* in Nature suggests a reasonable mixing time in practice. Regarding practical gate complexities, the locality of our algorithm for lattice Hamiltonian may be favorable as we merely need to simulate a $\tilde{\mathcal{O}}(\beta)$ -radius Hamiltonian patch localized around each jump \mathbf{A}^a .
- **Locality and complexity of quantum Gibbs state.** Our algorithm opens new angles on the locality and complexity of Gibbs states (such as the decay of correlation, quantum conditional mutual information, recovery channels, and quantum belief propagation). In particular, the combination of localized jumps and exact detailed balance enables the rigorous study of convergence [KB16, CRSF21] for noncommuting lattice Hamiltonians. Rapid mixing also directly implies the circuit complexity of the purification (Appendix C) through the Lindbladian gap, giving a dynamic perspective on the area law of entanglement [Has07].
- **New open-system physics.** Just as quantum computing lacks a go-to Monte Carlo algorithm, open system physics lacks a simple, universal Lindbladian that succinctly captures open system thermodynamics. Our algorithm qualifies due to its elegant properties. For example, our Lindbladian enables a precise definition of *dynamical thermal phase transitions* in terms of mixing time that may contrast with static thermal phase transitions. Related concepts include metastable states, the energy landscape, *quantum spin glass*, and self-correcting quantum memories, whose precise formulation for noncommuting Hamiltonian has also been lacking.
- **A new algorithmic subroutine.** Classical MCMC algorithms have been widely employed to solve other problems beyond physical simulation, and we may expect the same for our algorithm. A natural example is optimization problems (e.g., constraint satisfaction problems and modern optimization problems), whether applying to classical Hamiltonian (in a setting similar to Quantum Approximate Optimization Algorithms (QAOA) [FGG14]) or quantum Hamiltonians. Another application is Quantum Semidefinite Program Solvers [BS17, vAGGdW20], where Quantum Gibbs state preparation is routinely invoked.
- **Comparison with existing algorithms.** With a new algorithm at hand, we expect fruitful comparison with existing (quantum or classical) algorithms such as the adiabatic algorithm [FGGS00], phase estimation with trial states, tensor network, Quantum Monte Carlo, etc. In particular, understanding the distinction from classical algorithms could either inspire better classical algorithms or expose potential sources of quantum advantage in quantum simulation (e.g., the sign problem or difficulty in contracting PEPS).
- **Numerical studies.** As the complement to theory, the explicit form of our Lindbladian also enables direct numerical studies regarding the above notions, e.g., the scaling of mixing time for thermal state or ground states, dynamic phase transitions, and noncommuting quantum memories, and the interplay with tensor networks.

To conclude, given the celebrated theoretical and empirical triumph of Markov chain Monte Carlo methods and its successors over the past 70 years, we argue that this work should serve similar roles in quantum computing. Especially given the current skepticism on the practical applicability of quantum computers, our new algorithms bring hope to the community by initiating a new wave of directions covering theory, experiment, numerics, and application.

ACKNOWLEDGMENTS

We thank Jonathan Moussa for raising the question of whether exact detailed balance is possible and pointing us to his related work [Mou19] after the precursor of this work [CKBG23] became public; at that time, we thought that exact detailed balance is incompatible with the energy-time uncertainty principle. We also thank

Aaron J. Friedman, Jinkang Guo, Oliver Hart, and Andrew Lucas for collaborations on related topics and Alvaro Alhambra, Anurag Anshu, Simon Apers, Mario Berta, Fernando Brandao, Angela Capel, Garnet Chan, ChatGPT-4, Alex Dalzell, Zhiyan Ding, Steve Flammia, Hsin-Yuan (Robert) Huang, Lin Lin, Yunchao Liu, Sam McArdle, Mehdi Soleimanifar, Frederik Nathan, Umesh Vazirani, and Tong Yu for helpful discussions. CFC was supported through an internship of the AWS Center for Quantum Computing. AG acknowledges funding from the AWS Center for Quantum Computing.

-
- [Ali76] Robert Alicki. [On the detailed balance condition for non-hamiltonian systems](#). *Reports on Mathematical Physics*, 10:249–258, 1976. [35](#)
- [vAGGdW20] Joran van Apeldoorn, András Gilyén, Sander Gribling, and Ronald de Wolf. [Quantum SDP-solvers: Better upper and lower bounds](#). *Quantum*, 4:230, 2020. Earlier version in FOCS’17. arXiv: [1705.01843](#) [19](#)
- [BMNS12] Sven Bachmann, Spyridon Michalakis, Bruno Nachtergaele, and Robert Sims. Automorphic equivalence within gapped phases of quantum lattice systems. *Communications in Mathematical Physics*, 309(3):835–871, 2012. [32](#)
- [BS17] Fernando G. S. L. Brandão and Krysta M. Svore. [Quantum speed-ups for solving semidefinite programs](#). In *Proceedings of the 58th IEEE Symposium on Foundations of Computer Science (FOCS)*, pages 415–426, 2017. arXiv: [1609.05537](#) [19](#)
- [vBLH⁺21] Vera von Burg, Guang Hao Low, Thomas Häner, Damian S. Steiger, Markus Reiher, Martin Roetteler, and Matthias Troyer. [Quantum computing enhanced computational catalysis](#). *Physical Review Research*, 3(3), Jul 2021. [1](#), [19](#)
- [BWM⁺18] Ryan Babbush, Nathan Wiebe, Jarrod McClean, James McClain, Hartmut Neven, and Garnet Kin-Lic Chan. [Low-depth quantum simulation of materials](#). *Phys. Rev. X*, 8:011044, 2018. [1](#)
- [CB21] Chi-Fang Chen and Fernando G. S. L. Brandão. Fast thermalization from the eigenstate thermalization hypothesis, 2021. arXiv: [2112.07646](#) [1](#)
- [CKBG23] Chi-Fang Chen, Michael J. Kastoryano, Fernando G. S. L. Brandão, and András Gilyén. Quantum thermal state preparation. arXiv: [2303.18224](#), 2023. [1](#), [2](#), [3](#), [4](#), [5](#), [6](#), [8](#), [13](#), [14](#), [16](#), [17](#), [18](#), [19](#), [32](#), [36](#), [37](#)
- [CL17] Andrew M. Childs and Tongyang Li. [Efficient simulation of sparse Markovian quantum dynamics](#). *Quantum Information and Computation*, 17(11&12):901–947, 2017. arXiv: [1611.05543](#) [13](#)
- [CM17] Eric A Carlen and Jan Maas. Gradient flow and entropy inequalities for quantum markov semigroups with detailed balance. *Journal of Functional Analysis*, 273(5):1810–1869, 2017. [35](#), [38](#)
- [CNAA⁺20] Christopher Chamberland, Kyungjoo Noh, Patricio Arrangoiz-Arriola, Earl T. Campbell, Connor T. Hann, Joseph K. Iverson, Harald Putterman, Thomas C. Bohdanowicz, Steven T. Flammia, A. J. Keller, Gil Refael, John Preskill, Liang Jiang, Amir H. Safavi-Naeini, Oskar J. Painter, and Fernando G. S. L. Brandão. Building a fault-tolerant quantum computer using concatenated cat codes. *PRX Quantum*, 2020. [1](#), [19](#)
- [CRSF21] Ángela Capel, Cambyse Rouzé, and Daniel Stilck França. The modified logarithmic Sobolev inequality for quantum spin systems: classical and commuting nearest neighbour interactions, 2021. arXiv: [2009.11817](#) [19](#), [33](#)
- [CW17] Richard Cleve and Chunhao Wang. [Efficient quantum algorithms for simulating Lindblad evolution](#). In *Proceedings of the 44th International Colloquium on Automata, Languages, and Programming (ICALP)*, pages 17:1–17:14, 2017. arXiv: [1612.09512](#) [13](#)
- [Dav74] Edward Brian Davies. [Markovian master equations](#). *Communications in Mathematical Physics*, 39(2):91–110, 1974. [8](#), [38](#)
- [Dav76] Edward Brian Davies. [Markovian master equations. II](#). *Mathematische Annalen*, 219(2):147–158, 1976. [8](#)
- [DCL23] Zhiyan Ding, Chi-Fang Chen, and Lin Lin. Single-ancilla ground state preparation via lindbladians. *arXiv preprint arXiv:2308.15676*, 2023. [1](#), [33](#)
- [DMB⁺23] Alexander M. Dalzell, Sam McArdle, Mario Berta, Przemyslaw Bienias, Chi-Fang Chen, András Gilyén, Connor T. Hann, Michael J. Kastoryano, Emil T. Khabiboulline, Aleksander Kubica, Grant Salton, Samson Wang, and Fernando G. S. L. Brandão. Quantum algorithms: A survey of applications and end-to-end complexities. arXiv: [2310.03011](#), 2023. [1](#)
- [Fey82] Richard P. Feynman. [Simulating physics with computers](#). *International Journal of Theoretical Physics*, 21(6-7):467–488, 1982. [1](#)
- [FF07] Veronica Umanità Franco Fagnola. [Generators of detailed balance quantum Markov semigroups](#). *Infinite Dimensional Analysis, Quantum Probability and Related Topics*, 10(03):335–363, 2007. arXiv: [0707.2147](#) [9](#), [35](#), [36](#)
- [FGG14] Edward Farhi, Jeffrey Goldstone, and Sam Gutmann. A quantum approximate optimization algorithm. arXiv: [1411.4028](#), 2014. [19](#)
- [FGGS00] Edward Farhi, Jeffrey Goldstone, Sam Gutmann, and Michael Sipser. Quantum computation by adiabatic evolution. arXiv: [quant-ph/0001106](#), 2000. [19](#)
- [GHC⁺on] Jinkang Guo, Oliver Hart, Chi-Fang Chen, Aaron J. Friedman, and Andrew Lucas. Quantum active matter, in preparation. [8](#)
- [GSLW19] András Gilyén, Yuan Su, Guang Hao Low, and Nathan Wiebe. [Quantum singular value transformation and beyond: Exponential improvements for quantum matrix arithmetics](#). In *Proceedings of the 51st ACM Symposium on the Theory of Computing (STOC)*, pages 193–204, 2019. arXiv: [1806.01838](#) [2](#)
- [Has07] Matthew B. Hastings. An area law for one-dimensional quantum systems. *Journal of Statistical Mechanics: Theory and Experiment*, 2007:P08024 – P08024, 2007. [19](#)
- [HHKL18] Jeongwan Haah, Matthew B. Hastings, Robin Kothari, and Guang Hao Low. [Quantum algorithm for simulating real time evolution of lattice hamiltonians](#). In *Proceedings of the 59th IEEE Symposium on Foundations of Computer Science (FOCS)*, pages 350–360, 2018. arXiv: [1801.03922](#) [33](#)

- [HW05] Matthew B Hastings and Xiao-Gang Wen. Quasiadiabatic continuation of quantum states: The stability of topological ground-state degeneracy and emergent gauge invariance. *Physical review b*, 72(4):045141, 2005. [32](#)
- [KAA21] Tomotaka Kuwahara, Álvaro M Alhambra, and Anurag Anshu. Improved thermal area law and quasilinear time algorithm for quantum gibbs states. *Physical Review X*, 11(1):011047, 2021. [33](#)
- [KB16] Michael J. Kastoryano and Fernando G. S. L. Brandao. Quantum Gibbs samplers: the commuting case, 2016. arXiv: [1409.3435](#) [19](#)
- [LBG⁺21] Joonho Lee, Dominic W. Berry, Craig Gidney, William J. Huggins, Jarrod R. McClean, Nathan Wiebe, and Ryan Babbush. [Even more efficient quantum computations of chemistry through tensor hypercontraction](#). *PRX Quantum*, 2(3), Jul 2021. [1](#), [19](#)
- [LC17] Guang Hao Low and Isaac L. Chuang. [Optimal Hamiltonian simulation by quantum signal processing](#). *Physical Review Letters*, 118(1):010501, 2017. arXiv: [1606.02685](#) [2](#)
- [LLZ⁺22] Seunghoon Lee, Joonho Lee, Huanchen Zhai, Yu Tong, Alexander M Dalzell, Ashutosh Kumar, Phillip Helms, Johnnie Gray, Zhi-Hao Cui, Wenyuan Liu, Michael Kastoryano, Ryan Babbush, John Preskill, David R. Reichman, Earl T. Campbell, Edward F. Valeev, Lin Lin, and Garnet Kin-Lic Chan. Is there evidence for exponential quantum advantage in quantum chemistry?, 2022. arXiv: [2208.02199](#) [1](#)
- [LPW⁺17] David Asher Levin, Yuval Peres, Elizabeth L. Wilmer, James Propp, and David B. Wilson. *Markov chains and mixing times*. American Mathematical Society, 2017. [1](#)
- [LW22] Xiantao Li and Chunhao Wang. Simulating Markovian open quantum systems using higher-order series expansion. arXiv: [2212.02051](#), 2022. [13](#)
- [ML20] Evgeny Mozgunov and Daniel Lidar. [Completely positive master equation for arbitrary driving and small level spacing](#). *Quantum*, 4:227, February 2020. [1](#)
- [Mou19] Jonathan Edward Moussa. Low-depth quantum Metropolis algorithm. arXiv: [1903.01451](#), 2019. [3](#), [4](#), [19](#)
- [MS13] Juan Maldacena and Leonard Susskind. Cool horizons for entangled black holes. *Fortschritte der Physik*, 61, 2013. [2](#)
- [Pro23] ProofWiki. [Laplace transform of error function](#). Accessed on May 1, 2023. [29](#)
- [RWW22] Patrick Rall, Chunhao Wang, and Pawel Wocjan. Thermal state preparation via rounding promises, 2022. arXiv: [2210.01670](#) [1](#), [2](#), [4](#)
- [SM21] Oles Shtanko and Ramis Movassagh. Algorithms for Gibbs state preparation on noiseless and noisy random quantum circuits, 2021. [1](#)
- [Szeg04] Mária Szegedy. [Quantum speed-up of Markov chain based algorithms](#). In *Proceedings of the 45th IEEE Symposium on Foundations of Computer Science (FOCS)*, pages 32–41, 2004. arXiv: [quant-ph/0401053](#) [2](#)
- [TOV⁺11] Kristan Temme, Tobias J. Osborne, Karl G. Vollbrecht, David Poulin, and Frank Verstraete. [Quantum Metropolis sampling](#). *Nature*, 471(7336):87–90, 2011. arXiv: [0911.3635](#) [1](#), [2](#), [4](#)
- [VAMV13] Karel Van Acoleyen, Michaël Mariën, and Frank Verstraete. [Entanglement rates and area laws](#). *Physical Review Letters*, 111(17):170501, 2013. arXiv: [1304.5931](#) [33](#)
- [WT21] Pawel Wocjan and Kristan Temme. Szegedy walk unitaries for quantum maps, 2021. arXiv: [2107.07365](#) [1](#), [2](#), [4](#), [5](#), [6](#)
- [YAG12] Man-Hong Yung and Alán Aspuru-Guzik. [A quantum-quantum Metropolis algorithm](#). *Proceedings of the National Academy of Sciences*, 109(3):754–759, 2012. arXiv: [1011.1468](#) [1](#), [2](#), [4](#)
- [Zor16] Vladimir Antonovich Zorich. *Mathematical Analysis II*. Universitext. Springer, 2nd edition, 2016. [29](#)

NOMENCLATURE

This section recapitulates notations. We write scalars, functions, and vectors in normal font, matrices in bold font \mathbf{O} , and superoperators in curly font \mathcal{L} . Natural constants e, i, π are denoted in Roman font.

$\mathbf{H} = \sum_i E_i \psi_i\rangle\langle\psi_i $	the Hamiltonian of interest and its eigendecomposition
$\text{Spec}(\mathbf{H}) := \{E_i\}$	the spectrum of the Hamiltonian
$\nu \in B = B(\mathbf{H}) := \text{Spec}(\mathbf{H}) - \text{Spec}(\mathbf{H})$	the set of Bohr frequencies
$\mathbf{P}_E := \sum_{i:E_i=E} \psi_i\rangle\langle\psi_i $	eigenspace projector for energy E
$\mathcal{L} :$	a Lindbladian in the Schrödinger Picture
$n :$	system size (number of qubits) of the Hamiltonian \mathbf{H}
$\beta :$	inverse temperature
$\rho_\beta := \frac{e^{-\beta\mathbf{H}}}{\text{Tr}[e^{-\beta\mathbf{H}}]}$	the Gibbs state with inverse temperature β
$ \sqrt{\rho_\beta}\rangle := \frac{1}{\sqrt{\text{Tr}[e^{-\beta\mathbf{H}}]}} \sum_i e^{-\beta E_i/2} \psi_i\rangle \otimes \psi_i^*\rangle$	the purified Gibbs state
$\{\mathbf{A}^a\}_{a \in A} :$	set of jump operators
$ A :$	cardinality of the set of jumps
$\mathbf{I} :$	the identity operator
$\tilde{\mathcal{O}}(\cdot), \tilde{\Omega}(\cdot) :$	complexity expression ignoring (poly)logarithmic factors

Fourier transform notations:

$\hat{\mathbf{A}}_{(f)}(\omega) := \frac{1}{\sqrt{2\pi}} \int_{-\infty}^{\infty} e^{-i\omega t} f(t) \mathbf{A}(t) dt$	operator Fourier Transform for \mathbf{A} weighted by f
$\hat{f}(\omega) = \mathcal{F}(f) = \lim_{K \rightarrow \infty} \frac{1}{\sqrt{2\pi}} \int_{-K}^K e^{-i\omega t} f(t) dt$	the Fourier transform of a scalar function f over inputs t
$\mathbf{A}_\nu := \sum_{E_2 - E_1 = \nu} \mathbf{P}_{E_2} \mathbf{A} \mathbf{P}_{E_1}$	operator \mathbf{A} at exact Bohr frequency ν

Norms:

$\ f(x)\ _p := \left(\int f(x) ^p dx \right)^{1/p}$	the p -norm of a scalar function f over inputs x for $p \in [1, \infty]$
$\ell_p(\mathbb{R}) := \{f : \mathbb{R} \rightarrow \mathbb{C}, \quad \ f\ _p < \infty\}$	the set of integrable functions
$\ f(x)\ := \ f(x)\ _2 = \sqrt{\int f(x) ^2 dx}$	the 2-norm of a scalar function f over inputs x
$\ \psi\ :$	the Euclidean norm of a vector $ \psi\rangle$
$\ \mathbf{O}\ := \sup_{ \psi\rangle, \phi\rangle} \frac{\langle\phi \mathbf{O} \psi\rangle}{\ \psi\ \cdot \ \phi\ }$	the operator norm of a matrix \mathbf{O}
$\ \mathbf{O}\ _p := (\text{Tr} \mathbf{O} ^p)^{1/p}$	the Schatten p -norm of a matrix \mathbf{O}
$\ \mathcal{L}\ _{p-p} := \sup_{\mathbf{O}} \frac{\ \mathcal{L}[\mathbf{O}]\ _p}{\ \mathbf{O}\ _p}$	the induced $p - p$ norm of a superoperator \mathcal{L}

Linear algebra:

$\lambda_i(\mathbf{O}) :$	the i -th largest eigenvalue of a matrix \mathbf{O} sorted by their real parts
$\lambda_{gap}(\mathbf{O}) := \Re\lambda_1(\mathbf{O}) - \Re\lambda_2(\mathbf{O}) \geq 0$	the real spectral gap of a matrix \mathbf{O}
$\mathbf{O}^* :$	the entry-wise complex conjugate of a matrix \mathbf{O}
$\mathbf{O}^\dagger :$	the Hermitian conjugate of a matrix \mathbf{O}
$ \psi^*\rangle :$	entry-wise complex conjugate of a vector $ \psi\rangle$

Appendix A: Deriving time-domain representations

Our calculation for detailed balance has focused on the frequency domain. This appendix applies Fourier transforms to obtain the time-domain representation. The arguments are conceptually straightforward but require some bookkeeping.

For both the Lindbladians and the parent Hamiltonians, we will often encounter a two-dimensional sum over Bohr frequencies. Since there are two energy labels, we employ a two-dimensional Fourier Transform. For any function of frequencies $\hat{f}(\nu_1, \nu_2)$, the time-domain representation of the bilinear expression gives

$$\sum_{a \in A} \sum_{\nu_1, \nu_2 \in B} \hat{f}(\nu_1, \nu_2) \mathbf{A}_{\nu_1}^a \otimes (\mathbf{A}_{\nu_2}^a)^\dagger = \sum_{a \in A} \frac{1}{2\pi} \int_{-\infty}^{\infty} \int_{-\infty}^{\infty} f(t_1, t_2) \mathbf{A}^a(t_1) \otimes \mathbf{A}^{a\dagger}(-t_2) dt_1 dt_2$$

where we introduced the two-dimensional Fourier Transform

$$f(t_1, t_2) := \frac{1}{2\pi} \int_{-\infty}^{\infty} \int_{-\infty}^{\infty} \hat{f}(\nu_1, \nu_2) e^{i\nu_1 t_1} e^{i\nu_2 t_2} d\nu_1 d\nu_2.$$

Fortunately, for our usage, the Fourier Transform *decouples* into two iterations of one-dimensional Fourier Transforms, significantly simplifying the presentation and implementation.

Corollary A.1 (Factorized time-domain functions). *If the function factorizes in the energy domain such that*

$$\frac{1}{2\pi} \hat{f}(\nu_1, \nu_2) = \hat{f}_+(\nu_1 + \nu_2) \cdot \hat{f}_-(\nu_1 - \nu_2),$$

then

$$\sum_{a \in A} \sum_{\nu_1, \nu_2 \in B} \hat{f}(\nu_1, \nu_2) \mathbf{A}_{\nu_1}^a \otimes (\mathbf{A}_{\nu_2}^a)^\dagger = \sum_{a \in A} \int_{-\infty}^{\infty} \int_{-\infty}^{\infty} f_-(t_-) f_+(t_+) \mathbf{A}^a(-t_- - t_+) \otimes \mathbf{A}^{a\dagger}(t_+ - t_-) dt_+ dt_- \quad (\text{A1})$$

and

$$\sum_{a \in A} \sum_{\nu_1, \nu_2 \in B} \hat{f}(\nu_1, \nu_2) (\mathbf{A}_{\nu_2}^a)^\dagger \mathbf{A}_{\nu_1}^a = \sum_{a \in A} \int_{-\infty}^{\infty} f_-(t_-) e^{-i\mathbf{H}t_-} \left(\int_{-\infty}^{\infty} f_+(t_+) \mathbf{A}^{a\dagger}(t_+) \mathbf{A}^a(-t_+) dt_+ \right) e^{i\mathbf{H}t_-} dt_-$$

where the function f_{\pm} are inverse Fourier Transforms of \hat{f}_{\pm} .

Crucially, the RHS can be implemented via Linear Combination of Unitaries by discretizing the integral.

Proof. Since the expression is linear in the sum over jumps $a \in A$, it suffices to prove for any operator \mathbf{A} , dropping the jump labels a .

$$\begin{aligned} & \sum_{\nu_1, \nu_2 \in B} 2\pi \hat{f}_+(\nu_1 + \nu_2) \cdot \hat{f}_-(\nu_1 - \nu_2) \mathbf{A}_{\nu_1} \otimes (\mathbf{A}_{\nu_2})^\dagger \\ &= \sum_{\nu_1, \nu_2 \in B} 2\pi \hat{f}_+(\nu_+) \cdot \hat{f}_-(\nu_-) \left(\mathbf{A}_{\frac{\nu_+ + \nu_-}{2}} \otimes \mathbf{A}_{\frac{\nu_+ - \nu_-}{2}} \right)^\dagger \quad (\text{Let } \nu_+ := \nu_1 + \nu_2 \text{ and } \nu_- := \nu_1 - \nu_2) \\ &= \sum_{\nu_1, \nu_2 \in B} \int_{-\infty}^{\infty} f_+(t_+) e^{-i\nu_+ t_+} dt_+ \int_{-\infty}^{\infty} f_-(t_-) e^{-i\nu_- t_-} dt_- \mathbf{A}_{\frac{\nu_+ + \nu_-}{2}} \otimes \left(\mathbf{A}_{\frac{\nu_+ - \nu_-}{2}} \right)^\dagger \quad (\text{Fourier Transform}) \\ &= \sum_{\nu_1, \nu_2 \in B} \int_{-\infty}^{\infty} \int_{-\infty}^{\infty} f_+(t_+) f_-(t_-) \mathbf{A}_{\frac{\nu_+ + \nu_-}{2}}(-t_+ - t_-) \otimes \left(\mathbf{A}_{\frac{\nu_+ - \nu_-}{2}} \right)^\dagger(t_+ - t_-) dt_+ dt_- \quad (\text{Since } (\mathbf{A}_\nu)^\dagger = (\mathbf{A}^\dagger)_{-\nu}) \\ &= \int_{-\infty}^{\infty} \int_{-\infty}^{\infty} f_+(t_+) f_-(t_-) \mathbf{A}(-t_+ - t_-) \otimes \mathbf{A}^\dagger(t_+ - t_-) dt_+ dt_- . \end{aligned}$$

The fourth equality uses that

$$e^{-i\nu_+ t_+} e^{-i\nu_- t_-} = \exp\left(\frac{i(\nu_+ - \nu_-)(t_+ - t_-)}{2}\right) \cdot \exp\left(\frac{i(\nu_+ + \nu_-)(-t_+ - t_-)}{2}\right)$$

to conclude the proof. ■

Now, we plug in the appropriate functions to arrive at the time-domain functions.

1. Our Lindbladians

We evaluate the Fourier transform for the coherent term \mathbf{B} . The expression looks intimidating, but all that matters for the algorithmic complexity is that they decay rapidly (in the time domain).

Corollary A.2 (Explicit time-domain functions). *In the time domain, the coherent term \mathbf{B} in (2.5) corresponding to coefficients constructed in (2.6) reads*

$$f_+(t) = \int_{\frac{\beta\sigma_E^2}{2}}^{\infty} g(x)\sigma_\gamma(x) \exp\left(-\frac{4t^2x}{\beta} - 2itx\right) dx, \quad (\text{A2})$$

$$f_-(t) = \frac{\sigma_E}{\pi\beta} e^{\frac{\beta^2\sigma_E^2}{8}} \left(\frac{1}{\cosh\left(\frac{2\pi t}{\beta}\right)} *_t \sin(-\beta\sigma_E^2 t) e^{-2\sigma_E^2 t^2} \right), \quad (\text{A3})$$

depending on parameters $\sigma_E, g(x), \beta$.¹²

Recall that the convolution of two functions over variable t is defined by

$$(f *_t g)(t) := \int_{-\infty}^{\infty} f(s)g(t-s)ds.$$

Nicely, the product structure persists under a convex combination of Gaussians as only $f_+(t)$ depends on $g(x)$. Otherwise, we could have had to consider a linear combination of function products, which is messier to implement.

Proof. First, we confirm that the energy domain function indeed has a product structure $\frac{1}{2\pi}\hat{f}(\nu_1, \nu_2) = \hat{f}_+(\nu_1 + \nu_2) \cdot \hat{f}_-(\nu_1 - \nu_2)$ due to (2.3), (2.6) and (2.5) for

$$\hat{f}_+(\nu) = \int_{\frac{\beta\sigma_E^2}{2}}^{\infty} \frac{g(x)\sigma_\gamma(x)}{2\sqrt{\sigma_E^2 + \sigma_\gamma^2(x)}} \exp\left(-\frac{(\nu + 2x)^2}{16x/\beta}\right) dx, \text{ and} \quad (\text{A4})$$

$$\hat{f}_-(\nu) = \frac{1}{2\pi} \frac{\tanh(-\beta\nu/4)}{2i} \exp\left(-\frac{\nu^2}{8\sigma_E^2}\right) = \frac{1}{2\pi} \frac{1}{\cosh(-\beta\nu/4)} \cdot \frac{\sinh(-\beta\nu/4)}{2i} \exp\left(-\frac{\nu^2}{8\sigma_E^2}\right).$$

Since we work with well-concentrated integrable functions, the Fourier Transforms exist, and we can compute them as follows. We begin with the Gaussian integral associated with f_+

$$\frac{1}{\sqrt{2\pi}} \int_{-\infty}^{\infty} \exp\left(-\frac{(\nu + 2x)^2}{16x/\beta}\right) e^{i\nu t} d\nu = 2\sqrt{\frac{2x}{\beta}} \exp\left(-\frac{4t^2x}{\beta} - 2itx\right).$$

Thus, using (A4) and the definition of $\sigma_\gamma(x) = \sqrt{2x/\beta - \sigma_E^2}$, we get (A2). In order to compute $f_-(t)$, we use the convolution theorem $\mathcal{F}^{-1}(\mathcal{F}(f) \cdot \mathcal{F}(g)) = f *_t g/\sqrt{2\pi}$. Individually, we have

$$\begin{aligned} \frac{1}{\sqrt{2\pi}} \int_{-\infty}^{\infty} \frac{\sinh(-\beta\nu/4)}{2i} \exp\left(-\frac{\nu^2}{8\sigma_E^2}\right) e^{i\nu t} d\nu &= \sigma_E e^{\frac{\beta^2\sigma_E^2}{8}} \sin(-\beta\sigma_E^2 t) e^{-2\sigma_E^2 t^2} \\ \frac{1}{\sqrt{2\pi}} \int_{-\infty}^{\infty} \frac{1}{2\pi \cosh(-\beta\nu/4)} e^{i\nu t} d\nu &= \frac{2}{\sqrt{2\pi}\beta \cosh\left(\frac{2\pi t}{\beta}\right)}. \end{aligned} \quad (\text{A5})$$

Take the convolution to conclude the calculation. ■

The above explicit form allows us to compute the explicit form of the function $f_+(t)$ corresponding to our two main settings. We begin with the Gaussian case.

Corollary III.1 (Coherent term for the Gaussian case). *For each $\beta > 0$ and parameters $\sigma_E = \sigma_\gamma = \omega_\gamma = \frac{1}{\beta}$, the coherent term \mathbf{B} (2.5) corresponding to the Gaussian weight $\gamma(\omega) = \exp\left(-\frac{(\beta\omega+1)^2}{2}\right)$ can be written as*

$$\mathbf{B} := \sum_{a \in A} \int_{-\infty}^{\infty} b_1(t) e^{-i\beta \mathbf{H}t} \left(\int_{-\infty}^{\infty} b_2(t') \mathbf{A}^{a\dagger}(\beta t') \mathbf{A}^a(-\beta t') dt' \right) e^{i\beta \mathbf{H}t} dt, \quad (\text{3.1})$$

¹² Note that the function $b_1(t)$ seems to have width $\sim \beta\sigma_E$ due to the convolution by $\frac{1}{\cosh(4\pi t/(\beta\sigma_E))}$, meaning that the integral in t seems to require Hamiltonian evolution times up to $\sim \beta$. In fact, the numerics show a $1/\text{poly}$ decay until about $\sim \beta\sigma_E$ (after which the exponential decay starts), suggesting that about $\min(\sigma_E^{-1} \text{Poly}(1/\epsilon), \beta \log(1/\epsilon))$ Hamiltonian simulation time is required in order to achieve ϵ precision for the block-encoding of the coherent term. Thus, it might be difficult to obtain exact detailed balance below $\Omega(\beta)$ Hamiltonian evolution times. On the contrary, the function $b_2(t')$ has a width only about $1/\sqrt{\beta\omega_\gamma}$, implying that the corresponding other integral in t' can be well-approximated by only using Hamiltonian evolution time $\sim \sqrt{\beta/\omega_\gamma}$.

where

$$b_1(t) := 2\sqrt{\pi}e^{\frac{1}{8}} \left(\frac{1}{\cosh(2\pi t)} *_t \sin(-t) \exp(-2t^2) \right) \quad \text{such that } \|b_1\|_1 < 1 \quad (3.2)$$

$$b_2(t) := \frac{1}{2\pi} \sqrt{\frac{1}{\pi}} \exp(-4t^2 - 2it) \quad \text{such that } \|b_2\|_1 < \frac{1}{16}. \quad (3.3)$$

Indeed, both functions of time are rapidly decaying and have bounded ℓ_1 -norm (as required for LCU implementation).

Proof. Setting $g(x) = \delta(x - \omega_\gamma)$ in [Corollary A.1](#) yields the desired Gaussian weight and $f_+(t)$ in [\(A2\)](#) becomes

$$f_+(t) = \int_{-\infty}^{\infty} \delta(x - \omega_\gamma) \sigma_\gamma \exp\left(-\frac{4t^2 x}{\beta} - 2itx\right) dx = \sqrt{\frac{2\omega_\gamma}{\beta} - \sigma_E^2} \exp\left(-\frac{4t^2 \omega_\gamma}{\beta} - 2it\omega_\gamma\right).$$

Setting $b_1(t) := 2\pi\sqrt{\pi}f_-(t/\sigma_E)$ and $b_2(t) := f_+(\beta t)/(2\pi\sqrt{\pi})$ and applying a change of variables in the integral [\(A1\)](#) yields the desired result [\(3.1\)](#). Note that the convolution $*_t$ implicitly is an integral over t , so we should not forget to rescale dt there.

Lastly, we bound the ℓ_1 -norm of the functions by Hölder's inequality

$$\|b_1\|_1 \leq \|(1+t^2)^{-1}\|_2 \|(1+t^2)b_1\|_2 = \sqrt{\frac{\pi}{2}} \|(1+t^2)b_1\|_2 \leq 1,$$

using individual bounds $\int_{-\infty}^{\infty} \frac{1}{(1+2t^2)^2} dt = \frac{\pi}{2}$ and $\int_{-\infty}^{\infty} \left| (1+t^2)b_1(t) \right|^2 dt < 0.625$. The norm $\|b_2\|_1 = \frac{e^{-1/4}}{4\pi} < \frac{1}{16}$ is a Gaussian integral ([Fact II.1](#)). \blacksquare

The explicit weights corresponding to Metropolis weights are slightly more cumbersome due to taming a logarithmic singularity; see [Section B](#).

2. Our parent Hamiltonians

Based on the Lindbladian, we explicitly evaluate the discriminant in the frequency domain.

Proposition A.1 (Symmerized discriminant). *In the setting of [Corollary II.2](#), the discriminant corresponding to the ρ_β -DB Lindbladian reads*

$$\begin{aligned} \mathcal{H}_\beta &= \sum_{a \in A} \sum_{\nu_1, \nu_2 \in B} h_{\nu_1, \nu_2} \mathbf{A}_{\nu_1}^a(\cdot) (\mathbf{A}_{\nu_2}^a)^\dagger + \frac{1}{2} (\mathbf{N}(\cdot) + (\cdot) \mathbf{N}) \\ \text{or } \mathcal{H}_\beta &= \sum_{a \in A} \sum_{\nu_1, \nu_2 \in B} \underbrace{h_{\nu_1, \nu_2} \mathbf{A}_{\nu_1}^a \otimes (\mathbf{A}_{\nu_2}^a)^*}_{\text{transition part}} + \underbrace{\frac{1}{2} (\mathbf{N} \otimes \mathbf{I} + \mathbf{I} \otimes \mathbf{N}^*)}_{\text{coherent and decay part}} \end{aligned}$$

where $h_{\nu_1, \nu_2} := e^{\beta(\nu_1 + \nu_2)/4} \alpha_{\nu_1, \nu_2} = h_{-\nu_2, -\nu_1}$ and

$$\mathbf{N} := - \sum_{a \in A} \sum_{\nu_1, \nu_2 \in B} \frac{\alpha_{\nu_1, \nu_2}}{\cosh(\beta(\nu_1 - \nu_2)/4)} (\mathbf{A}_{\nu_2}^a)^\dagger \mathbf{A}_{\nu_1}^a = \mathbf{N}^\dagger.$$

Proof. We calculate

$$\begin{aligned} \mathcal{H}_\beta &= \rho^{-1/4} \mathcal{L}[\rho^{1/4} \cdot \rho^{1/4}] \rho^{-1/4} \\ &= \sum_{a \in A} \sum_{\nu_1, \nu_2 \in B} e^{\beta(\nu_1 + \nu_2)/4} \alpha_{\nu_1, \nu_2} \mathbf{A}_{\nu_1}^a(\cdot) (\mathbf{A}_{\nu_2}^a)^\dagger \\ &\quad - i \sum_{\nu \in B} \left(e^{\frac{\beta\nu}{4}} \mathbf{B}_\nu(\cdot) - e^{-\frac{\beta\nu}{4}} (\cdot) \mathbf{B}_\nu \right) - \frac{1}{2} \sum_{a \in A} \sum_{\nu_1, \nu_2 \in B} \left(\alpha_{\nu_1, \nu_2} e^{\frac{\beta(\nu_1 - \nu_2)}{4}} (\mathbf{A}_{\nu_2}^a)^\dagger \mathbf{A}_{\nu_1}^a(\cdot) + \alpha_{\nu_1, \nu_2} e^{-\frac{\beta(\nu_1 - \nu_2)}{4}} (\cdot) (\mathbf{A}_{\nu_2}^a)^\dagger \mathbf{A}_{\nu_1}^a \right) \\ &= \sum_{a \in A} \sum_{\nu_1, \nu_2 \in B} h_{\nu_1, \nu_2} \mathbf{A}_{\nu_1}^a(\cdot) (\mathbf{A}_{\nu_2}^a)^\dagger + \frac{1}{2} \mathbf{N}(\cdot) + \frac{1}{2} (\cdot) \mathbf{N}^\dagger \end{aligned}$$

where

$$\mathbf{N} = -2i \sum_{\nu \in B} e^{\beta\nu/4} \mathbf{B}_\nu - \sum_{a \in A} \sum_{\nu_1, \nu_2 \in B} \alpha_{\nu_1, \nu_2} e^{\frac{\beta(\nu_1 - \nu_2)}{4}} (\mathbf{A}_{\nu_2}^a)^\dagger \mathbf{A}_{\nu_1}^a.$$

We further simplify \mathbf{N} by expressing \mathbf{B} as a linear combination of $(\mathbf{A}_{\nu_2}^a)^\dagger \mathbf{A}_{\nu_1}^a$ as in (2.5).

$$\begin{aligned} \mathbf{N} &= \sum_{a \in A} \sum_{\nu_1, \nu_2 \in B} \left(\exp(\beta(\nu_1 - \nu_2)/4) \tanh(\beta(\nu_1 - \nu_2)/4) - \exp(\beta(\nu_1 - \nu_2)/4) \right) \alpha_{\nu_1, \nu_2} (\mathbf{A}_{\nu_2}^a)^\dagger \mathbf{A}_{\nu_1}^a \\ &= - \sum_{a \in A} \sum_{\nu_1, \nu_2 \in B} \frac{\alpha_{\nu_1, \nu_2}}{\cosh(\beta(\nu_1 - \nu_2)/4)} (\mathbf{A}_{\nu_2}^a)^\dagger \mathbf{A}_{\nu_1}^a && \text{(By } e^x(\tanh(x) - 1) = \frac{-1}{\cosh(x)} \text{)} \\ &= \mathbf{N}^\dagger, && \text{(Invariance under } \nu_1 \leftrightarrow \nu_2 \text{)} \end{aligned}$$

as advertised. ■

a. The transition part

For the transition part, we quickly obtain the time-domain representation using a two-dimensional Fourier Transform as a corollary of [Corollary A.1](#).

Corollary A.3 (Time integrals). *Suppose $h_{\nu_1, \nu_2} = 2\pi \cdot \hat{h}_+(\nu_+) \cdot \hat{h}_-(\nu_-)$, then*

$$\sum_{a \in A} \sum_{\nu_1, \nu_2 \in B} h_{\nu_1, \nu_2} \mathbf{A}_{\nu_1}^a \otimes (\mathbf{A}_{\nu_2}^a)^* = \sum_{a \in A} \int_{-\infty}^{\infty} \int_{-\infty}^{\infty} h_-(t_-) h_+(t_+) \cdot \mathbf{A}^a(t_+ - t_-) \otimes \mathbf{A}^a(-t_- - t_+)^T dt_+ dt_-$$

where $h_\pm(t)$ are Fourier Transforms of $\hat{h}_\pm(\nu)$.

Now, we can evaluate the Fourier transforms explicitly.

Proposition A.2 (Linear combination for h). *For α_{ν_1, ν_2} defined in (2.6) and each $\sigma_E, g(x)$, we have that $h_{\nu_1, \nu_2} = 2\pi \hat{h}_+(\nu_+) \cdot \hat{h}_-(\nu_-)$ for the discriminant ([Proposition A.1](#)) where*

$$\hat{h}_+(\nu) = \int_{\frac{\beta\sigma_E^2}{2}}^{\infty} \frac{g(x)\sigma_\gamma(x)}{2\sqrt{\sigma_E^2 + \sigma_\gamma^2(x)}} \exp\left(-\frac{\beta\nu^2}{16x} - \frac{\beta x}{4}\right) dx \quad \text{and} \quad \hat{h}_-(\nu) := \frac{1}{2\pi} \exp\left(-\frac{\nu^2}{8\sigma_E^2}\right),$$

with the corresponding time-domain functions

$$h_+(t) = \int_{\frac{\beta\sigma_E^2}{2}}^{\infty} g(x)\sigma_\gamma(x) \exp\left(-\frac{4t^2x}{\beta} - \frac{\beta x}{4}\right) dx \quad \text{and} \quad h_-(t) = \frac{\sigma_E}{\pi} \exp(-2\sigma_E^2 t^2). \quad (\text{A6})$$

Proof. For $\hat{h}_+(\nu)$ term, the cross term in the exponential $e^{-\beta\nu/4}$ is precisely cancelled by $h_{\nu_1, \nu_2} := e^{\beta(\nu_1 + \nu_2)/4} \alpha_{\nu_1, \nu_2}$; the $\hat{h}_-(\nu)$ term remains the same. To obtain the time-domain functions, we simply carry out the Gaussian integral

$$\frac{1}{\sqrt{2\pi}} \int_{-\infty}^{\infty} \exp\left(-\frac{\beta\nu^2}{16x} - \frac{\beta x}{4}\right) e^{i\nu t} d\nu = 2\sqrt{\frac{2x}{\beta}} \exp\left(-\frac{4t^2x}{\beta} - \frac{\beta x}{4}\right)$$

and use that $\sigma_E^2 + \sigma_\gamma^2(x) = \beta/2x$. ■

Proposition A.3 (The Gaussian case). *In the setting of [Proposition A.2](#) and for α_{ν_1, ν_2} defined in (2.4), we have*

$$\hat{h}_+(\nu) := \frac{\sigma_\gamma}{2\sqrt{\sigma_E^2 + \sigma_\gamma^2}} \cdot \exp\left(-\frac{\nu^2 + (2\omega_\gamma)^2}{8(\sigma_E^2 + \sigma_\gamma^2)}\right) \quad \text{and} \quad \hat{h}_-(\nu) := \frac{1}{2\pi} \exp\left(-\frac{\nu^2}{8\sigma_E^2}\right).$$

Corollary III.3 (The transition part for Gaussian weights). *For the Gaussian weight $\gamma(\omega) = \exp\left(-\frac{(\beta\omega+1)^2}{2}\right)$ with $\omega_\gamma = \sigma_E = \sigma_\gamma = 1/\beta$, the discriminant \mathcal{H}_β is described in the time domain by*

$$h_+(t) = \frac{1}{\beta} e^{-1/4} \exp\left(-\frac{4t^2}{\beta^2}\right) \quad \text{and} \quad h_-(t) = \frac{1}{\pi\beta} \exp\left(-\frac{2t^2}{\beta^2}\right) \quad \text{such that} \quad \|h_-\|_1, \|h_+\|_1 \leq 1. \quad (\text{3.7})$$

Corollary III.4 (The transition part for Metropolis weights). *For $\sigma_E = \frac{1}{\beta}$, the Metropolis-like weight $\gamma^M(\omega) = \exp\left(-\beta \max\left(\omega + \frac{1}{2\beta}, 0\right)\right)$ yields \mathcal{H}_β described in the time domain by the same $h_-(t)$ as in Eq. (3.7) and by*

$$h_+(t) = \frac{e^{-1/8}}{\beta} \frac{e^{-2t^2/\beta^2}}{4\sqrt{2\pi}\left(\frac{t^2}{\beta^2} + \frac{1}{16}\right)} \quad \text{such that} \quad \|h_+(t)\|_1 \leq 1.$$

Proof. Setting $g(x) = \frac{1}{\sqrt{2\pi}\sigma_\gamma(x)}$ on the interval $\left(\frac{\beta\sigma_E^2}{2}, \infty\right)$, yields in (A6)

$$\begin{aligned} h_+(t) &= \int_{\frac{\beta\sigma_E^2}{2}}^{\infty} g(x)\sigma_\gamma(x) \exp\left(-\frac{4t^2x}{\beta} - \frac{\beta x}{4}\right) dx = \frac{1}{\sqrt{2\pi}} \int_{\frac{\beta\sigma_E^2}{2}}^{\infty} \exp\left(-\frac{4t^2x}{\beta} - \frac{\beta x}{4}\right) dx \\ &= \frac{1}{\beta} \frac{e^{-2\sigma_E^2 t^2 - \beta^2 \sigma_E^2 / 8}}{4\sqrt{2\pi}\left(\frac{t^2}{\beta^2} + \frac{1}{16}\right)}. \end{aligned}$$

Set $\sigma_E = 1/\beta$ to conclude the calculation. To obtain the ℓ_1 -norm bound, integrate $\frac{1}{e^{1/84}\sqrt{2\pi}} \int_{-\infty}^{\infty} \frac{e^{-2x^2}}{x^2+1/16} dx = \sqrt{\frac{\pi}{2}} \operatorname{erfc}(1/\sqrt{8}) < 0.78$. \blacksquare

b. The \mathbf{N} -term

We instantiate the time-domain presentation of the \mathbf{N} term (adapted from the calculation for the coherent term \mathbf{B} (Corollary A.2)).

Corollary A.4 (Explicit time-domain functions). *In the time domain, the \mathbf{N} term corresponding to coefficients constructed in (2.6) can be written as*

$$\mathbf{N} = \sum_{a \in A} \int_{-\infty}^{\infty} f_-(t_-) e^{-i\mathbf{H}t_-} \left(\int_{-\infty}^{\infty} f_+(t_+) \mathbf{A}^{a\dagger}(t_+) \mathbf{A}^a(-t_+) dt_+ \right) e^{i\mathbf{H}t_-} dt_-$$

for $f_+(t)$ as in (A2) and

$$f_-(t) = \frac{2\sigma_E}{\pi\beta} \left(\frac{1}{\cosh\left(\frac{2\pi t}{\beta}\right)} *_t e^{-2\sigma_E^2 t^2} \right),$$

depending on parameters $\sigma_\gamma, \sigma_E, g(x), \beta$.

Proof. Follow the proof of Corollary A.2, but drop the $\sinh(-\beta\nu/4)/(2i)$ term in (A5). The convolution then gives

$$\frac{1}{\sqrt{2\pi}} \int_{-\infty}^{\infty} \exp\left(-\frac{\nu^2}{8\sigma_E^2}\right) e^{i\nu t} d\nu = 2\sigma_E e^{-2\sigma_E^2 t^2}.$$

\blacksquare

We instantiate similar results with minor modifications without replicating the proofs.

Corollary III.5 (\mathbf{N} term for Gaussian weights). *For each β , the Gaussian weight $\gamma(\omega) = \exp\left(-\frac{(\beta\omega+1)^2}{2}\right)$ with $\sigma_E = \sigma_\gamma = \omega_\gamma = \frac{1}{\beta}$ corresponds to the discriminant where*

$$\mathbf{N} = \sum_{a \in A} \int_{-\infty}^{\infty} n_1(t) e^{-i\beta\mathbf{H}t} \left(\int_{-\infty}^{\infty} n_2(t') \mathbf{A}^{a\dagger}(\beta t') \mathbf{A}^a(-\beta t') dt' \right) e^{i\beta\mathbf{H}t} dt,$$

where

$$\begin{aligned} n_1(t) &:= \frac{1}{4} \cdot 2\sqrt{\pi} \left(\frac{1}{\cosh(2\pi t)} *_t \exp(-2t^2) \right) & \text{such that } \|n_1\|_1 &= \frac{\pi}{4\sqrt{2}} < 1 \\ n_2(t) &:= 4 \cdot 2 \cdot \frac{1}{2\pi} \sqrt{\frac{1}{\pi}} \exp(-4t^2 - 2it) = 8 \cdot b_2(t) & \text{such that } \|n_2\|_1 &< \frac{1}{2} \end{aligned} \quad (3.8)$$

with b_2 as in (3.3).

Proof. As both functions are positive $\frac{1}{\cosh(2\pi t)}, \exp(-2t^2) > 0$, we have that $\|n_1(t)\|_1 = \int_{-\infty}^{\infty} n_1(t) dt = \frac{\sqrt{\pi}}{2} \left(\int_{-\infty}^{\infty} \frac{1}{\cosh(2\pi t)} dt \right) \cdot \left(\int_{-\infty}^{\infty} \exp(-2t^2) dt \right)$, where the second equality follows from the fact that the integral of a convolution is the product of the integrals of the convolved functions due to Fubini's theorem. The first integral evaluates to $1/2$ and the second evaluates to $\sqrt{\pi/2}$ due to Fact II.1, therefore $\|n_1(t)\|_1 = \pi/\sqrt{32}$. The second bound follows from the analogous bound on b_2 in Corollary III.1. The factor of 4 and $\frac{1}{4}$ is redistributed to ensure both n_1 and n_2 are normalized. Note the overall extra factor of 2 in Corollary A.4 compared with Corollary A.2. \blacksquare

Corollary III.6 (N term for Metropolis weights). *If $\sigma_E = \frac{1}{\beta}$, then the Metropolis-like weight $\gamma^M(\omega) = \exp\left(-\beta \max\left(\omega + \frac{1}{2\beta}, 0\right)\right)$ corresponds to the discriminant where \mathbf{N}^M satisfies*

$$\|\mathbf{N}^M - \mathbf{N}^{M,\eta}\| \leq \sum_{a \in A} \|\mathbf{A}^{a\dagger} \mathbf{A}^a\| \min\left(\frac{\eta\beta\|\mathbf{H}\|}{\sqrt{2\pi}}, \mathcal{O}((\eta\beta\|\mathbf{H}\|)^3)\right),$$

where

$$\mathbf{N}^{M,\eta} := \sum_{a \in A} \int_{-\infty}^{\infty} n_1(t) e^{-i\beta \mathbf{H}t} \left(\int_{-\infty}^{\infty} n_2^{M,\eta}(t') \mathbf{A}^{a\dagger}(\beta t') \mathbf{A}^a(-\beta t') dt' + \frac{1}{16\sqrt{2\pi}} \mathbf{A}^{a\dagger} \mathbf{A}^a \right) e^{i\beta \mathbf{H}t} dt,$$

with $n_1(t)$ as in (3.8), and $n_2^{M,\eta} = b_2^{M,\eta}$ as in (3.6).

Appendix B: Calculating the coherent term for the Metropolis-like weights

In this section, we dedicate to calculating the weights corresponding to the Metropolis-like weight in order to arrive at an expression that enables efficient implementation via LCU.

Proposition B.1 (Metropolis-like weights). *Setting $g(x) = \frac{1}{\sqrt{2\pi}\sigma_\gamma(x)}$ on the interval $\left(\frac{\beta\sigma_E^2}{2}, \frac{s^2}{\beta}\right)$, yields in (A2)*

$$f_+^{(s)}(t) = \frac{1}{\beta} \frac{e^{-2\sigma_E^2 t^2 - i\beta\sigma_E^2 t} - e^{-4\frac{t^2}{\beta^2} s^2 - 2i\frac{t}{\beta} s^2}}{2\sqrt{2\pi}\frac{t}{\beta}(2\frac{t}{\beta} + i)}. \quad (\text{B1})$$

In particular, in the $s \rightarrow \infty$ limit, the second term vanishes, but we can only interpret the result as a distribution

$$f_+^{(\infty)}(t) = \lim_{\eta \rightarrow 0^+} \mathbb{1}(|t| \geq \eta) \frac{1}{\beta} \frac{e^{-2\sigma_E^2 t^2 - i\beta\sigma_E^2 t}}{2\sqrt{2\pi}\frac{t}{\beta}(2\frac{t}{\beta} + i)} + \sqrt{\frac{\pi}{8}} \delta(t).$$

Which again decays rapidly; we would need to pay attention to the $t \sim 0$ regime due to the delta function $\delta(t)$ and $1/t$ dependence.

Proof. We substitute $g(x) = \frac{1}{\sqrt{2\pi}\sigma_\gamma(x)}$ in (A2), which due to $\sigma_E^2 + \sigma_\gamma^2 = \frac{2\omega_\gamma}{\beta}$ gives

$$\begin{aligned} f_+^{(s)}(t) &:= \int_{\frac{\beta\sigma_E^2}{2}}^{\infty} \frac{1}{\sqrt{2\pi}\sigma_\gamma(x)} \sigma_\gamma(x) \exp\left(-\frac{4t^2 x}{\beta} - 2itx\right) dx = \frac{1}{\sqrt{2\pi}} \int_{\frac{\beta\sigma_E^2}{2}}^{\frac{s^2}{\beta}} \exp\left(-\frac{4t^2 x}{\beta} - 2itx\right) dx \\ &= \frac{1}{\beta} \frac{e^{-2\sigma_E^2 t^2 - i\beta\sigma_E^2 t} - e^{-4\frac{t^2}{\beta^2} s^2 - 2i\frac{t}{\beta} s^2}}{2\sqrt{2\pi}\frac{t}{\beta}(2\frac{t}{\beta} + i)}. \end{aligned}$$

In order to properly understand the $s \rightarrow \infty$ limit we also need to analyze (A4):

$$\begin{aligned} \hat{f}_+^{(s)}(\nu) &= \int_{\frac{\beta\sigma_E^2}{2}}^{\infty} \frac{g(x)\sigma_\gamma}{2\sqrt{\sigma_E^2 + \sigma_\gamma^2}} \exp\left(-\frac{(\nu + 2x)^2}{16x/\beta}\right) dx = \int_{\frac{\beta\sigma_E^2}{2}}^{\frac{s^2}{\beta}} \sqrt{\frac{\beta}{16\pi x}} \exp\left(-\frac{(\nu + 2x)^2}{16x/\beta}\right) dx \\ &= \frac{1}{4} \left(e^{-\frac{\beta\nu}{2}} \operatorname{erf}\left(\frac{\nu}{\sqrt{8}\sigma_E} - \frac{\beta\sigma_E}{\sqrt{8}}\right) - \operatorname{erf}\left(\frac{\nu}{\sqrt{8}\sigma_E} + \frac{\beta\sigma_E}{\sqrt{8}}\right) + e^{-\frac{\beta\nu}{2}} \operatorname{erf}\left(\frac{s}{2} - \frac{\beta\nu}{4s}\right) + \operatorname{erf}\left(\frac{s}{2} + \frac{\beta\nu}{4s}\right) \right), \end{aligned} \quad (\text{B2})$$

which in the $s \rightarrow \infty$ limit becomes

$$\hat{f}_+^{(\infty)}(\nu) = \frac{1}{4} \left(\operatorname{erfc}\left(\frac{\beta\sigma_E}{\sqrt{8}} + \frac{\nu}{\sqrt{8}\sigma_E}\right) + e^{-\frac{\beta\nu}{2}} \operatorname{erfc}\left(\frac{\beta\sigma_E}{\sqrt{8}} - \frac{\nu}{\sqrt{8}\sigma_E}\right) \right). \quad (\text{B3})$$

In order to compute $f_+^{(\infty)}(\nu)$, let us consider the function $\hat{f}_{+,0}^{(\infty)}(\nu) := \hat{f}_+^{(\infty)}(\nu) - \frac{1 - \operatorname{sgn}(\nu)}{4}$, where

$$\operatorname{sgn}(\nu) = \begin{cases} 0 & \text{if } \nu = 0 \\ \operatorname{sgn}(\nu) = \nu/|\nu| & \text{if } \nu \neq 0 \end{cases}.$$

Since $\hat{f}_{+,0}^{(\infty)}(\nu) \in \ell_1$, its inverse Fourier Transform exists, and it can be computed as $f_{+,0}^{(\infty)}(t) = \frac{1}{\beta} \frac{e^{-2\sigma_E^2 t^2 - i\beta\sigma_E^2 t + 2i\frac{t}{\beta} - 1}}{2\sqrt{2\pi}\frac{t}{\beta}(2\frac{t}{\beta} + i)}$ after a change of variables by utilizing the (complex) Laplace transform of the error function erf [Pro23]. Moreover, since $\hat{f}_{+,0}^{(\infty)}(\nu)$ is smooth, apart from $\nu = 0$ where its value is the mean of its left and right side limits, standard results in the theory of Fourier integrals (see, e.g., [Zor16, Chapter 18.3.1.d]) imply

$$\hat{f}_{+,0}^{(\infty)}(\nu) = \lim_{\eta \rightarrow 0^+} \frac{1}{\sqrt{2\pi}} \int_{-\frac{1}{\eta}}^{\frac{1}{\eta}} f_{+,0}^{(\infty)}(\nu) e^{-i\nu t} dt = \lim_{\eta \rightarrow 0^+} \frac{1}{\sqrt{2\pi}} \int_{-\frac{1}{\eta}}^{\frac{1}{\eta}} \frac{1}{\beta} \frac{e^{-2\sigma_E^2 t^2 - i\beta\sigma_E^2 t + 2i\frac{t}{\beta} - 1}}{2\sqrt{2\pi}\frac{t}{\beta}(2\frac{t}{\beta} + i)} dt.$$

On the other hand, it is a standard calculation that

$$\frac{1}{4} \operatorname{sgn}(\nu) = \lim_{\eta \rightarrow 0^+} \frac{1}{8\pi} \int_{\eta}^{\infty} \frac{\sin(\nu t)}{t} dt = \lim_{\eta \rightarrow 0^+} \frac{1}{\sqrt{2\pi}} \left(\int_{-\frac{1}{\eta}}^{-\eta} \frac{i}{\sqrt{8\pi t}} e^{-i\nu t} dt + \int_{\eta}^{\frac{1}{\eta}} \frac{i}{\sqrt{8\pi t}} e^{-i\nu t} dt \right).$$

Since $f_{+,0}^{(\infty)}(\nu)$ is bounded in the neighborhood of 0 we can combine the above two expressions, yielding

$$\begin{aligned} \hat{f}_{+,0}^{(\infty)}(\nu) - \frac{\operatorname{sgn}(\nu)}{4} &= \hat{f}_{+,0}^{(\infty)}(\nu) - \frac{1}{4} \\ &= \lim_{\eta \rightarrow 0^+} \frac{1}{\sqrt{2\pi}} \int_{-\infty}^{\infty} \mathbb{1}(|t| \in (\eta, 1/\eta)) \left(f_{+,0}^{(\infty)}(\nu) - \frac{i}{\sqrt{8\pi t}} \right) e^{-i\nu t} dt \\ &= \lim_{\eta \rightarrow 0^+} \frac{1}{\sqrt{2\pi}} \int_{-\infty}^{\infty} \mathbb{1}(|t| \in (\eta, 1/\eta)) \frac{1}{\beta} \frac{e^{-2\sigma_E^2 t^2 - i\beta\sigma_E^2 t}}{2\sqrt{2\pi}\frac{t}{\beta}(2\frac{t}{\beta} + i)} e^{-i\nu t} dt \\ &= \lim_{\eta \rightarrow 0^+} \frac{1}{\sqrt{2\pi}} \int_{-\infty}^{\infty} \mathbb{1}(|t| \geq \eta) \frac{1}{\beta} \frac{e^{-2\sigma_E^2 t^2 - i\beta\sigma_E^2 t}}{2\sqrt{2\pi}\frac{t}{\beta}(2\frac{t}{\beta} + i)} e^{-i\nu t} dt, \end{aligned}$$

where the last equality holds because of the rapid decay of the function for large t values. We can conclude the proof by observing that the Fourier Transform of $\sqrt{\frac{\pi}{8}}\delta(t)$ is $\frac{1}{4}$. \blacksquare

In the $s = \infty$ case, the diverging ℓ_1 norm of $f_{+,0}^{(\infty)}(t)$ raises the question: how big could the norm $\|\mathbf{B}^M\|$ be? In the following we spell out the explicit form of \mathbf{B} by removing the singularity at $t = 0$, which shows that in fact $\|\mathbf{B}^M\| \leq \mathcal{O}(\log(\beta\|\mathbf{H}\|))$, because $\|f_{-,0}\|_1 = \mathcal{O}(1)$. Although the exact formula becomes cumbersome, it enables us to find a very precise approximation by a much simpler formula in Corollary III.2.

Proposition B.2 (Exact form of Metropolis coherent term). *The coherent term \mathbf{B}^M corresponding to the quasi-Metropolis weight $\gamma_{\sigma_E}^{(\infty)}(\omega)$ in (2.8) can be written as*

$$\mathbf{B}^M = \sum_{a \in A} \int_{-\infty}^{\infty} f_{-,0}(t_-) e^{-i\mathbf{H}t_-} \mathbf{O}_a^M e^{i\mathbf{H}t_-} dt_-,$$

where $f_{-,0}(t_-)$ is defined in (A3), and for arbitrary $\theta > 0$ we have

$$\begin{aligned} \mathbf{O}_a^M &= \int_{-\infty}^{\infty} e^{i\mathbf{H}t} \mathbf{A}^{a\dagger} \left(\frac{e^{-2\sigma_E^2 t^2 - i\beta\sigma_E^2 t} + \mathbb{1}(|t| \leq \theta) i \left(2\frac{t}{\beta} + i \right)}{\sqrt{8\pi t} \left(2\frac{t}{\beta} + i \right)} e^{-2i\mathbf{H}t} - \mathbb{1}(|t| \leq \theta) \mathbf{H} \frac{\operatorname{sinc}(2\mathbf{H}t)}{\sqrt{2\pi}} \right) \mathbf{A}^a e^{i\mathbf{H}t} dt \\ &+ \frac{1}{\sqrt{8\pi}} \int_{-\theta}^{\theta} \cos(\mathbf{H}t) \mathbf{A}^{a\dagger} \cos(2\mathbf{H}t) \mathbf{A}^a \mathbf{H} \operatorname{sinc}(\mathbf{H}t) + \operatorname{sinc}(\mathbf{H}t) \mathbf{H} \mathbf{A}^{a\dagger} \cos(2\mathbf{H}t) \mathbf{A}^a \cos(\mathbf{H}t) dt + \sqrt{\frac{\pi}{8}} \mathbf{A}^{a\dagger} \mathbf{A}^a. \end{aligned}$$

Proof. By Corollary A.1-Proposition B.1 we know that

$$\mathbf{O}_a^M = \lim_{\eta \rightarrow 0^+} \int_{-\infty}^{\infty} \left(\mathbb{1}(|t| \geq \eta) \frac{e^{-2\sigma_E^2 t^2 - i\beta\sigma_E^2 t}}{\sqrt{8\pi t} \left(2\frac{t}{\beta} + i \right)} + \sqrt{\frac{\pi}{8}} \delta(t) \right) \mathbf{A}^{a\dagger}(t) \mathbf{A}^a(-t) dt.$$

We decompose the above integral in order to remove its singularity at $t = 0$. We start with the decomposition

$$\frac{e^{-2\sigma_E^2 t^2 - i\beta\sigma_E^2 t}}{\sqrt{8\pi t} \left(2\frac{t}{\beta} + i \right)} = \frac{e^{-2\sigma_E^2 t^2 - i\beta\sigma_E^2 t} + \mathbb{1}(|t| \leq \theta) i \left(2\frac{t}{\beta} + i \right)}{\sqrt{8\pi t} \left(2\frac{t}{\beta} + i \right)} - \mathbb{1}(|t| \leq \theta) \frac{i}{\sqrt{8\pi t}},$$

implying that

$$\begin{aligned} \frac{e^{-2\sigma_E^2 t^2 - i\beta\sigma_E^2 t}}{\sqrt{8\pi t}(2\frac{t}{\beta} + i)} \mathbf{A}^{a\dagger}(t) \mathbf{A}^a(-t) &= e^{i\mathbf{H}t} \mathbf{A}^{a\dagger} \cdot \left(\frac{e^{-2\sigma_E^2 t^2 - i\beta\sigma_E^2 t}}{\sqrt{8\pi t}(2\frac{t}{\beta} + i)} e^{-2i\mathbf{H}t} \right) \mathbf{A}^a e^{i\mathbf{H}t} \\ &= e^{i\mathbf{H}t} \mathbf{A}^{a\dagger} \cdot \left(\frac{e^{-2\sigma_E^2 t^2 - i\beta\sigma_E^2 t} + \mathbb{1}(|t| \leq \theta) i \left(2\frac{t}{\beta} + i\right)}{\sqrt{8\pi t}(2\frac{t}{\beta} + i)} - \mathbb{1}(|t| \leq \theta) \frac{i}{\sqrt{8\pi t}} \right) e^{-2i\mathbf{H}t} \mathbf{A}^a e^{i\mathbf{H}t}, \end{aligned}$$

where

$$\frac{i}{\sqrt{8\pi t}} e^{-2i\mathbf{H}t} = \frac{i}{\sqrt{8\pi t}} \cos(2\mathbf{H}t) + \frac{1}{\sqrt{8\pi t}} \underbrace{\sin(2\mathbf{H}t)}_{2\mathbf{H}t \operatorname{sinc}(2\mathbf{H}t)} = i \frac{\cos(2\mathbf{H}t)}{\sqrt{8\pi t}} + \mathbf{H} \frac{\operatorname{sinc}(2\mathbf{H}t)}{\sqrt{2\pi}}.$$

Finally, observe that due to parity reasons, we have

$$\begin{aligned} &\int_{-\infty}^{\infty} \mathbb{1}(|t| \geq \eta) e^{i\mathbf{H}t} \mathbf{A}^{a\dagger} \mathbb{1}(|t| \leq \theta) \frac{i}{\sqrt{8\pi}} \frac{\cos(2\mathbf{H}t)}{t} \mathbf{A}^a e^{i\mathbf{H}t} dt \\ &= \frac{-1}{\sqrt{8\pi}} \int_{-\infty}^{\infty} \mathbb{1}(\eta \leq |t| \leq \theta) \left(\cos(\mathbf{H}t) \mathbf{A}^{a\dagger} \frac{\cos(2\mathbf{H}t)}{t} \mathbf{A}^a \sin(\mathbf{H}t) + \sin(\mathbf{H}t) \mathbf{A}^{a\dagger} \frac{\cos(2\mathbf{H}t)}{t} \mathbf{A}^a \cos(\mathbf{H}t) \right) dt \\ &= \frac{-1}{\sqrt{8\pi}} \int_{-\infty}^{\infty} \mathbb{1}(\eta \leq |t| \leq \theta) \left(\cos(\mathbf{H}t) \mathbf{A}^{a\dagger} \cos(2\mathbf{H}t) \mathbf{A}^a \mathbf{H} \operatorname{sinc}(\mathbf{H}t) + \operatorname{sinc}(\mathbf{H}t) \mathbf{H} \mathbf{A}^{a\dagger} \cos(2\mathbf{H}t) \mathbf{A}^a \cos(\mathbf{H}t) \right) dt. \end{aligned}$$

Since in the above provided decomposition, every (matrix) function is bounded in the neighborhood of 0, we can obtain the $\eta \rightarrow 0+$ limit by simply removing the indicator $\mathbb{1}(|t| \geq \eta)$.

$$\begin{aligned} &\lim_{\eta \rightarrow 0+} \int_{-\infty}^{\infty} \mathbb{1}(|t| \geq \eta) \frac{e^{-2\sigma_E^2 t^2 - i\beta\sigma_E^2 t}}{\sqrt{8\pi t}(2\frac{t}{\beta} + i)} \mathbf{A}^{a\dagger}(t) \mathbf{A}^a(-t) dt \\ &= \int_{-\infty}^{\infty} e^{i\mathbf{H}t} \mathbf{A}^{a\dagger} \cdot \left(\frac{e^{-2\sigma_E^2 t^2 - i\beta\sigma_E^2 t} + \mathbb{1}(|t| \leq \theta) i \left(2\frac{t}{\beta} + i\right)}{\sqrt{8\pi t}(2\frac{t}{\beta} + i)} e^{-2i\mathbf{H}t} - \mathbb{1}(|t| \leq \theta) \mathbf{H} \frac{\operatorname{sinc}(2\mathbf{H}t)}{\sqrt{2\pi}} \right) \mathbf{A}^a e^{i\mathbf{H}t} dt \\ &+ \frac{1}{\sqrt{8\pi}} \int_{-\theta}^{\theta} \cos(\mathbf{H}t) \mathbf{A}^{a\dagger} \cos(2\mathbf{H}t) \mathbf{A}^a \mathbf{H} \operatorname{sinc}(\mathbf{H}t) + \operatorname{sinc}(\mathbf{H}t) \mathbf{H} \mathbf{A}^{a\dagger} \cos(2\mathbf{H}t) \mathbf{A}^a \cos(\mathbf{H}t) dt. \end{aligned}$$

We conclude by noting that $\int_{-\infty}^{\infty} \sqrt{\frac{\pi}{8}} \delta(t) \mathbf{A}^{a\dagger}(t) \mathbf{A}^a(-t) dt = \sqrt{\frac{\pi}{8}} \mathbf{A}^{a\dagger} \mathbf{A}^a$. ■

Note that this exact formula could be directly and efficiently implemented using QSVT. However, the gains are minimal, as it would only reduce subnormalization from $\mathcal{O}(\log(\beta\|\mathbf{H}\|/\epsilon))$ (this being the ℓ_1 norm required to achieve ϵ precision in [Corollary III.2](#)) to $\mathcal{O}(\log(\beta\|\mathbf{H}\|))$ (the ℓ_1 norm of the weight function corresponding to the natural choice $\theta = 1/\beta\|\mathbf{H}\|$ in [Proposition B.2](#)).

More interestingly, this exact formula seems also to hold in the infinite-dimensional case, giving rise to exact detailed balance in the infinite-dimensional version as well. We leave it for future work to verify that the construction and its analysis can indeed be generalized to infinite dimensional systems.

Moreover, the above result actually also implies that the Lindbladian corresponding to [\(B1\)](#) also well-approximates its $s \rightarrow \infty$ limit, i.e., the above Metropolis-like Lindbladian. The argument goes as follows: first, ‘‘round’’ the Hamiltonian \mathbf{H} to discretize its spectrum at some finite resolution $\ll 1/\beta$. Due to the form of [\(B1\)](#), the resulting perturbation of the Lindbladian is bounded. Then, take the $s \rightarrow \infty$ limit. Since [\(B2\)](#) is exponentially close to its limit [\(B3\)](#) and there is a limited number of Bohr frequencies due to rounding, the resulting perturbation of the Lindbladian is once again bounded. Finally, undo the rounding, which again causes a bounded perturbation due to the exact form of Metropolis coherent term ([Proposition B.2](#)). Carefully executing these bounds in the $\sigma_E = \beta$ case should show that for $s = \Theta((\beta\|\mathbf{H}\| + \log(1/\epsilon) + 1)^2)$ the resulting Lindbladian is ϵ -close to its $s = \infty$ limit.

Now we show how to approximate the exact Metropolis Lindbladian in a different efficient way.

Corollary III.2 (Approximate coherent term for the Metropolis-like weight). *If $\sigma_E = \frac{1}{\beta}$, then the coherent term \mathbf{B}^M corresponding to the Metropolis-like weight $\gamma^M(\omega) = \exp\left(-\beta \max\left(\omega + \frac{1}{2\beta}, 0\right)\right)$ satisfies*

$$\|\mathbf{B}^M - \mathbf{B}^{M,\eta}\| \leq \left\| \sum_{a \in A} \mathbf{A}^{a\dagger} \mathbf{A}^a \right\| \min\left(\frac{\eta\beta\|\mathbf{H}\|}{\sqrt{2\pi}}, \mathcal{O}((\eta\beta\|\mathbf{H}\|)^3)\right), \quad (3.4)$$

where

$$\mathbf{B}^{M,\eta} := \sum_{a \in A} \int_{-\infty}^{\infty} b_1(t) e^{-i\beta \mathbf{H}t} \left(\int_{-\infty}^{\infty} b_2^{M,\eta}(t') \mathbf{A}^{a\dagger}(\beta t') \mathbf{A}^a(-\beta t') dt' + \frac{1}{16\sqrt{2}\pi} \mathbf{A}^{a\dagger} \mathbf{A}^a \right) e^{i\beta \mathbf{H}t} dt, \quad (3.5)$$

with $b_1(t)$ as in (3.2), and

$$b_2^{M,\eta}(t) := \frac{1}{4\sqrt{2}\pi} \frac{\exp(-2t^2 - it) + \mathbb{1}(|t| \leq \eta) i(2t + i)}{t(2t + i)} \quad \text{such that} \quad \|b_2^{M,\eta}\|_1 < \frac{1}{5} + \frac{1}{2\sqrt{2}\pi} \ln(1/\eta). \quad (3.6)$$

Further, if $[\sum_{a \in A} \mathbf{A}^{a\dagger} \mathbf{A}^a, \mathbf{H}] = 0$, we can drop the second term in (3.5) after the integral in t' since $\int_{-\infty}^{\infty} b_1(t) = 0$.

Proof. First, let us establish the norm bound (3.6). Observe that

$$b_2^{M,\eta}(t) = b_2^{M,1}(t) - \frac{1}{4\sqrt{2}\pi} \mathbb{1}(\eta < |t| \leq 1) \frac{i}{t}.$$

Using the above identity and applying a triangle inequality and then Hölder's inequality gives

$$\|b_2^{M,\eta}\|_1 \leq \|(1 + 4t^2)^{-1}\|_2 \left\| (1 + 4t^2) b_2^{M,1} \right\|_2 + \frac{1}{4\sqrt{2}\pi} \left\| \mathbb{1}(\eta < |t| \leq 1) \frac{i}{t} \right\|_1$$

To obtain (3.6), use that $\int_{\eta}^1 \frac{1}{t} dt = \ln(1/\eta)$, $\int_{-\infty}^{\infty} \frac{1}{(1+4t^2)^2} dt = \frac{\pi}{4}$, $\int_1^{\infty} \left| \frac{\exp(-2t^2)(2t-i)}{t} \right|^2 dt = e^{-4} - \sqrt{\pi} \operatorname{erfc}(2)$, and a direct computation of $\int_{-1}^1 \left| \frac{\exp(-2t^2-it)(2t-i) + i(1+4t^2)}{t} \right|^2 < 16$.

Next, setting $\theta = \eta\beta$ in Proposition B.2 and scaling the variables t, t' by a factor of β reveals that

$$\mathbf{B}^M - \mathbf{B}^{M,\eta} = \frac{1}{2\sqrt{2}\pi^2} \sum_{a \in A} \int_{-\infty}^{\infty} b_1(t) e^{-i\beta \mathbf{H}t} \mathbf{Q}_a e^{i\beta \mathbf{H}t} dt, \quad (\text{B4})$$

where

$$\begin{aligned} \mathbf{Q}_a &= \frac{1}{2} \int_{-\eta}^{\eta} \cos(\beta \mathbf{H}t') \mathbf{A}^{a\dagger} \cos(2\beta \mathbf{H}t') \mathbf{A}^a \beta \mathbf{H} \operatorname{sinc}(\beta \mathbf{H}t') + \operatorname{sinc}(\beta \mathbf{H}t') \beta \mathbf{H} \mathbf{A}^{a\dagger} \cos(2\beta \mathbf{H}t') \mathbf{A}^a \cos(\beta \mathbf{H}t') dt' \\ &\quad - \int_{-\eta}^{\eta} e^{i\beta \mathbf{H}t'} \mathbf{A}^{a\dagger} (\beta \mathbf{H} \operatorname{sinc}(2\beta \mathbf{H}t')) \mathbf{A}^a e^{i\beta \mathbf{H}t'} dt'. \end{aligned}$$

We can decompose in the second term $e^{i\beta \mathbf{H}t'} = \cos(\beta \mathbf{H}t') + i \sin(\beta \mathbf{H}t')$. Due to parity reasons, we can see that the second term can be replaced by

$$- \int_{-\eta}^{\eta} \cos(\beta \mathbf{H}t') \mathbf{A}^{a\dagger} (\beta \mathbf{H} \operatorname{sinc}(2\beta \mathbf{H}t')) \mathbf{A}^a \cos(\beta \mathbf{H}t') - \sin(\beta \mathbf{H}t') \mathbf{A}^{a\dagger} (\beta \mathbf{H} \operatorname{sinc}(2\beta \mathbf{H}t')) \mathbf{A}^a \sin(\beta \mathbf{H}t') dt'.$$

Now, let us define

$$\begin{aligned} \mu_a(\mathbf{X}) &:= \cos(\mathbf{X}) \mathbf{A}^{a\dagger} \cos(2\mathbf{X}) \mathbf{A}^a \mathbf{X} \operatorname{sinc}(\mathbf{X}) + \operatorname{sinc}(\mathbf{X}) \mathbf{X} \mathbf{A}^{a\dagger} \cos(2\mathbf{X}) \mathbf{A}^a \cos(\mathbf{X}) \\ &\quad - 2 \cos(\mathbf{X}) \mathbf{A}^{a\dagger} (\mathbf{X} \operatorname{sinc}(2\mathbf{X})) \mathbf{A}^a \cos(\mathbf{X}) + 2 \sin(\mathbf{X}) \mathbf{A}^{a\dagger} (\mathbf{X} \operatorname{sinc}(2\mathbf{X})) \mathbf{A}^a \sin(\mathbf{X}), \end{aligned}$$

so that

$$\mathbf{Q}_a = \int_{-\eta}^{\eta} \frac{\mu_a(\beta \mathbf{H}t')}{2t'} dt'.$$

If \mathbf{X} is Hermitian, by the triangle inequality, we can see that $\|\mu_a(\mathbf{X})\| \leq 6\|\mathbf{A}^a\|^2 \|\mathbf{X}\|$. Moreover, from its definition, we can see that $\mu_a(\mathbf{X})$ is an odd analytic entire function, and its derivative is 0 at $\mathbf{X} = 0$. From this it directly follows that $\mu_a(\mathbf{X}) = \mathcal{O}(\|\mathbf{A}^a\|^2 \|\mathbf{X}\|^3)$ for every Hermitian \mathbf{X} . Due to the triangle inequality,

$$\|\mathbf{Q}_a\| \leq \int_{-\eta}^{\eta} \frac{\|\mu_a(\beta \mathbf{H}t')\|}{2|t'|} dt' \leq \int_{-\eta}^{\eta} \|\mathbf{A}^a\|^2 \|\beta \mathbf{H}\| \min\left(\frac{6}{2}, \mathcal{O}(\|\beta \mathbf{H}t'\|^2)\right) dt' = \|\mathbf{A}^a\|^2 \min\left(6\eta\beta \|\mathbf{H}\|, \mathcal{O}((\eta\beta \|\mathbf{H}\|)^3)\right).$$

Finally, we can prove (3.4) for individual jumps by combining the above bound and the inequality $\|b_1\|_1 \leq 1$ within (B4). To obtain the bound in terms of the norm-of-sum $\|\sum_a \mathbf{A}^{a\dagger} \mathbf{A}^a\|$, note that for any matrices $\mathbf{X}, \mathbf{Y}, \mathbf{Z}$, we have

$$\begin{aligned} \left\| \sum_a \mathbf{X} \mathbf{A}^{a\dagger} \mathbf{Y} \mathbf{A}^a \mathbf{Z} \right\| &\leq \|\mathbf{X}\| \cdot \left\| \sum_a \mathbf{A}^{a\dagger} \otimes \langle a | \right\| \cdot \|\mathbf{Y} \otimes \mathbf{I}\| \cdot \left\| \sum_a \mathbf{A}^a \otimes |a\rangle \right\| \cdot \|\mathbf{Z}\| \\ &= \|\mathbf{X}\| \|\mathbf{Y}\| \|\mathbf{Z}\| \cdot \left\| \sum_a \mathbf{A}^{a\dagger} \mathbf{A}^a \right\|. \end{aligned}$$

And rewrite $\mu_a(\mathbf{X})$ as a linear combination of terms each bounded by $\mathcal{O}(\|\sum_a \mathbf{A}^{a\dagger} \mathbf{A}^a\| \|\mathbf{X}\|^3)$ by canceling out the linear $\mathcal{O}(\mathbf{X})$ terms. \blacksquare

Appendix C: The discriminant gap and area law

The fact that the discriminant \mathcal{H}_β can be regarded as frustration-free, spatially local Hamiltonian (Proposition I.1) has direct implications on the ‘‘locality’’ of its zero-eigenstate, the purified Gibbs state. In particular, existing analytic techniques for studying gapped phases immediately lead to *explicit* low-depth circuits assuming a large discriminant gap for \mathcal{H}_β . Elegantly, lowering the temperature can now be interpreted as the Nature-given adiabatic paths parameterized by the inverse temperature β (known as quantum simulated annealing).

The particularly helpful tool is quasi-adiabatic evolution [HW05], a version of adiabatic evolution that exploits spatial locality.

Lemma C.1 (Quasi-adiabatic evolution [BMNS12, Proposition 2.4]). *Consider a one-parameter family of Hamiltonians*

$$\mathbf{H}(s) \quad \text{for each } s \in [0, 1] \quad \text{with minimal gap } \Delta.$$

Then, the family of ground-state projectors can be generated by a time-dependent Hamiltonian

$$\mathbf{P}'(s) = i[\mathbf{W}(s), \mathbf{P}(s)] \quad \text{where} \quad \mathbf{W}(s) := \int_{-\infty}^{\infty} dt w(t) \int_0^t du e^{iu\mathbf{H}(s)} \mathbf{H}'(s) e^{-iu\mathbf{H}(s)} \quad \text{for each } s \in [0, 1]$$

for any weight function $w(t)$ satisfying

$$\int_{-\infty}^{\infty} w(t) dt = 1 \quad \text{and} \quad \tilde{w}(\omega) = 0 \quad \text{if } |\omega| \geq |\Delta|.$$

For geometrically local Hamiltonian on d -dimension lattice with single-site jumps $\|\mathbf{A}^a\| = 1$ (note that the natural normalization here is to make the strength extensive $\|\sum_{a \in A} \mathbf{A}^{a\dagger} \mathbf{A}^a\| \propto n$), we can plug the discriminant into the above by

$$\mathbf{H}(s) \rightarrow \mathcal{H}_{s\beta} \quad \text{and} \quad \Delta \rightarrow \min_s \lambda_{gap}(\mathcal{H}_{s\beta}).$$

Strictly speaking, we are interested in the top eigenvector instead of the ground state due to its Lindbladian origin (Lindbladian spectrum is always nonpositive), but this is also handled by quasi-adiabatic continuation. We obtain a unitary circuit preparing the purified Gibbs state driven by the following time-dependent Hamiltonian

$$\mathbf{W}(s) = \sum_a \underbrace{\int_{-\infty}^{\infty} dt w(t) \int_0^t du e^{iu\mathcal{H}_{s\beta}} \mathcal{H}_{s\beta}^{a'} e^{-iu\mathcal{H}_{s\beta}}}_{=:\mathbf{W}^a(s)}. \quad (\text{C1})$$

Algorithmically, the above should be considered an alternative to modernized adiabatic algorithms based on amplitude amplification [CKBG23, Appedix G]. The Heisenberg evolution is particularly powerful in the case of local Hamiltonians as it manifestly gives a quasi-local unitary circuit. Based on existing tools, we quickly instantiate several notations of locality. First, the unitary preserves spatially local operators.

Proposition C.1 (Quasi-local unitary [BMNS12]). *Consider the one-parameter family of unitaries generated by the time-dependent Hermitian matrix $\mathbf{W}(s)$ as in (C1)*

$$\mathbf{V}'(s) = i\mathbf{W}(s)\mathbf{V}(s) \quad \text{for each } s \in [0, 1].$$

Then, the unitary satisfies a Lieb-Robinson bound with almost exponential decay

$$\|[\mathbf{V}(s)\mathbf{O}_1 \mathbf{V}^\dagger(s), \mathbf{O}_2]\| \leq \mathcal{O}\left(\exp\left(-\frac{d}{\text{Poly}_D(\beta) \ln(d^2)}\right)\right) \quad \text{where } d = d(\mathbf{O}_1, \mathbf{O}_2).$$

Second, the unitary generates limited entanglement. Since the unitary is generated by (quasi)-local operators, integrating the entangling rate from $0 \rightarrow \beta$ ¹³ gives an area law of entanglement [VAMV13] for purified Gibbs state.

Corollary C.1 (Thermal area-law from entangling rates (similar argument to [VAMV13])). *The purified Gibbs state satisfies an entanglement area-law*

$$(the\ entanglement\ entropy\ for\ any\ region\ R) \leq \frac{\text{Poly}_D(\beta)}{\Delta} \cdot |\partial R|.$$

The above thermal area-law is weaker than existing bounds¹⁴ and should be thought of as a sanity check. However, what's new is the explicitly parameterized low-depth unitary circuit (which is not a consequence of the area law). The unitary $V(1)$ corresponding to (C1) for a D -dimensional lattice Hamiltonian can be decomposed in to a

$$\text{depth} \quad \frac{\text{Poly}_D(\beta)}{\Delta} \cdot \text{Poly} \log(n/\epsilon) \quad \text{circuit of 2-qubit gates}$$

up to ϵ -error in the operator norm using the HHKL algorithm [HHKL18]. The discriminant gap Δ is expected to be independent of the system size in the rapid mixing regime (under the normalization $\|\mathbf{A}^a\| = 1$). To obtain gapped ground states, we could scale the inverse temperature with the Hamiltonian gap $\Delta(\mathbf{H})$ (not to confuse with the discriminant gap Δ)

$$\beta = \mathcal{O}(\Delta(\mathbf{H}) \log(n/\epsilon)).$$

Of course, there might be phase transitions at low temperatures where the discriminant gap may close. The logarithmic dependence on the system size marks a technical difference from the area law setting. Nevertheless, the explicit circuit appears novel and could potentially lead to new numerical ansatz for low-energy states.

1. The Lindbladian case

Of course, we may apply the same line of thought to Lindbladians, assuming the quasi-local Lindbladian mixes in logarithmic time. However, there are subtle differences. The spectral gap of the parent Hamiltonian is qualitatively the same as the mixing time of our Lindbladian (which has a vanishing anti-Hermitian part)

$$\frac{\ln(2)}{\lambda_{gap}(\mathcal{H})} \leq t_{mix}(\mathcal{L}) \leq \frac{\ln(2\|\rho^{-1/2}\|)}{\lambda_{gap}(\mathcal{H})}.$$

The conversion overhead $\ln(2\|\rho^{-1/2}\|) = \mathcal{O}(\beta\|\mathbf{H}\|)$ could scale with the system size in general. However, to drop this $\mathcal{O}(\beta\|\mathbf{H}\|)$ factor (i.e., proving *rapid mixing* such that the mixing time scaling logarithmically with the system size) amounts to proving a more stringent quantum log-Sobolev inequality, which has been highly nontrivial [CRSF21]. Even if we assume rapid mixing, to get a low-depth circuit for the Gibbs state, we still need an efficient algorithm to implement the Lindbladian evolution that parallelizes the Lindblad operators. However, the HHKL algorithm [HHKL18] achieving this parallelization for local Hamiltonians made critical use of *reversing* time evolutions, which does not obviously apply to the dissipative setting.

As a remedy, one may consider trotterizing into quasi-local brickwork nonunitary circuits, giving a *discrete-time* Quantum Markov chain¹⁵

$$e^{\mathcal{L}\theta} \rightarrow \mathcal{N} := \prod_g e^{\mathcal{L}_g\theta} \quad \text{where} \quad \mathcal{L} = \sum_g \mathcal{L}_g \quad \text{such that each} \quad \mathcal{L}_g \quad \text{is a sum of quasi-local, nearly commuting block.}$$

That is, we regroup the Lindbladian $\mathcal{L} = \sum_{a \in A} \mathcal{L}^a$ into quasi-local blocks to exploit the fact that nearly disjoint Lindbladians can be efficiently implemented in parallel (after spatial truncation). However, the Trotter error from first-order product formulas is extensive; thus, the discrete-time channel would not approximate the continuous-time evolution in general, and the mixing time analysis might require quantitatively different formalism. Nevertheless, the Gibbs state remains stationary

$$\mathcal{N}[\rho_\beta] = \rho_\beta,$$

and could potentially share similar mixing behavior as the continuous case in practice.

¹³ The infinite temperature Gibbs state is the maximally entangled state. It is a tensor product of bell pairs across the two copies and has trivially entanglement across regions.

¹⁴ Ref. [KAA21] states that the *mutual information* between regions satisfies $I(R : R') \leq \mathcal{O}(\beta^{2/3})|\partial R|$ in any D -dimension lattice.

¹⁵ The observation that discretization can be helpful despite deviating from the continuum was made in [DCL23].

Appendix D: Why Gaussians?

Our direct calculation confirms the correctness of our ansatz. But why does the filter $f(t)$ need to be Gaussian (1.3)? In this section, we try to derive the Gaussians from scratch, which can be viewed as an alternative view of detailed balance in the time domain. While we try to make our arguments precise, we stop at physicists' level of rigor and do not attempt to extract a mathematical theorem.

Assume that the filter function is real on the real axis

$$f(t) = f(t)^* \quad \text{for each } t \in \mathbb{R}$$

and complex analytic, independent of β , and that the jump operator $\mathbf{A} = \mathbf{A}^\dagger$ is Hermitian (Let us focus on a single jump and drop the jump labels $a \in A$). The goal is to solve for the viable choices of $f(t)$.

We calculate the associated ‘‘transition’’ part (1.1) in the time domain

$$\begin{aligned} \mathcal{T}^\dagger[\cdot] &= \int_{-\infty}^{\infty} \gamma(\omega) \hat{\mathbf{A}}(\omega)^\dagger(\cdot) \hat{\mathbf{A}}(\omega) d\omega \\ &= \int \gamma(\omega) e^{i\omega(t-t')} f(t) f(t') \mathbf{A}(t)(\cdot) \mathbf{A}(t') d\omega dt dt' \quad (\text{using } f(t) = f(t)^*) \\ &= \frac{1}{\sqrt{2\pi}} \int c(t-t') f(t) f(t') \mathbf{A}(t)(\cdot) \mathbf{A}(t') dt dt'. \end{aligned}$$

The third line uses the inverse Fourier Transform

$$c(t) = \frac{1}{\sqrt{2\pi}} \int_{-\infty}^{\infty} e^{i\omega t} \gamma(\omega) d\omega.$$

We may interpret $c(t)$ as a certain correlation function (hence the notation). Now, note that conjugating the Gibbs state yields

$$\begin{aligned} \Lambda(\hat{\mathbf{A}}(\omega)) &= \int_{-\infty}^{\infty} e^{-i\omega t} f(t) e^{i\mathbf{H}(t-i\beta/2)} \mathbf{A} e^{-i\mathbf{H}(t-i\beta/2)} dt \\ &= \int e^{-is\omega} e^{\beta\omega/2} \mathbf{A}(s) f(s+i\beta/2) ds \quad (\text{setting } s := t - i\beta/2). \end{aligned}$$

Then, we get that

$$\begin{aligned} &\Gamma^{-1} \circ \mathcal{T} \circ \Gamma[\cdot] \\ &= \int_{-\infty}^{\infty} \gamma(\omega) \Lambda(\hat{\mathbf{A}}(\omega))(\cdot) \Lambda^{-1}(\hat{\mathbf{A}}(\omega)^\dagger) d\omega \\ &= \int_{-\infty}^{\infty} \int \int \gamma(\omega) e^{-i\omega(s-s'+i\beta)} f(s+i\beta/2) f(s'-i\beta/2) \mathbf{A}(s)(\cdot) \mathbf{A}(s') ds ds' d\omega \quad (\text{setting } s' := t' + i\beta) \\ &= \frac{1}{\sqrt{2\pi}} \int \int c(s' - s - i\beta) f(s+i\beta/2) f(s' - i\beta/2) \mathbf{A}(s)(\cdot) \mathbf{A}(s') ds ds' \quad (\text{continuing } c(z), z \in \mathbb{C}) \\ &= \frac{1}{\sqrt{2\pi}} \int \int c(t' - t - i\beta) f(t+i\beta/2) f(t' - i\beta/2) \mathbf{A}(t)(\cdot) \mathbf{A}(t') dt dt' \quad (\text{shifting integration}). \end{aligned}$$

The third line uses that $(\mathbf{A}(z))^\dagger = \mathbf{A}(z^*)$ for Heisenberg evolution at complex times. The last line shifts the integrals by $s \rightarrow t$ and $s' \rightarrow t'$ (assuming the absence of poles across the strip).

Comparing the coefficient of product integrals over $\mathbf{A}(t) \cdot \mathbf{A}(t')$ for each t, t' , the condition

$$c(t-t') f(t) f(t') = c(t' - t - i\beta) f(t+i\beta/2) f(t' - i\beta/2) \quad \text{for each } t, t' \in \mathbb{R} \quad \text{ensures } \mathcal{T}^\dagger = \Gamma^{-1} \circ \mathcal{T} \circ \Gamma.$$

This condition can be rearranged as (whenever the denominators are non-zero)

$$\frac{c(t-t')}{c(t' - t - i\beta)} = \frac{f(t+i\beta/2) f(t' - i\beta/2)}{f(t) f(t')} \quad \text{for each } t, t' \in \mathbb{R}. \quad (\text{D4})$$

1. Solving the functional equation

We proceed to solve (D4) for a fixed β . Consider a change of variable $t \leftrightarrow t'$

$$\frac{c(t' - t)}{c(t - t' - i\beta)} = \frac{f(t' + i\beta/2) f(t - i\beta/2)}{f(t') f(t)}. \quad (\text{D5})$$

Then, divide the two equations and observe that the LHS depends only on the time difference $t - t'$

$$(D4)/(D5) : f_1(t - t') = \frac{f(t + i\beta/2)}{f(t - i\beta/2)} \cdot \frac{f(t' - i\beta/2)}{f(t' + i\beta/2)} := g(t)/g(t').$$

We must have that

$$g(t) = ae^{bt} \quad \text{for constants } a, b \text{ independent of } t.$$

Thus,

$$\begin{aligned} & ae^{bt} f(t - i\beta/2) = f(t + i\beta/2) \\ \implies & ae^{bt} e^{-i\beta/2 \cdot \partial_t} f(t) = e^{i\beta/2 \cdot \partial_t} f(t) && \text{(analyticity)} \\ \implies & e^{a' + b't - i\beta \cdot \partial_t} f(t) = f(t) && \text{(since } [t, \partial_t] \propto 1). \end{aligned}$$

The last equality regards t and ∂_t as linear operators acting on functions and use the matrix-exponential fact that

$$[\mathbf{X}, \mathbf{Y}] \text{ commutes with } \mathbf{X}, \mathbf{Y} \text{ implies } e^{\mathbf{X}} e^{\mathbf{Y}} = e^{\mathbf{X} + \mathbf{Y} + [\mathbf{X}, \mathbf{Y}]/2}.$$

We can get rid of the exponential by regarding it as an eigenproblem

$$e^{\mathbf{X}} |v\rangle = |v\rangle \quad \text{implies} \quad \mathbf{X} |v\rangle = i2\pi\mathbb{Z} \cdot |v\rangle.$$

This amounts to solving the differential equation

$$(a_1 \partial_t + a_2 t + a_3) f(t) = 0$$

which has the general solution being Gaussians (the constants may depend on the fixed β). Plugging back into (D4), we can solve for $c(t)$, which would not be unique as it allows for linear combinations.

As a sanity check, we re-derive the constraints between the Gaussian parameters and the temperature in the time picture. Let

$$c(x) = e^{-iax} e^{-x^2/\delta^2}, \quad \text{and} \quad f(t) = e^{-t^2/\kappa^2},$$

where a, δ, κ are all real parameters. Then, letting $t - t' := x$ we get:

$$\begin{aligned} & \log \left[\frac{c(t - t')}{c(t' - t - i\beta)} \right] = \log \left[\frac{f(t + i\beta/2) f(t' - i\beta/2)}{f(t) f(t')} \right] \\ \implies & \log \left[\frac{e^{-iax} e^{-x^2/\delta^2}}{e^{ia(x+i\beta)} e^{-(x+i\beta)^2/\delta^2}} \right] = \log \left[\frac{e^{-(t+i\beta/2)^2/\kappa^2} e^{-(t'-i\beta/2)^2/\kappa^2}}{e^{-t^2/\kappa^2} e^{-t'^2/\kappa^2}} \right], \\ \text{it suffices if} & \quad 2ix \left(\frac{\beta}{\delta^2} - a \right) + a\beta - \frac{\beta}{\delta^2} = \frac{-ix\beta}{\kappa^2} + \frac{\beta^2}{2\kappa^2}. \end{aligned}$$

Equating the imaginary and real parts leads to two linearly dependent equations with the same solution:

$$a = \beta \left(\frac{1}{\delta^2} + \frac{1}{2\kappa^2} \right).$$

Then identifying $a \equiv \omega_\gamma$, $\gamma^{-2} = \sigma_\gamma^2/2$, and $\kappa^{-2} = \sigma_E^2$ leads to the same relationship between $\omega_\gamma, \sigma_\gamma^2, \sigma_E^2$ and β as in (1.4).

Appendix E: Other notions of detailed balance

In addition to our KMS detailed balance condition (Definition II.1), other quantum detailed balance has also been studied (see, e.g., [Ali76, FF07, CM17]). In this section, we will discuss two variants of quantum detailed balance, and only the first one seems to work.

1. Detailed balance with unitary drift

We constructed a Lindbladian satisfying the KMS detailed balance condition. However, much of our results remain to hold even if we add a suitable Hamiltonian term, which might enable alternative constructions.

Definition E.1 (KMS-detailed balance with unitary drift [FF07, Section 5]). *We say that the Lindbladian \mathcal{L} satisfies ρ -detailed balance with unitary drift (in short ρ -DBU) with respect to a full-rank state ρ if there exists a Hermitian operator \mathbf{Q} such that*

$$\mathcal{L}^\dagger[\cdot] - \sqrt{\rho}^{-1} \mathcal{L}[\sqrt{\rho} \cdot \sqrt{\rho}] \sqrt{\rho}^{-1} = i[\mathbf{Q}, \cdot]. \quad (\text{E1})$$

Or, in terms of discriminants,

$$\mathcal{A}(\rho, \mathcal{L}) := \frac{\mathcal{D}(\rho, \mathcal{L}) - \mathcal{D}(\rho, \mathcal{L})^\dagger}{2} = -i\rho^{1/4}[\mathbf{Q}, \rho^{-1/4}(\cdot)\rho^{-1/4}]\rho^{1/4}.$$

That is, we relax the KMS detailed balance condition (Definition II.1) by allowing the RHS to be any commutator term $i[\mathbf{Q}, \cdot]$ ¹⁶; this enlarges the family of possible Lindbladian for the stationary state ρ .

Proposition E.1 (Fixed point). *If a Lindbladian \mathcal{L} is ρ -detailed-balanced with unitary drift, then*

$$\mathcal{L}[\rho] = 0.$$

Proof. Evaluate the superoperator (E1) for the identity \mathbf{I} and conclude $\sqrt{\rho}^{-1} \mathcal{L}[\sqrt{\rho} \mathbf{I} \sqrt{\rho}] \sqrt{\rho}^{-1} = \mathcal{L}^\dagger[\mathbf{I}] = 0$. ■

Intuitively, we can certainly add any Hermitian \mathbf{Q} that commutes with ρ without changing the stationary state. In fact, this is the only possibility¹⁷.

Proposition E.2 (Structure of \mathbf{Q} [FF07, Lemma 28]). *In the setting of Definition E.1, \mathbf{Q} must commute with ρ .*

Indeed, we can solve for \mathbf{B} and \mathbf{Q} by modifying the argument for Corollary II.1

$$\begin{aligned} \mathbf{Q} &= \mathbf{Q}^\dagger \\ &\Updownarrow \\ (\Lambda - \Lambda^{-1})(\mathbf{B}) &= \frac{i}{2}(2\mathbf{I} - (\Lambda + \Lambda^{-1}))(\mathbf{R}) \\ &\Updownarrow \\ \sum_{\nu \in B} (e^{\frac{\beta\nu}{2}} - e^{-\frac{\beta\nu}{2}}) \mathbf{B}_\nu &= \frac{i}{2} \sum_{\nu \in B} (2 - e^{-\frac{\beta\nu}{2}} - e^{\frac{\beta\nu}{2}}) \mathbf{R}_\nu \\ &\Updownarrow \\ \sum_{\nu \in B \setminus \{0\}} \mathbf{B}_\nu &= \frac{i}{2} \sum_{\nu \in B \setminus \{0\}} \tanh\left(\frac{\beta\nu}{4}\right) \mathbf{R}_\nu. \end{aligned} \quad (e^{\frac{\beta\nu}{2}} - e^{-\frac{\beta\nu}{2}} \neq 0 \iff \nu \neq 0) \quad (\text{E2})$$

Thus, allowing the term $\mathbf{Q} \neq 0$ merely amounts to dropping constraints on the \mathbf{B}_0 component (which is exactly the set of operators that commute with the Hamiltonian).

This relaxed version of detailed balance comes with the conceptual price of making the Lindbladian “non-self-adjoint” under similarity transformation. Due to the anti-self-adjoint component $\mathcal{A}(\rho, \mathcal{L})^\dagger$, the spectral theory of convergence (at first glance) seems to break since the right eigenvectors are not orthogonal in the Hilbert-Schmidt norm. Fortunately, the following observation comes to the rescue.

Proposition E.3. *If a Lindbladian \mathcal{L} is ρ -detailed-balanced with unitary drift, then*

$$\mathcal{A}(\rho, \mathcal{L})[\sqrt{\rho}] = \mathcal{H}(\rho, \mathcal{L})[\sqrt{\rho}] = 0.$$

In other words, the specific form of detailed balance implies that the anti-self-adjoint component preserves the eigenvector $\sqrt{\rho}$; the particular eigenvector $\sqrt{\rho}$, which we care about, is orthogonal to other eigenvectors. Therefore, the second eigenvalue of \mathcal{H} corresponds to the contraction of the Hilbert-Schmidt norm of the other eigenvector, controlling the mixing time.

Proposition E.4 (Mixing time from spectral gap (adapted from [CKBG23, Proposition II.2])). *If a Lindbladian \mathcal{L} satisfies ρ -DBU, then*

$$t_{\text{mix}}(\mathcal{L}) \leq \frac{\ln(2\|\rho^{-1/2}\|)}{\lambda_{\text{gap}}(\mathcal{H})} \quad \text{where} \quad \mathcal{H} := \frac{\mathcal{D}(\rho, \mathcal{L})^\dagger + \mathcal{D}(\rho, \mathcal{L})}{2},$$

and the mixing time t_{mix} is the smallest time for which

$$\|e^{\mathcal{L}t_{\text{mix}}}[\rho_1 - \rho_2]\|_1 \leq \frac{1}{2}\|\rho_1 - \rho_2\|_1 \quad \text{for any states } \rho_1, \rho_2.$$

¹⁶ In an email exchange with Jonathan Moussa, he mentioned analogous unitary effect for discrete quantum channels.

¹⁷ We thank Jonathan Moussa for pointing us to [FF07, Lemma 28]. This further simplifies the derivation and the presentation, clarifying that our construction actually has $\mathbf{Q} = 0$ and a vanishing anti-Hermitian component.

In other words, adding a coherent term only seems to help with the convergence.

Proof. Write $\mathbf{R} = \rho_1 - \rho_2$, then

$$\begin{aligned} \|e^{\mathcal{L}t}[\mathbf{R}]\|_1 &= \left\| \rho^{1/4} e^{\mathcal{D}t} [\rho^{-1/4} \mathbf{R} \rho^{-1/4}] \rho^{1/4} \right\|_1 \\ &\leq \left\| \rho^{1/4} \right\|_4 \cdot \left\| e^{\mathcal{D}t} [\rho^{-1/4} \mathbf{R} \rho^{-1/4}] \right\|_2 \cdot \left\| \rho^{1/4} \right\|_4 \\ &\leq e^{-\lambda_{gap}(\mathcal{H})t} \left\| \rho^{-1/4} \mathbf{R} \rho^{-1/4} \right\|_2 \\ &\leq e^{-\lambda_{gap}(\mathcal{H})t} \|\rho^{-1/4}\|_2^2 \|\mathbf{R}\|_2 \\ &\leq e^{-\lambda_{gap}(\mathcal{H})t} \|\rho^{-1/4}\|_2^2 \|\mathbf{R}\|_1 \\ &= e^{-\lambda_{gap}(\mathcal{L}^\dagger)t} \|\rho^{-1/2}\| \|\mathbf{R}\|_1. \end{aligned}$$

The first inequality uses Hölder's inequality. The second inequality uses the orthogonality to the leading eigenvector such that $\text{Tr}[\sqrt{\rho} \cdot \rho^{-1/4} \mathbf{R} \rho^{-1/4}] = \text{Tr}[\mathbf{R}] = 0$. Take the logarithm to conclude the proof. \blacksquare

However, if we wish to obtain a parent Hamiltonian corresponding to this Lindbladian, the anti-Hermitian component forces us to consider the *symmetrized discriminant*

$$\mathcal{H}_\beta = \frac{\mathcal{D} + \mathcal{D}^\dagger}{2}.$$

Unfortunately, the presence of the anti-Hermitian component breaks the qualitative analogy between mixing times and discriminant gaps; fast mixing can hold despite a small symmetrized discriminant gap, marking a limitation of the parent Hamiltonian approach. Incorporating a coherent term, the general conversion bound is as follows [CKBG23]; unfortunately, some bounds are only meaningful if the anti-Hermitian part \mathcal{A} is small enough.

Proposition E.5 (Spectral gap from mixing time [CKBG23, Proposition E.5]). *For any Lindbladian \mathcal{L} , let $-\lambda_{\text{Re}(gap)}(\mathcal{L})$ be the second largest real part in its spectrum (counted by algebraic multiplicity), then*

$$\lambda_{gap}(\mathcal{H}) + 2\|\mathcal{A}\|_{2-2} \geq \|\mathcal{A}\|_{2-2} - \lambda_2(\mathcal{H}) \geq \lambda_{\text{Re}(gap)}(\mathcal{L}) \geq \frac{\ln(2)}{t_{mix}(\mathcal{L})}. \quad (\text{E3})$$

Moreover, if $\lambda_{\text{Re}(gap)}(\mathcal{L}) \geq 2\|\mathcal{A}\|_{2-2}$, then there is unique eigenvalue $\lambda_1(\mathcal{H}) \geq -\|\mathcal{A}\|_{2-2}$ and

$$\lambda_{gap}(\mathcal{H}) + 2\|\mathcal{A}\|_{2-2} \geq \|\mathcal{A}\|_{2-2} - \lambda_2(\mathcal{H}) \geq \lambda_{\text{Re}(gap)}(\mathcal{L}). \quad (\text{E4})$$

Corollary E.1 (Spectral gap from mixing time). *If a Lindbladian \mathcal{L} satisfies ρ -DBU and $\frac{\ln(2)}{2t_{mix}(\mathcal{L})} \geq \|\mathcal{A}\|_{2-2}$, then¹⁸*

$$\lambda_{gap}(\mathcal{H}) \geq \frac{\ln(2)}{2t_{mix}(\mathcal{L})}.$$

Proof. Observe that $\frac{\ln(2)}{2t_{mix}(\mathcal{L})} \geq \|\mathcal{A}\|_{2-2}$ implies $\lambda_{\text{Re}(gap)}(\mathcal{L}) \geq 2\|\mathcal{A}\|_{2-2}$ due to (E3), which in turn by (E4) also implies that $\lambda_1(\mathcal{H}) = 0$ (since 0 is an eigenvalue due to Proposition E.3). Thus combining (E3)-(E4) yields

$$\|\mathcal{A}\|_{2-2} + \lambda_{gap}(\mathcal{H}) \geq \lambda_{\text{Re}(gap)}(\mathcal{L}) \geq \frac{\ln(2)}{t_{mix}(\mathcal{L})}. \quad \blacksquare$$

The proof of the above proceeds by showing that $\lambda_{\text{Re}(gap)}(\mathcal{L}) \geq \frac{\ln(2)}{t_{mix}(\mathcal{L})}$, however without any prior knowledge on $\|\mathcal{A}\|_{2-2}$ it does not seem to be possible to lower bound $\lambda_{gap}(\mathcal{H})$ in general. Indeed, if the Lindbladian \mathcal{L} satisfies ρ -detailed balance with unitary drift, then \mathcal{L} and $\mathcal{D}(\rho, \mathcal{L}) = \mathcal{H} + \mathcal{A}$ are related by a similarity transform and are thus co-spectral. Due to Proposition E.3 we know that $V := \text{Span}(\sqrt{\rho})^\perp$ is an invariant subspace of both \mathcal{H} and \mathcal{A} , and thus also of \mathcal{L} . Since $\mathcal{H}|_V \preceq -\lambda_{gap}(\mathcal{H})\mathcal{I}$ and $\mathcal{A}|_V$ is anti-Hermitian we get that every eigenvalue of $\mathcal{L}|_V$ has real part at most $-\lambda_{gap}(\mathcal{H})$, thus $\lambda_{\text{Re}(gap)}(\mathcal{L}) \geq \lambda_{gap}(\mathcal{H})$, which is an inequality in the “wrong” direction.

¹⁸ The bound cannot be qualitatively strengthened without additional structural understanding or assumptions. E.g., consider $\mathbf{H} := \mathbf{Z} - (1 + \epsilon)\mathbf{I}$, $\mathbf{A} := i\mathbf{X}$; the eigenvalues of $\mathbf{H} + \mathbf{A}$ are $-1 - \epsilon$, while $\lambda_1(\mathbf{H}) = -\epsilon$, $\|\mathbf{A}\| = 1$, and the relaxation (mixing) time is $\mathcal{O}(1)$.

2. s -detailed balance

Our KMS detailed balance condition (Definition E.2) is a special case ($s = 1/2$) of a larger family of s -detailed balance condition.

Definition E.2 (s -detailed balance condition). *For a normalized, full-rank state $\rho \succ 0$ and an scalar $0 \leq s \leq 1$, we say that an super-operator \mathcal{L} satisfies (s, ρ) -detailed balance (or s -DB in short) if*

$$\mathcal{L}^\dagger[\cdot] = \rho^{s-1} \mathcal{L}[\rho^{1-s} \cdot \rho^s] \rho^{-s}.$$

Since ρ is an operator, different choices of $0 \leq s \leq 1$ yield different detailed balance conditions. Nevertheless, they all prescribe the same fixed point.

Proposition E.6 (Fixed point). *If a Lindbladian \mathcal{L} is (s, ρ) -detailed-balanced, then $\mathcal{L}[\rho] = 0$.*

The case $s = 0$ corresponds to the so-called Gelfand-Naimark-Segal (GNS) inner product. One naturally wonders if our constructions also apply here. Unfortunately, the case $s = 1/2$ appears to be a special point in the interval $0 \leq s \leq 1$. Let us revisit the energy domain representation of detailed balance (Proposition II.2) for the transition part. Consider a super-operator parameterized by a Hamiltonian \mathbf{H} , β , and a set of operators including its adjoints $\{\mathbf{A}^a : a \in A\} = \{\mathbf{A}^{a^\dagger} : a \in A\}$:

$$\mathcal{T} = \sum_{a \in A} \sum_{\nu_1, \nu_2 \in B} \alpha_{\nu_1, \nu_2} \mathbf{A}_{\nu_1}^a(\cdot) (\mathbf{A}_{\nu_2}^a)^\dagger.$$

Then, the s -detailed balance condition

$$\mathcal{T}^\dagger[\cdot] = \rho^{s-1} \mathcal{T}[\rho^{1-s} \cdot \rho^s] \rho^{-s} \quad \text{demands that} \quad \alpha_{\nu_1, \nu_2} = \alpha_{-\nu_2, -\nu_1} \exp(-\beta(1-s)\nu_1 - \beta s \nu_2) \quad \text{for each } \nu_1, \nu_2 \in B.$$

However, this appears to be a strong condition; if we apply a change of variable $(\nu_1, \nu_2) \rightarrow (-\nu_2, -\nu_1)$,

$$\alpha_{-\nu_2, -\nu_1} = \alpha_{\nu_1, \nu_2} \exp(\beta(1-s)\nu_2 + \beta s \nu_1) \quad \text{for each } \nu_1, \nu_2 \in B.$$

Multiply the two to see that (see [CM17, Lemma 2.5] for an abstract argument)

$$\alpha_{\nu_1, \nu_2} \alpha_{-\nu_2, -\nu_1} = \alpha_{\nu_1, \nu_2} \alpha_{-\nu_2, -\nu_1} \exp(\beta(1-2s)(\nu_2 - \nu_1)) \quad \text{for each } \nu_1, \nu_2 \in B.$$

Therefore, if $s \neq \frac{1}{2}$ and $\beta \neq 0$, we must have that

$$\alpha_{\nu_1, \nu_2} = 0 \quad \text{if } \nu_1 \neq \nu_2 \tag{E5}$$

which contradicts our construction, and currently, we do not know how to algorithmically ensure (E5). The only existing Lindbladian we knew that satisfies (E5) is the Davies' generator [Dav74], which requires resolving the level spacing using a (exponentially) long Hamiltonian simulation time.

Appendix F: Mathematica code for symbolically verifying our calculations

This appendix displays the Mathematica code that symbolically verifies the heavy algebra calculations and Fourier Transforms, as well as

- Setting up proper parameters for the Fourier Transforms and globally applicable assumptions:

```
In[1]:= SetOptions[FourierTransform, FourierParameters -> {0, -1}];
SetOptions[InverseFourierTransform, FourierParameters -> {0, -1}];
$Assumptions = \beta > 0 && \sigma > 0 && \omega \in \mathbb{R} && t \in \mathbb{R};
```

- Verifying (2.7) by taking $c \leftarrow 0$ and (2.8) by additionally setting $s \leftarrow \infty$, finally (2.9) by resetting $c \leftarrow \beta \sigma_E$:

```
In[2]:= Exp[-(\omega + x)^2/(2 (2x/\beta - \sigma^2))] Sqrt[2Pi(2x/\beta - \sigma^2)];
Integrate[%, {x, \beta \sigma^2/2 + c^2/\beta, \beta \sigma^2/2 + s^2/\beta}, Assumptions -> $Assumptions && s > c > 0]
```

```
Out[2]= 1/2 E^(-(1/4)\beta(\beta \sigma^2 + 2\omega + Abs[\beta \sigma^2 + 2\omega]))
*(-Erf[c/2 - (\beta Abs[\beta \sigma^2 + 2\omega])/(4c)] + Erf[s/2 - (\beta Abs[\beta \sigma^2 + 2\omega])/(4s)]
+ E^(1/2 \beta Abs[\beta \sigma^2 + 2\omega])*( - Erf[c/2 + (\beta Abs[\beta \sigma^2 + 2\omega])/(4c)]
+ Erf[s/2 + (\beta Abs[\beta \sigma^2 + 2\omega])/(4s)] ) )
```

- Verifying the integral in the proof of Corollary III.4:

```
In[3]:= Integrate[Exp[-2 x^2]/(x^2 + 1/16), {x, -Infinity, Infinity}] / Sqrt[32 Pi Exp[1/4]]
% // N
```

```
Out[3]= Sqrt[Pi/2] Erfc[1/Sqrt[8]]
0.773389
```

- Verifying the inverse Fourier Transform computations at the end of the proof of [Corollary A.1](#):

```
In[4]:= InverseFourierTransform[Exp[-(2x + ω)^2/(16x/β)], ω, t, Assumptions → x > 0 && σ > 0]
InverseFourierTransform[Exp[-ω^2/(8σ^2)] Sinh[-βω/4]/(2 I), ω, t,
Assumptions → β > 0 && σ > 0 && x > 0];
Exp[-2 t^2 σ^2] σ;
%% / % // FullSimplify;
% * %%
InverseFourierTransform[1/Cosh[-βω/4]/(2Pi), ω, t] // FullSimplify
```

```
Out[4]= 2 Sqrt[2] E^(-2tx (I + (2t)/β))/Sqrt[β/x]
```

```
Out[5]= -E^(-2t^2σ^2 + (β^2σ^2)/8) σ Sin[tβσ^2]
```

```
Out[6]= (Sqrt[2/Pi] Sech[(2Pi t)/β])/β
```

- Verifying the computations in the proof of [Proposition B.1](#):

```
In[7]:= Integrate[Exp[-4t^2x/β - 2Itx]/Sqrt[2Pi], {x, 1/(2 β), s^2/β}]
Integrate[Sqrt[β/(16Pi x)] Exp[-(ω + 2 x)^2/(16x/β)], {x, βσ^2/2, s^2/β},
Assumptions → $Assumptions && s > βσ/Sqrt[2]];
% // FullSimplify[#, Assumptions → $Assumptions && s > βσ/Sqrt[2]] &
% /. {s → Infinity} // FullSimplify
InverseFourierTransform[%, ω, t];
((% - Sqrt[Pi/8] DiracDelta[t]) // FullSimplify) + Sqrt[Pi/8] DiracDelta[t]
```

```
Out[7]= ((E^-((t (2t + Iβ))/β^2)) - E^-((2s^2t (2t + Iβ))/β^2)) β/(2 Sqrt[2Pi] t (2t + Iβ))
```

```
Out[8]= 1/4 (-Erf[(βσ^2 + ω)/(2 Sqrt[2] σ)] + Erf[s/2 + (βω)/(4s)]
+ E^-((βω)/2) (Erf[s/2 - (βω)/(4s)] - Erf[(βσ^2 - ω)/(2 Sqrt[2] σ)]))
```

```
Out[9]= 1/4 (E^-((β ω)/2) Erfc[(βσ^2 - ω)/(2 Sqrt[2] σ)] + Erfc[(βσ^2 + ω)/(2 Sqrt[2] σ)])
```

```
Out[10]= (E^-t(2t + Iβ)σ^2β)/(2 Sqrt[2Pi] t(2t + Iβ)) + 1/2 Sqrt[Pi/2] DiracDelta[t]
```

- Verifying (E2):

```
In[11]:= I/2 (2 - Exp[-βω/2] - Exp[βω/2])/(Exp[-βω/2] - Exp[βω/2]) // FullSimplify
```

```
Out[11]= I/2 Tanh[βω/4]
```